Fall 2011

Investigations of the Tribological Effects of Engine Oil Dilution by Vegetable and Animal Fat Feedstock Biodiesel on Selected Surfaces

Sultana Mahbuba Shanta

INVESTIGATIONS OF THE TRIBOLOGICAL EFFECTS OF ENGINE OIL DILUTION BY VEGETABLE AND ANIMAL FAT FEEDSTOCK BIODIESEL ON SELECTED SURFACES

by

SULTANA MAHBUBA SHANTA

(Under the Direction of Gustavo J. Molina)

ABSTRACT

Biodiesels have become attractive alternative fuel to replace traditional fossil fuels. Biodiesels can be used in diesel engines with no major modification, but its use leads to some degree of engine oil dilution because of biodiesel leaking and scrapping to engine oil pan. Biodiesels can be made from vegetable and animal fat feedstocks. Therefore, the fatty acid methyl ester components of biodiesel may vary upon these sources of feedstock. In this thesis work, engine oil is diluted with vegetable (canola oil, peanut oil and soybean oil biodiesel) and animal (chicken fat) feedstock biodiesels at known percentages and these mixtures are tested in a pin-on-disk tribometer. In-process friction force and temperature changes are observed and specific wear on the tested surface and dilution effects on viscosity are measured. The oxidative stability of diluted engine oils is also assessed by observation. Experimental results suggest that a higher fraction of palmitic and a lower fraction of linoleic acid contents of the biodiesel play a role for providing good lubricity when mixed with the engine oil in the tested condition and animal feedstock biodiesel perform better than that of vegetable feedstock biodiesel.

INDEX WORDS: Biodiesel, Engine oil dilution, Vegetable feedstock, Animal feedstock

INVESTIGATIONS OF THE TRIBOLOGICAL EFFECTS OF ENGINE OIL DILUTION BY VEGETABLE AND ANIMAL FAT FEEDSTOCK BIODIESEL ON SELECTED SURFACES

by

SULTANA MAHBUBA SHANTA

B.Sc. Bangladesh University of Engineering and Technology, Bangladesh, 2005

A Thesis Submitted to the Graduate Faculty of Georgia Southern University in Partial Fulfillment
of the Requirements for the Degree

MASTERS OF SCIENCE IN APPLIED ENGINEERING

STATESBORO, GEORGIA

2011

INVESTIGATIONS OF THE TRIBOLOGICAL EFFECTS OF ENGINE OIL DILUTION BY VEGETABLE AND ANIMAL FAT FEEDSTOCK BIODIESEL ON SELECTED SURFACES

by

SULTANA MAHBUBA SHANTA

Major Professor: Gustavo J. Molina

Committee: Valentin A. Soloiu

Norman E. Schmidt

Electronic Version Approved:
December 2011

DEDICATION

This thesis work is dedicated to my parents who give me inspiration through continuous encouragement, advisement and cordial care.

ACKNOWLEDGMENTS

I would like to express my sincere gratitude to my supervisor Dr. Gustavo J. Molina for his valuable direction, encouragement and supports in the progress of this research and thesis work. I would also express my most sincere gratitude and thanks to my co-supervisor Dr. Valentin A. Soloiu for his advice, efforts and time in the accomplishment of this thesis.

A special thanks to the biodiesel formulation group and Mr. Jeff Lewis of the Renewable Energy & Engines Lab at Georgia Southern University for supplying the vegetable feedstock biodiesel. My gratitude also goes to Mr. Andrew Michaud for helping with machining the disk and setup the data acquisition system. I also appreciate the support of my thesis committee member Dr. Norman E. Schmidt. Finally I want to thank the Department of Mechanical and Electrical Engineering at Georgia Southern University for supplying materials and equipments used for this work.

TABLE OF CONTENTS

LIST OF TABLES

LIST OF FIGURES

NOMENCLATURE

Acronym	Definition
ASTM	American Society of Testing and materials
B100	100% Biodiesel
BDC	Bottom Dead Center
BOCLE	Ball on Cylinder Lubricity Evaluator
CFB	Chicken Fat Biodiesel
CSO	Cotton Seed Biodiesel
COB	Canola Oil Biodiesel
DG	Diglycerides
DPF	Diesel Particle Filters
ECR	Electrical Contact Resistant
EE	Ethyl ester
EN	EuroNorme
EMA	Engine Manufacturer's Association
EPA	Environment Protection Agency
EO	Engine Oil
FAME	Fatty Acid Methyl Ester
FFA	Free Fatty acids
FIE	Fuel Injection Equipment
FTIR	Fourier Transform InfraRed (spectrometer)
HFRR	High Frequency Reciprocating Rig

HSDI	High Speed Direct Injection
LN	Lubricity Number
LOME	Methyl Ester of Linseed oil
MG	Monoglycerides
ME	Methyl Ester
MEE	Methyl Ethyl Ester
M-ROCLE	Munson Roller in Cylinder Lubricity Evaluator
NCWM	National Conference on Weights and Measure
NMR	Nuclear Magnetic Resonance Spectroscopy
P^{31}-NMR	Phosphorous 31 nuclear magnetic resonance (analytical technique)
PRA	Piston Ring Assembly
PF	Poultry Fat Biodiesel
POB	Peanut Oil Biodiesel
S8	Synthetic Fuel Blend
SBO	Soybean Oil Biodiesel
SOB	Soybean Oil Biodiesel
SLBOCLE	Scuffing Load Ball On cylinder Lubricity Evaluator.
SRV	Optimol Reciprocating Rig
TAE	Trends in Agricultural Engineering
TDC	Top Dead Center
TG	Triglyceride
ULSD	Ultra Low Sulfur Diesel
WSD	Wear Scar Diameter
YG	Yellow Grease Biodiesel
ZDDP	Zinc Dialkyl Dithio Phosphate

CHAPTER 1

INTRODUCTION

1.1 General

The recent energy crisis of the world draws attentions towards bio-fuels and biodiesels. Biodiesel development started in the 19th century. The process of transesterification that is used to derive biodiesel from vegetable oil is a more than one hundred year old technology. This process was used initially to derive glycerin from vegetable oil. The byproduct of that glycerin production process was methyl ester and what is today called biodiesel. Rudolf Diesel envisioned using vegetable oil as a fuel of his engine, as he stated in his 1912 speech saying "the use of vegetable oils for engine fuels may seem insignificant today, but such oils may become, in the course of time, as important as petroleum and the coal-tar products of the present time" (Chasen & Fasano, 2009). At the 1900 World Exhibition in Paris, a diesel engine was demonstrated running on peanut oil. In fact, the general feeling in the early 20^{th}century was that vegetable fuels would be the primary fuel for diesel engines, and biodiesels were widely used until the 1920s. However, during the 1920's, diesel engine manufacturers altered their engines to utilize the lower viscosity of fossil fuel, best known as petro diesel, rather than to run on biomass vegetable oil fuel. The first patent of biodiesel fuel derived from palm oil was granted in 1937. In 1938, J. Walton promote the use of FAME (Fatty Acid Methyl Ester) from which glycerol had been removed (Chasen & Fasano, 2009). During the shortage of fuel in 1970's and 1980's, interest in alternative fuels was again revived.

(a)

(b)

Figure 1: Rudolf Diesel and first model of diesel engine run by peanut oil. (Chasen & Fasano,2009)

1.2 Biodiesel Characterization and Standards

Bio-diesel is an alternative fuel for diesel engine that is obtained from renewable agricultural sources such as canola, soybean, peanut, and olive oil; animal fat and waste vegetable oil, through a process called transesterification. All vegetable oils and animal fats consist primarily of triglyceride molecules as shown in Figure 2.

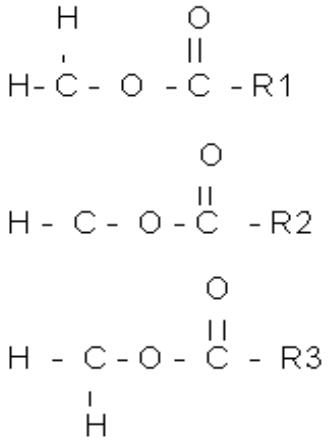

Figure 2: Typical molecular structure of Triglyceride

In Figure 2, R_1, R_2, and R_3 represent the hydrocarbon chains of the fatty acid elements of the triglyceride. The properties of the triglyceride and the biodiesel fuel will be determined by the amounts of each fatty acid that are present in the molecules. Biodiesel consists of the monoesters, formed when the triglycerides react with an alcohol such as methanol. This process is known as transesterification. In the transesterification process, vegetable oil or animal fat reacts with the alcohol in presence of catalyst (e.g. KOH, NaOH, $NaOCN_{3,}$) and produces glycerol and biodiesel as shown in the Figure 3.

Triglyceride + Methanol ⟶ Mixture of fatty esters (biodiesel) + glycerol

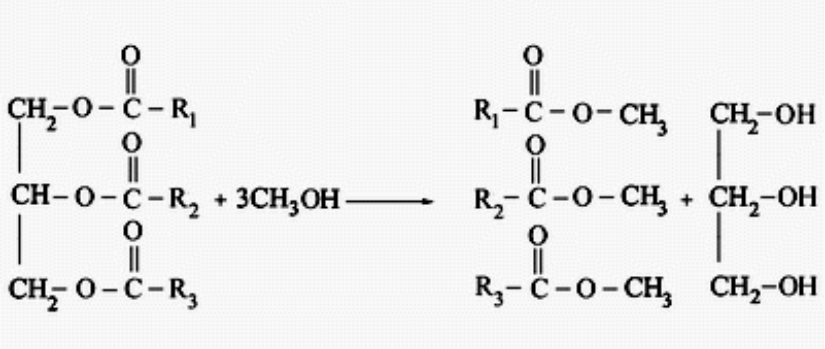

Triglyceride (oil) Biodiesel

Figure 3: Reaction of transesterification process

Typical feedstock is transformed into fatty acid methyl ester (FAME) by transesterification. The chemistry in biodiesel production involves a single step transesterifiction process. Major by-product of the transesterifiction process is glycerin but as it is more polarize and have higher density than FAME, it is immediately separate during the reaction and can be easily removed, once the reaction is completed.

Biodiesel is manufactured both in US and Europe, and there are currently several large biodiesel manufacturers in US. Biodiesel can be obtained from vegetable oil, animal fat or grease, but the large variation of feedstock oils, of their chemistry, and of control used in manufacturing process, make the biodiesel production process more expensive than that of diesel fuel. Requirements for biodiesel are established by the ASTM D6751, a standard specification for biodiesel fuel (B100) blend stock for distillate fuel. Feedstock oil or fat which are used in biodiesel production do not follow any standard for consistent quality control of transesterification (Weiksner, Crump, & White) .There is some controversy in the biodiesel

industry about how much control should be required to obtain an adequate quality product. A strict quality control can yield an improved quality biodiesel but increases the cost for manufacturer, feedstock supplier and finally the consumer. The schematic of biodiesel production is presented in the Figure 4. Failure to control the process of manufacturing, blending and storage of biodiesel can lead to performance failure problems in biodiesel fueled vehicle.

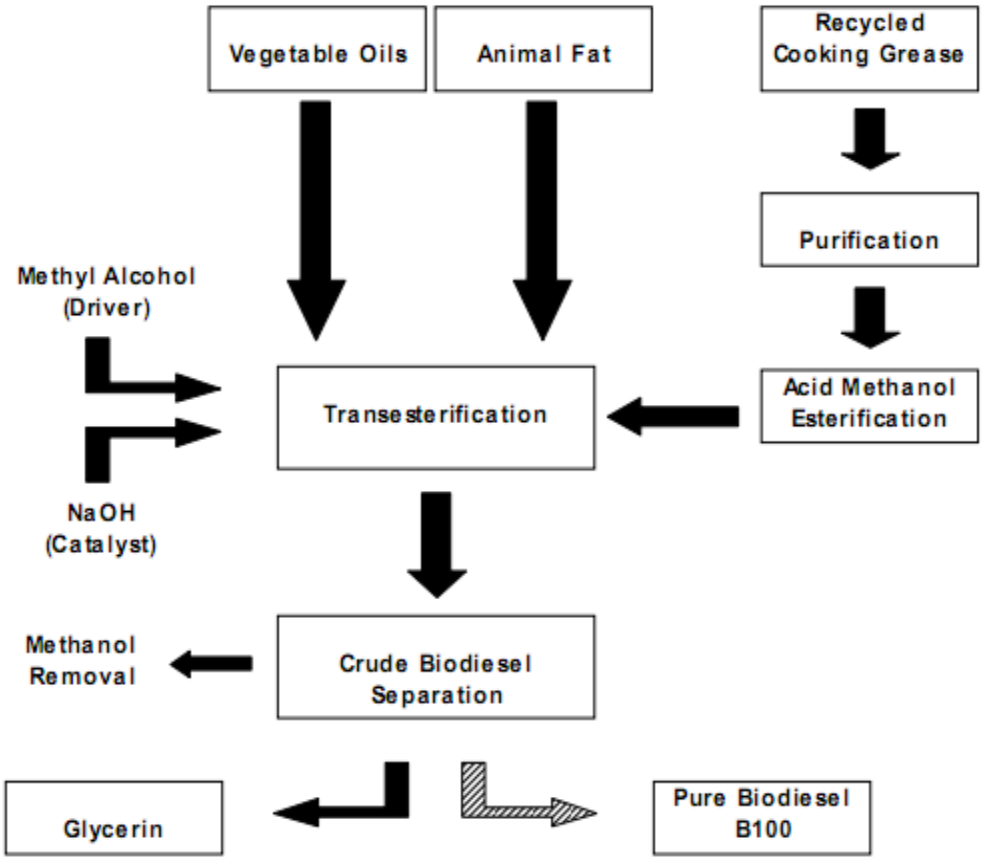

Figure 4: Block schematics of biodiesel manufacturing process (Weiksner, Crump, & White).

1.2.1Chemical Properties of Biodiesel as Fuel

Biodiesel chemical properties vary in a wide range due to the different composition of feedstock. Different feedstock creates biodiesels which may have advantages or disadvantage over petroleum diesel (Duffield, Shapouri, Graboski, McCormick, & Wilson, 1998). Table 1 presents properties of biodiesel and diesel fuel (No 2 Diesel fuel). In the distillation process of crude oil, there are four broad product fraction generated: refinery gas, liquefied petroleum gas, gasoline and distillate fuels. Distillate fuels are further subdivided according to the temperature boiling fraction. The lightest or lowest temperature boiling fraction is known as kerosene or No. 1 diesel fuel. The next fraction used in cold weather condition in automotives or trucks is known as diesel fuel or No.2 diesel fuel or D-2 (EPA, 1999). Table 1 indicates heat of combustion, ignition quality, flash point, oxidative stability, cold flow, viscosity and lubricity properties difference between biodiesel and No.2 diesel fuel. These seven key fuel properties are very important and good indication of fuel quality.

Table 1*:*
Properties of No.2 Diesel fuel and Biodiesel

Fuel Properties	Unit	No. 2 Diesel	Biodiesel
Fuel Standard	ASTM	D795	D6751
Lower Heating Value	Btu/gal	129,050	118,170
Kinematic Viscosity	@ 40^0C	1.3 -4.1	4.0-6.0
Specific Gravity	Kg/l @60^0F	0.85	0.88
Density	lb/gal @ 15^0C	7.079	7.328
Water and Sediment	Vol %	0.05 max	0.05 max
Carbon	Wt%	87	77
Hydrogen	Wt%	13	12
Oxygen	Wt%	0	11
Sulfur	Wt%	0.05 max	0-0.0024
Boiling point	^{0}C	180-340	315-350
Flash Point	^{0}C	60-80	100-170
Pour Point	^{0}C	-15 to 5	-3 to 12
Cetane Number	-	40-55	48-65
Lubricity	SLBOCLE gram	2000-5000	> 7000
Lubricity	HRFF microns	300-600	< 300

Source (biodiesel-b100)

1.2.1.1 Heat of Combustion

The heat of combustion is the energy released as heat, when a substance undergoes complete combustion with oxygen. The heat of combustion of a fuel is commonly referred to as the heating value or the caloric value. It can be determined as either the higher heating value (HHV) or the lower heating value (LHV). HHV is the amount of heat released when a unit amount of fuel at a given initial temperature is completely combusted, and the combustion products being cooled to the initial temperature, and any water vapor produced being condensed. The LHV is similarly defined except that any water in the combustion products is not condensed and remains as a vapor. Lower heating value of No.2 diesel is 132,000 Btu/gal where that of biodiesel is of approximately 10% less. Again No.2 diesel has a specific gravity of 0.85 according to ASTM D-287, but biodiesel specific gravity varies between 0.86 and 0.90.

Therefore the volumetric metering of biodiesel results in slightly higher mass of fuel compared to that of No. 2 diesel. Although a large mass of biodiesel fuel is delivered by the fuel injector, its energy delivery is lower than that of No.2 diesel (Duffield, Shapouri, Graboski, McCormick, & Wilson, 1998). Fuel consumption is in general proportional to the volumetric energy density of the fuel or energy per unit volume of fuel. As biodiesel has lower LHV (lower heating value) and higher specific gravity, it has lower volumetric energy density, which eventually leads to a lower mileage range. However, some research claim that energy efficiency based upon the lower heating value is almost same for No.2 diesel, biodiesel and biodiesel blend (Graboski, M. S.; McCormick, R. L.; J.D. Ross, 1996).

1.2.1.2 Ignition Quality

A common parameter of ignition quality is the dimensionless Cetane number (CN), which (for biodiesel) is also affected by hydrocarbon chain length, un-saturation and branching (F. D. Gunstone, 2007). The Cetane number of a fuel is specified by the ASTM D-613. A Cetane number implies a shorter time between the fuel injection and the ignition start in the cylinder. No-2 diesel has CN ranging from 40 to 52. While CN for soybean oil methyl ester ranges from 44 to 55 that for rapeseed oil methyl ester range from 48 to 61.8. CN for other types of methyl esters, range from 48 to 60 (Duffield, Shapouri, Graboski, McCormick, & Wilson, 1998). An increasing Cetane Number helps reducing No_x emissions. But higher CN (of above 55 to 60) have small additional positive effect in the reduction of emission (Heywood, 1988). Highly saturated esters are generally expected to show higher Cetane Number (Graboski, M. S.; McCormick, R. L.; J.D. Ross, 1996).

1.3.1.3 Flash Point

According to the U.S Department of Transportation neat biodiesel (B100) is much safer than petroleum biodiesel (Biodiesel blend). One of the parameters to assess safety of fuel handling and storage is flash point. A flash point is the temperature at which mixture of the fuel vapors and the air above the fuel is ignites. All No.2 diesel fuel has high flash point (from min 54^0C to 71^0C max) and it is considered safe under normal operating conditions. It is clear from the definition of flash point that the higher the fuels flash point the less likely it would accidentally ignite. Therefore, from this point biodiesel is even safer than diesel fuel because its flash point is typically greater than 100^0C (Duffield, Shapouri, Graboski, McCormick, & Wilson, 1998).

1.3.1.4 Viscosity

Viscosity measures the thickness of the fuel and it describes a fluid internal resistance to flow. It is also a measurement of the resistance of a fluid which is being deformed by either shear or tensile stress. Viscosity is generally independent of pressure, but liquids under extreme pressure often experience an increase in viscosity. Like every other fluid, engine oil viscosity varies with temperature. Based upon the anticipated operating condition of the engine, the viscosity behavior of engine oil would be specified in advance. In the United States, the organization that sets the standards for performance of motor oils is the Society of Automotive Engineers (SAE). Oils with low SAE numbers are generally less viscous or runnier than oils with high SAE numbers, which tend to be thicker. There are two related measurements of fluid viscosity, known as dynamic (or absolute) and kinematic viscosity. In most of the engineering application dynamic viscosity measurement is used.

High viscosity of oil may leads to poorer atomization of fuel spray from the fuel injector. Viscosity is the one of the main reason why vegetable oil or animal fat are converted to biodiesel through transesterifiction (Knothe & Steidley, 2005). Viscosity of biodiesel is however slightly greater than that of No.2 diesel. Biodiesel and its blends with petro diesel show the same temperature dependent viscosity behavior like the pure No.2 diesel.

Additionally, as temperature decreases the viscosity of biodiesel and biodiesel blend increases faster than that of petro diesel (Van Garpen, September, 1996). The effect of biodiesel content on the blend viscosity is lower than the prediction by linear combination model (i.e. according to the volume fraction in mixture). However, B30 soybean or rapeseed methyl ester exhibits the same viscosity as that of No.2 diesel fuel (Duffield, Shapouri, Graboski, McCormick, & Wilson, 1998). Table 2 presents the measured typical viscosity of petro-diesel and biodiesel according to ASTM and EN standard.

Table 2*:*
Kinematic viscosity in diesel fuel standards

Standards	Location	Fuel	Method	Kinematic Viscosity mm^2/s
ASTM	United States	Petrodiesel	ASTM D445	1.9-4.1
ASTM	United States	Biodiesel	ASTM D445	1.9-6.0
EN	Europe	Petrodiesel	ISO 3104	2.0-4.5
EN	Europe	Biodiesel	ISO 3104	3.5-5.0

Source: (Knothe & Steidley, 2005)

1.2.1.5 Lubricity

Lubricating properties of the diesel fuel are very important parameters for diesel engine performance because most of diesel fuel injection systems relied on fuel as a lubricant. In the fuel injection pump all the moving parts are lubricated by the fuel itself, and not by the engine oil. Lubricity of the fuel can give an indication of the wear that would occur between two surfaces in relative motion when covered by the fuel or lubricant.

Before 1993 lubricity of the typical diesel fuel was sufficient to maintain adequate performance of engines. But after 1993, the use of hydro-treating process changed diesel fuel composition by primarily reducing fuel sulfur and aromatic components which then reduced some of the compounds that provided fuel lubricity. This decrease of fuel lubricity can cause premature equipment breakdown and in some cases even catastrophic failure. The problem became more dramatic as EPA (Environment Protection Agency) introduced further reductions in acceptable sulfur levels of the diesel fuel.

Biodiesel typically has higher lubricity than that of reduced sulfur content No.2 diesel. Although lubricity of typical commercial diesel is acceptable, increased lubricity as that of biodiesel yields some benefits regarding engine frictional power loss. A premium diesel task force set up in 1996 by the NCWM (National Conference on Weights and Measure) with the support from ASTM (American Society of Testing and Materials), analyzed the merit of enhance lubricity of fuel in diesel engine (Duffield, Shapouri, Graboski, McCormick, & Wilson, 1998). Lubricity can be measured by Scuffing Load Ball on Cylinder Lubricity Evaluator (SLBOCLE) or High Frequency Reciprocating Rig (HFRR) test. The addition of biodiesel in the petro-diesel even in small amount has been showed to produce a significant amount of increase in lubricity. The Fuel Injection Equipment (FIE) manufacturer adopted the HFRR method and recommend that all diesel fuel meet a limit of 460 micron wear scar diameter (WSD) (Delphi Diesel System,

June, 2000). A typical experimental measurement of WSD of HFRR method for No.1 and No.2 diesel fuel blend is presented in Table 3. For HFRR, a lower wear scar indicates better lubricity. The detail methods for determining lubricity will be discussed in Chapter 2.

Table 3
WSD (Wear Scar Diameter) of different biodiesel blend

Percent Biodiesel	**HFRR WSD (micron)**	
	No.2 Diesel	**No.1 Diesel**
0.0	536	671
0.4	481	649
1.0	321	500
2.0	322	355
20	314	318
100	314	314

Source: (Fuel Fact Sheet)

Therefore, lubricity test shows that a biodiesel exhibit a superior lubricity when compared to a conventional low sulfur diesel fuel. Blending biodiesel with low sulfur diesel at 0.4 percent or higher percentage significantly improves fuel lubricity quality.

1.2.2 Biodiesel Limitations

Although biodiesels present big advantages for the environment and they are able to substitute a portion of fossil fuel use, there are still some major limitations for the massive use of biodiesels. The main limitations are a lower energetic yield and higher production cost.

Energetic yield represent the ratio of all energetic inputs for biodiesel production such as crops, cultivation, transport, transformation etc. to the all outputs (that is fuel and by product). For example, energetic yield of biodiesel from soybean is 3.2. This means that for every unit of energy used in the production of biodiesel, 3.2 unit of energy needs to be harvested (Pavesi & Fauchet, 2008) .

Engines fueled by biodiesel have a 10% reduced fuel economy and power as compared to those of diesel fuel vehicles. The biodiesel fueled engine also emits more nitrogen oxide than diesel fuel (Edwards, 2009) .

Another consideration is fuel price. Biodiesel are not yet economically competitive. Storage, transportation and handling require special management .Biodiesel also have good solvent properties which can be a problem for engines which are running for long time.

1.3 Purpose of the Research of This Thesis

At present biodiesel is already being used as diesel engine fuel in most of diesel engines without any major modification of engine, engine materials or engine oil. It is used as B100 (100% biodiesel) or in a blend with the diesel fuel. Although biodiesel is proved to be an energetically alternative to diesel engine fuel, in some aspects, especially in its chemical composition and fuel properties, biodiesel has some differences as compared to the regular petro-diesel fuel. For instance, biodiesel has lower LHV (lower heating value), higher kinematic and dynamic viscosity and higher specific gravity than those of regular petro diesel.

In a typical diesel engine some degree of engine oil dilution is expected. The reasons and the processes of engine oil dilution will explained in chapter 2. Engine oil performance is a very important factor regarding engine wear and frictional power loss. When biodiesel is used as blend with the regular petro diesel there may be some changes regarding lubricity of the fuel, which may depend upon the feedstock employed for biodiesel or corresponding fatty acid components. As with regular petro-diesel fueled engines, biodiesel or biodiesel blend fueled engines also have some degree of engine oil dilution problem. The purpose of this study is to investigate effects of both vegetable and animal fat feedstock biodiesels on the engine oil, in

terms of lubricity, wear protection properties and oxidative stability of biodiesel diluted engine oil.

1.5 Overview of the Thesis

Chapter 2 contains the theory behind engine wear, engine oil dilution and methods for laboratory estimation of wear. This chapter also contains some literature review about the effects of engine oil dilution by biodiesel and effects of biodiesel components on the diluted engine oil.

Chapter 3 describes the experimental methodology and employed equipments. The description of sample making and surface finishing processes is also included in this chapter.

Chapter 4 presents the experimental results and their discussion and chapter 5 includes conclusions and future research directions.

CHAPTER 2

LITERATURE REVIEW

2.1 Introduction

Biodiesel has become an attractive alternative renewable source of energy. According to the National Biodiesel Board of US, from 1999 to 2008, biodiesel production increased from 500,000 gallons to 700 million gallon. Figure 5 present the annual increment of the biodiesel production from 1999 to 2009 (Scott, 2009). Because of this increased use of biodiesel, it is essential to determine the impact of biodiesel on critical operation points of diesel engines. Figure 6 presents the interaction path of engine fuel with the engine lubricant. There are significant differences in composition between biodiesel and petroleum diesel fuels which have the potential to influence, for instance, ash emissions and thereby affecting after-treatment system performance. Although it is true that biodiesel can be used in diesel engine with no modification, no separate fuel tank or no heat exchanger but still yields acceptable engine performance. Engine oil dilution effect on engine frictional and wear patterns and on emissions are still under investigation.

The fuel also interacts directly with the lubricant through fuel dilution, and may impact lubricant properties ((Sappok & Wong, April 2009). The currently used engine oils produced from mineral hydrocarbons were mainly developed for low sulfur standardized hydrocarbon fuel. The main impact to engine oils by biodiesel compounds can occur from oil dilution by the fatty acid methyl ester (FMAE) and the oil thickening by oxidation of the diluted biodiesel. In this chapter engine oil dilution with biodiesel and its consequences on the lubricity properties of

engine oil, lubricity properties of biodiesel with the diesel fuel base oil, friction and wear on reciprocating surfaces will be discussed.

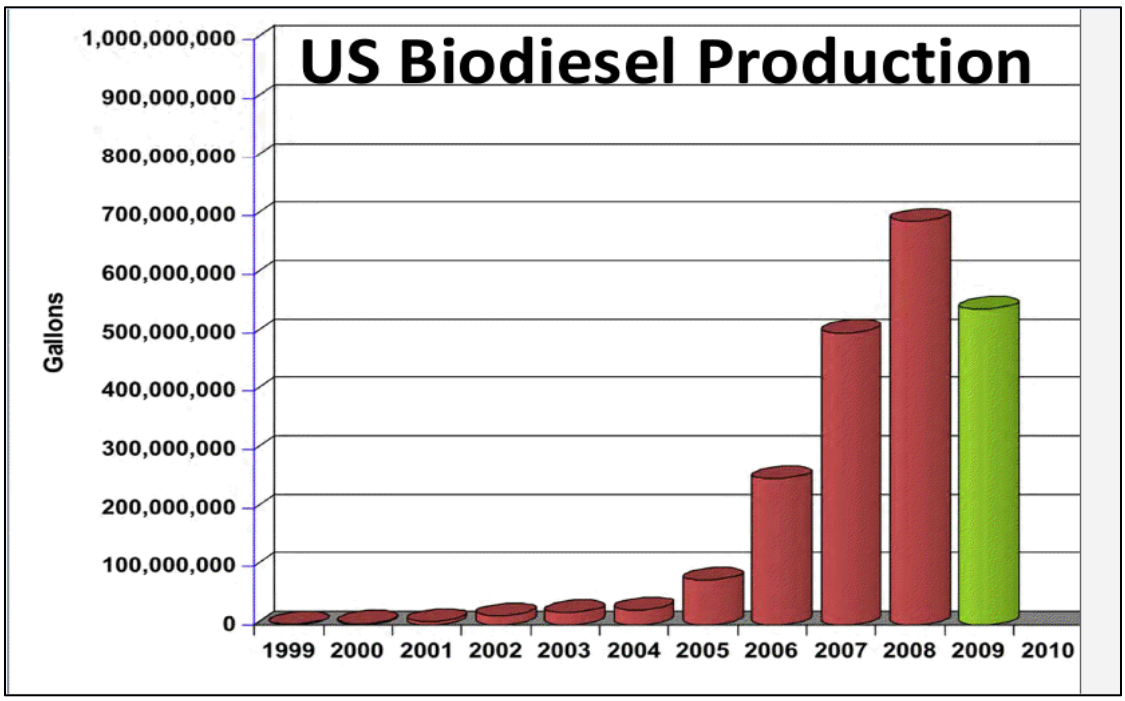

Figure 5: Biodiesel productions in US from 1999 to 2009.

(Scott, 2009)

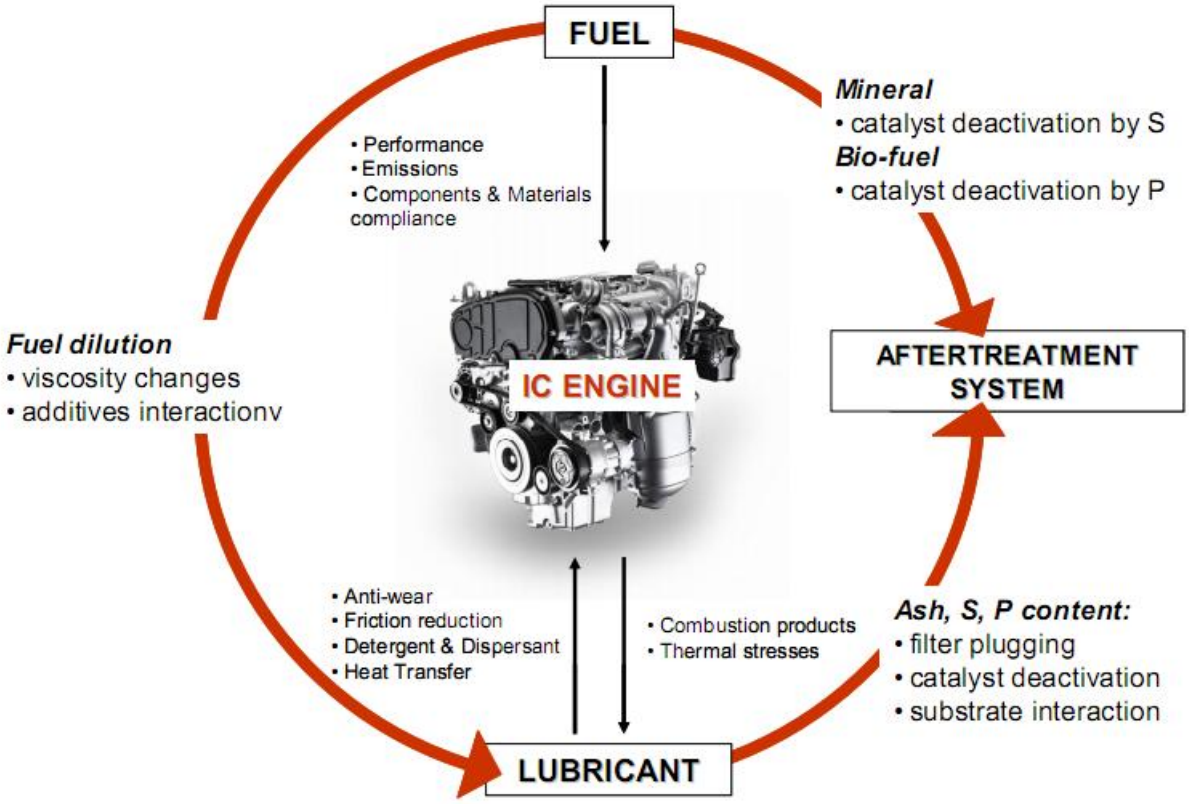

Figure 6: Overview of Engine Fluid Interaction.

(Gili, Igartua, Luther, & Woydt, January 2010)

2.2 How Engine Oil Works

Engine oil primarily provides for the lubrication of the engine moving parts. Figure 7 presents the elements of the lubrication circuit and flow path of oil in a typical engine. Lubricants are designed to reduce the friction between the surfaces that are or could be in contact with one another, which could cause wear at the contact point and they also hydro-dynamically separate the parts in relative motion. Along with the friction reduction modern diesel engine oil performs as a coolant, a cleaning agent and a sealant.

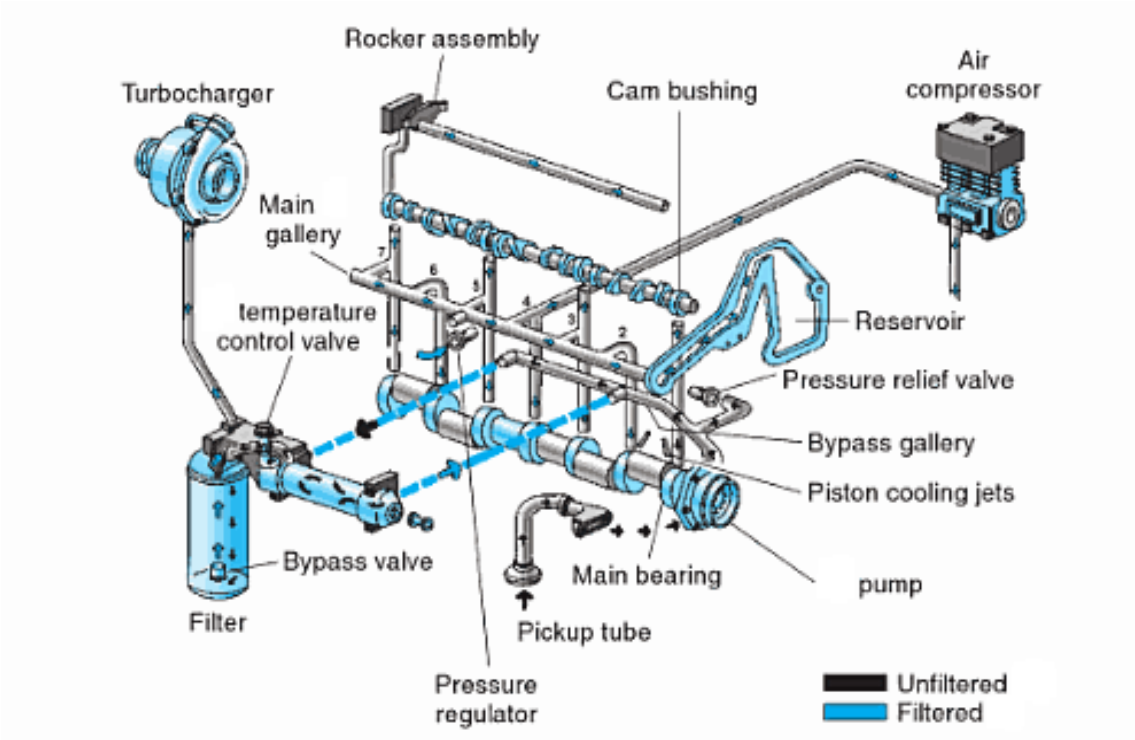

Figure 7: Lubrication Circuit and Flow Path of Oil in Engine

(Bennett, 2009)

Engine oil forms a film between the moving surfaces. The friction occurs in the oil itself preventing direct metal to metal contact. This phenomenon is known as fluid friction. Engine oil perform its lubricating action in two ways: (Bennett, 2009)

1. **Thick Film Lubrication**: It occurs when the distance between two moving surface are wider, such as between rotating crankshaft and its main bearing. This lubrication is also known as hydrodynamic lubrication. Figure 8(a) presents the film thickness pattern of hydrodynamic lubrication.
2. **Boundary lubrication:** It occurs when metal to metal surface distance are very narrow such as those between crankshaft and its main bearing when engine is not running or

during start and ideal periods. Boundary lubrication occurs when the lubricating film is of about same the thickness as that of the surface roughness. Figure 8 (b) presents the film thickness pattern of boundary lubrication. For a hydrostatic or hydrodynamic bearing this operating regime is undesirable, but during start-up, shutdown and low speed operation, the engine is in this boundary lubrication condition.

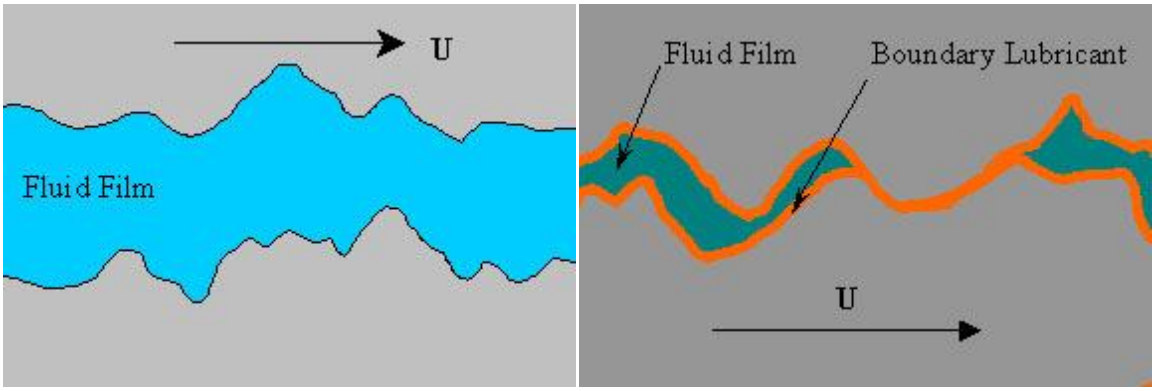

a: hydrodynamic lubrication b: boundary lubrication

Figure 8: The two typical lubricating condition of oil film formation (Bennett, 2009)

2.3 Engine Friction and Wear

Diesel engine achieves a high fuel efficiency, which can approach to 50%.This means that 50% of heat of the combusted fuel is converted into useful work. Although most of the energy is dissipated due to inherent thermodynamic limitations, still 5% of the combustion heat and approximately 10% of the potential useful power are lost due to mechanical loss (Dardalis, 2004). Various internal resistances determine the mechanical power loss of the diesel engine. About 70% of the mechanical power loss of the engine is due to frictional power loss. Power loss due to friction between piston and position rings is approximately 50-60% of the engine frictional loss (Macartchouk, 2002). Loss due to friction in crankshaft bearings is 30-35% of the

frictional loss and loss due to friction in inlet/outlet distributing system is 10-12% of total engine frictional loss. Therefore, the greatest frictional loss happens between piston and piston rings. Decrease the frictional loss is one of the main concerns of engine tribological design.

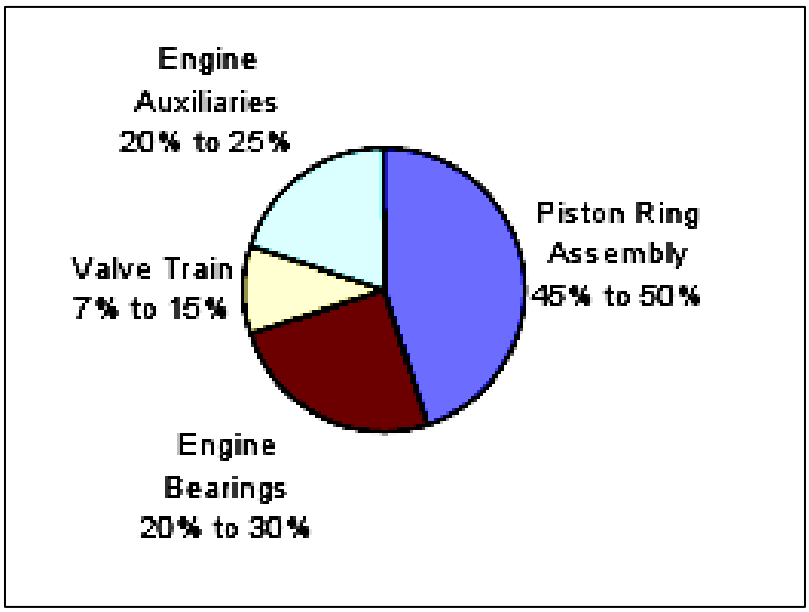

Figure 9: Distribution of total mechanical loss in a typical diesel engine.

(Comfort, 2003)

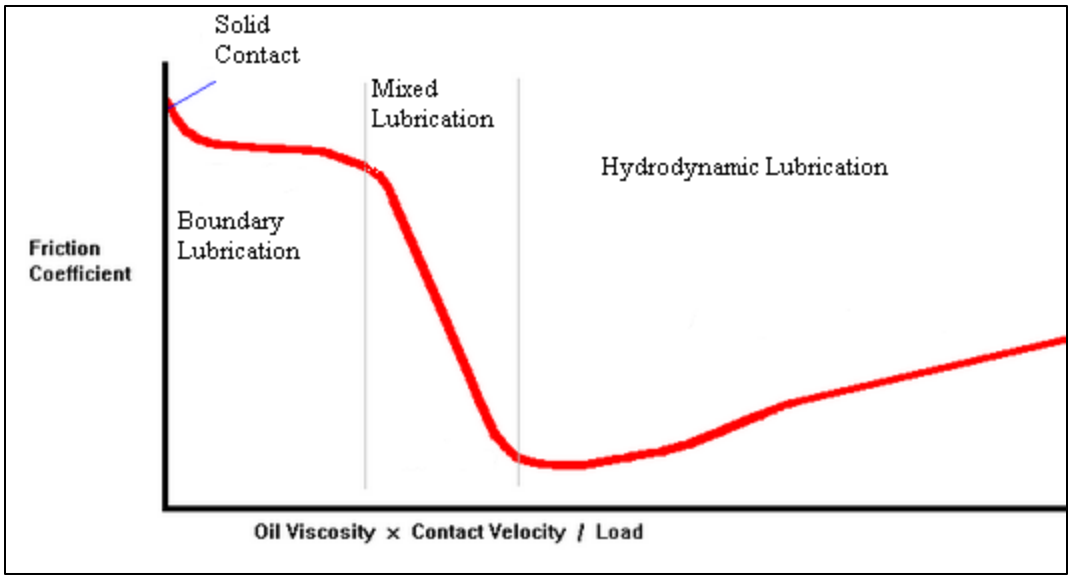

Figure 10: Typical Stribeck curve (Comfort, 2003)

Engine friction can be generally classified into two groups. First one is Coulomb Friction or Dry Friction: This friction occurs when asperities come into contact between two relatively moving surfaces. Second one is Fluid Friction: This occurs when adjacent layers of fluid are moving at different velocities. In real cases it is very difficult to assign an actual degree of engine friction to either group, instead each friction component lies somewhere in between these two categories of friction, and for engine friction there is a continuum between dry and fluid frictions. This continuum depends upon component geometry, surface roughness, and relative velocity of the moving surface, normal loads and various rheological properties of lubricant. This continuum approach can be expressed by the Stribeck curve. Figure 10 presents the regime of lubrication as described the Stribeck curve. Stribeck curve was initially developed for journal bearing studies but the result of those studies can be extended to other lubricated systems.

2.3.1 Piston Ring Assembly Friction (PRA)

Piston ring assembly consists of piston ring, skirt and cylinder liner .The primary role of the PRA is to maintain the effective gas seal between combustion chamber and crankcase. It also transfers heat from the piston to the cylinder wall and it limits the amount of oil transported from crankcase to combustion chamber.PRA should perform all these three tasks with minimum frictional power loss at the sliding interface with the cylinder wall, and with minimum wear. PRA friction was discussed using different theories and mathematical expression, which were based on experimental results and simulations. Velocity of the piston relative to cylinder liner can be modeled as a general plane motion and it plays important role to transfer momentum to the lubricating fluid film. According to the Stribeck curve this relative velocity is also a major factor to determine the lubricating regime of PRA.

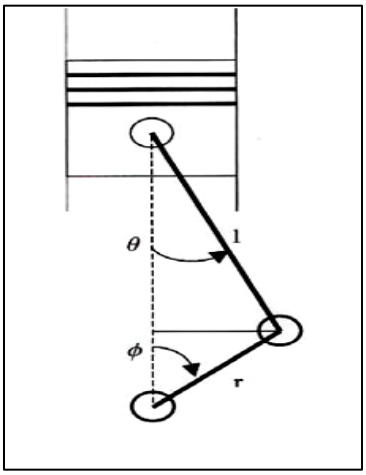

Figure 11:2-D Model of Piston and Crank-throw assembly (Comfort, 2003)

Figure 11 presents the model of piston and crank-throw assembly. The distance from the main journal center line to the piston pin can be expressed as:

$$y = l\cos\theta + r\sin\varphi \qquad 2.1$$

And the relative velocity of piston with respect to linear can be expressed as

$$v = -l\theta'\sin\theta + r\varphi'\sin\varphi \qquad 2.2$$

The type of friction occurring in the PRA can be predicted from the velocity profile of the piston. By comparison with the Stribeck curve, when piston velocity is zero both at top dead center (TDC) and bottom dead center (BDC) as presented in Figure12, lubricant regime would be boundary and some asperity contact would occur. When the piston velocity reaches the maximum, lubricant regime would be hydrodynamic. Any point in between these two extreme points would go to a transition from mixed lubrication to hydrodynamic lubrication.

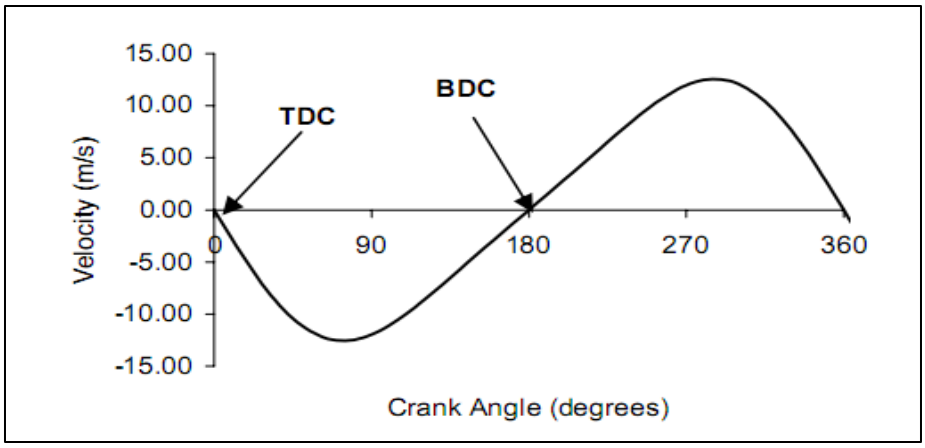

Figure 12: Relative Velocity of Piston with respect to Liner vs. Crank angle at 1800 rpm.

(Comfort, 2003)

2.3.2 Factors for the Modeling of Diesel Engine Friction and Wear

There are six main factors whose effects must be addressed while performing the laboratory scale tests of engine lubricants and wear. Most of the factors, which are presented in Figure 13, are interrelated. Therefore, the change of one factor may affect the several other

factors. This complexity makes it difficult to conduct friction and wear experiments with one controlled independent variable while considering everything else as constant.

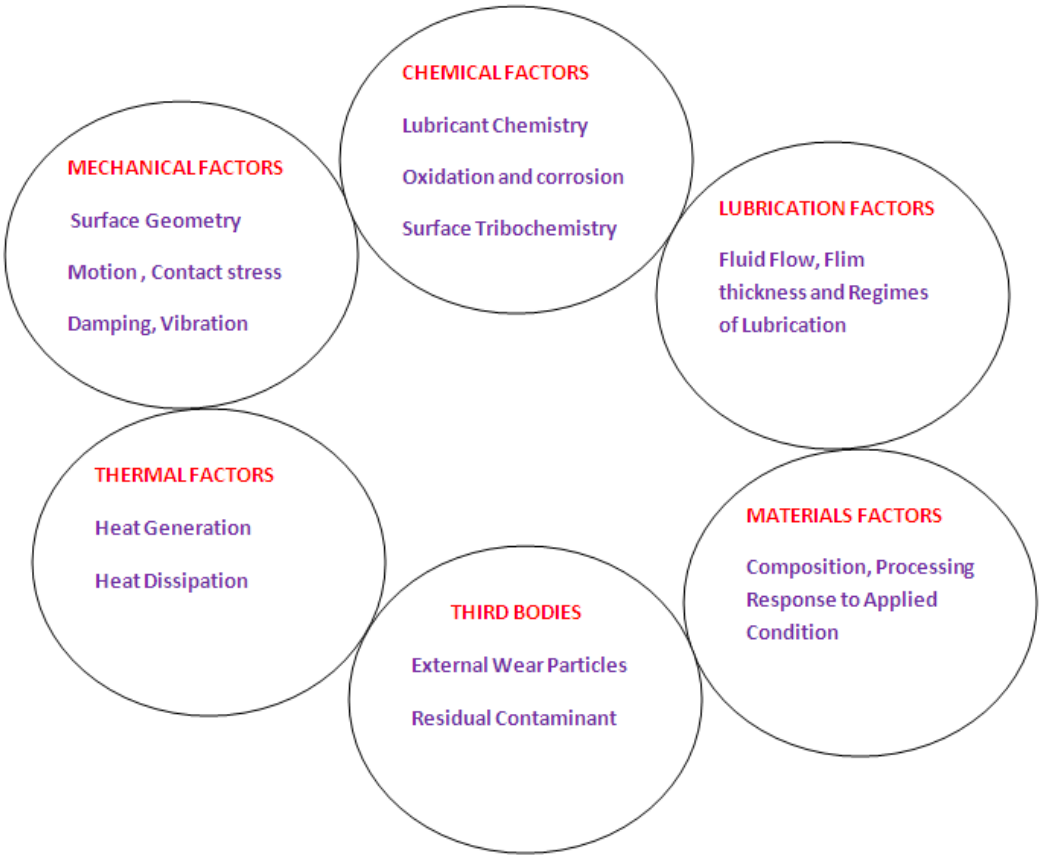

Figure 13: The factors that must be considered for developing accurate simulation of friction and wear in diesel engine.

Besides contact stress, relative motion, stiffness and damping capacity of the system is also considered important mechanical factors in friction and wear modeling. Under rubbing contact, chemical reactivity also change due to compound formation in the lubricant. But this chemical reactivity strongly varies with temperature and also third body particles need to consider. In abrasive wear, some particle is removed from the surface and this wear particles at

the interface need to be considered as third bodies. Lubricant chemistry, film thickness, lubrication regime, and surface tribo-chemistry may play an important role for modeling engine friction and wear. These factors are again strongly affected by engine oil characteristics. Therefore, to model engine friction and wear, engine oil dilution or change of lubricity property, chemical properties and corresponding interactions with the surface play very important roles.

2.4 Engine Oil Contamination by Diesel Engine Fuel

Engine oil contamination can be one main reason of early oil degradation and of eventual engine cessation. Engine oil can become contaminated when unburned or incomplete burnt fuel blows by through the piston rings and ends up in the crankcase. The presence of fuel in the crankcase can reduce oil viscosity and attenuate detergency or additives performance. Frequent engine starts, excessive idling and cold running conditions can lead to moderate and acceptable fuel dilution. Some fuel dilution is always expected and basically 0.36 percent of the total fuel consumption ends up in the crankcase (Fitch, 2007) in a typical engine. Figure 14 presents the flow path of engine fuel towards the crankcase.

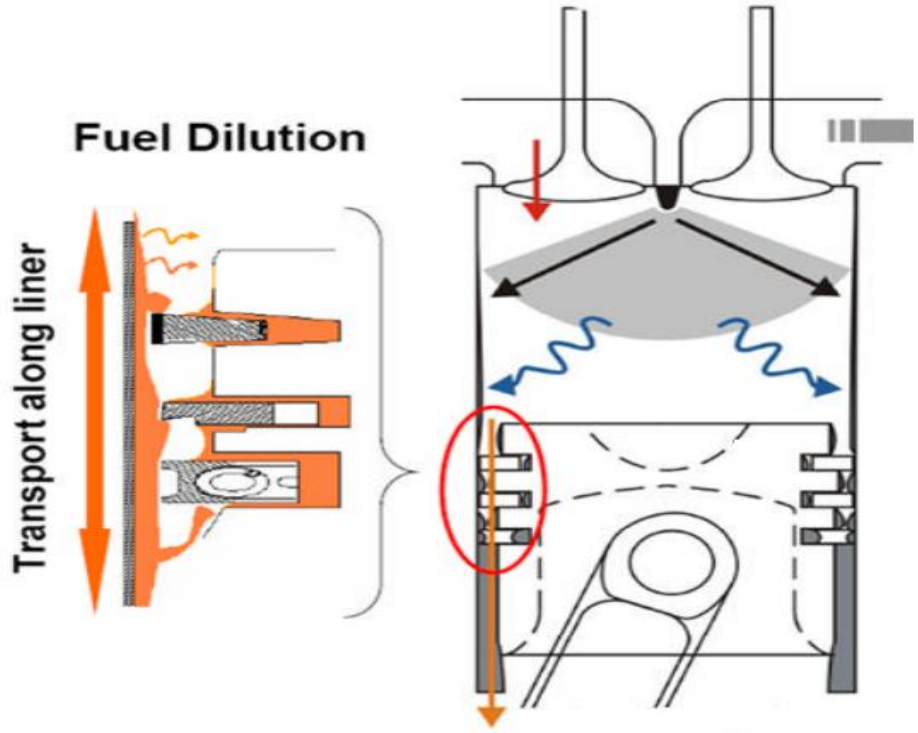

Figure 14: Basic path of the blow by of partially burn fuel as it enters the engine crankcase. (Schwaller, 2005)

In four cycle diesel engines more than four percent of fuel dilution in oil is considered abnormal (U.S Oilchek). Fuel dilution above this percentage indicates that a potential problem may occur with injectors, fuel pumps, gaskets or seals. Faulty operation of fuel system then may lead to excessively rich mixture and defective pressure regulator, poor combustion, bad timing or worn piston. Leakage of oil/fuel heat exchanger may also cause the fuel to enter into the crankcase (Schwaller, 2005). In some newer model diesel engines, late post- injection method is used as a strategy of emission control but it is also can creates more oil dilution.

Engine oil contamination can be detected in the laboratory by three methods: Viscosity, flash point and gas chromatography. Viscosity of the contaminated oil can drop, but sometimes fuel soot level and oil oxidation can nullify such viscosity reduction effect. Measurement of flash

point of the oil is better way to determine the percentage of fuel contamination. The most accurate method of quantitative measurement of oil dilution is gas chromatography (Booser, 1994).

2.5 Primary Cause of Engine Oil Dilution by biodiesel

Some limited engine oil dilution by diesel engine fuel is acceptable and it happens in all engines. But when the engine is fueled by biodiesel or biodiesel blend then engine oil dilution rate and its effect can be different than those from the regular diesel fuel. Gili at el. (Gili F. , Igartua, Luther, & Woydt, 2010) discussed three reasons that are responsible for the biodiesel dilution in the engine oil.

1. Compared to the equi-viscous hydrocarbons (diesel fuel), ester fluids (biodiesel) have more penetrating and solvencies properties. These properties lead to more unburned biodiesel fuel dilution in the engine oil.
2. Today most of the diesel engines with DPF (Diesel Particle Filters), use filter generation system. This system involves a periodic injection of small quantity of a fuel with the burn fuel in order to increase the exhaust temperature and to burn-off all the unburned carbon at exhaust. This procedure increases the dilution of unburned biodiesel fuel in the engine oil.
3. The distillation temperature of the biodiesel is shifted by about 100^0C lower than the diesel fuel, therefore it tends to accumulate in the engine oil and it leads to a long term dilution.

2.6 Problems Associated with Engine Oil Dilution by Diesel Engine Fuel

Service properties of the engine oil may change or sometimes oil can lose its working capacity when contaminated by fuel. Problems associated with engine oil dilution are (Fitch, 2007):

- In cold operating conditions, engine oil dilution can create wax which eventually leads to low oil pressure and to starvation during start up conditions.
- Fuel dilution can cause reduction of engine oil viscosity and have a detrimental effect on the critical oil film thickness. This results in premature combustion-zone wear and crankcase bearing wear.
- High fuel dilution changes the concentration of engine oil and their effectiveness. Figure 15 presents a typical viscosity degradation of engine oil with the increase of fuel dilution percentage.
- If the fuel dilution is caused by a faulty fuel injector, it can wash-down cylinder liner oil. This may lead to piston ring, piston and cylinder wear. It can also increase blow-by and fuel consumptions.
- Engine oil diluted by biodiesel fuel can create some additional problems such as oxidation stability; filter plugging, deposit formation and crankcase accumulation.

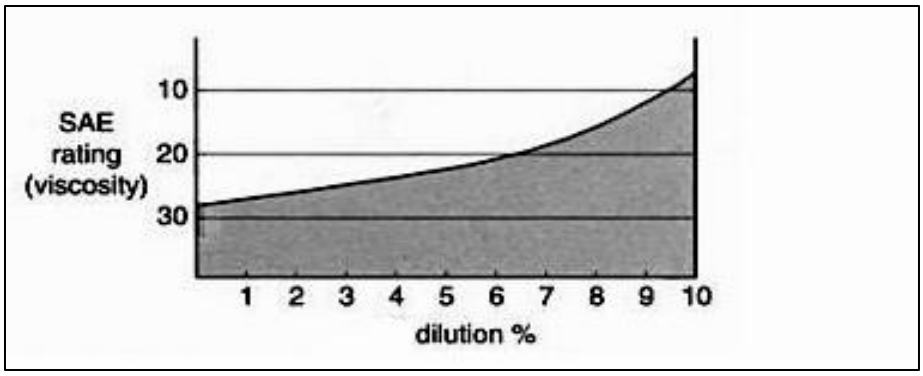

Figure 15: SAE viscosity rating decrease as the percentage of fuel contamination of the engine oil increase (Schwaller, 2005).

2.7 Methods for Determining Lubricity of the Engine Fluid

Lubrication properties are important parameters that determine engine wear and frictional properties. Lubricity test assess frictional properties of the fluid. There are three types of test to evaluate the lubricity of engine fluid (Knothe, Gerpen, & Krahl, The Biodiesel Handbook, 2005):

- Vehicle Tests,
- Fuel Injection Equipment Tests, and
- Laboratory Tests.

Most type of vehicle test and fuel injection equipment test need 500-1000hr of closely monitored operation, and are expensive and lengthy. Laboratory test methods are of low cost, faster moreover able to give accurate evaluation (Munson & Hetz, 1999). There are several standard laboratory test methods available to evaluate lubricity:

- Munson Roller in Cylinder Lubricity Evaluator (M-ROCLE)
- Scuffing Load Ball On Cylinder Lubricity Evaluator(SLBOCLE)
- Ball On Cylinder Lubricity Evaluator (BOCLE)
- High Frequency Reciprocating Rig.(HFRR)

- Optimol Reciprocating Rig(SRV)
- Pin-on-disk Tribometer

The BOCLE and SLBOCLE test devices press a steel ball against a steel rotating ring which is partially immerse in the test fluid. A load is applied until a scuff mark is seen on the rotating cylinder. The gram of load or force is needed to produce a scuff is recorded. In the United States EMA (Engine manufacturer's Association) suggested use of SL-BOCLE test with minimum 3100g load. Figure 16 presents the schematic experimental setup of the SL-BOCLE test.

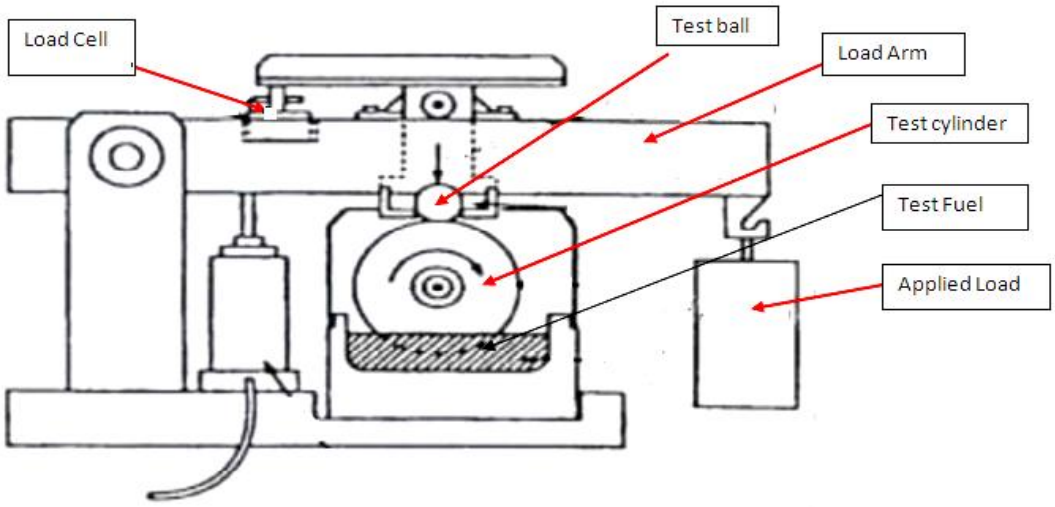

Figure 16: Basic Schematic of SLBOCLE (Garpen, 2004)

HFRR (High Frequency Reciprocating Rig) is the most widely used method and it consists of a reciprocating friction and wears measurement system. This test setup includes a ball which is oscillating with a 1mm stroke length and a 200g load applied on the ball. After 75 minutes of contact, the worn spot of the steel ball is measured with a 100X microscope. The

width of the spot diameter (WSD) directly relates to lubricating properties of the fluid being tested. The WSD (Wear scar diameter) value of HRFF test of different biodiesel blends is presented in Table 3 of section 1.2.1.5. Figure 17 presents the basic schematics and working principle of High Frequency Reciprocating Rig test.

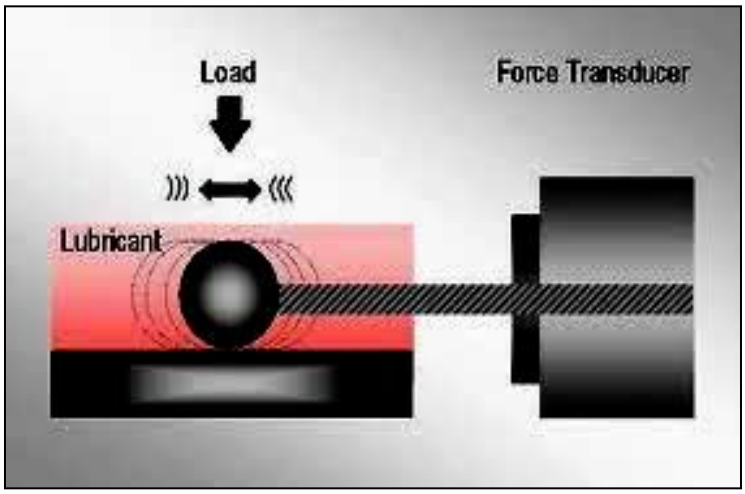

Figure 17: Basic Schematics of HFRR test method. (Garpen, 2004)

In the SRV (Optimol Reciprocating Rig) test method a 10 mm steel ball is sliding against a 25 mm diameter disk, in an off-center mode. Disk and ball are flooded by fuel or oil in the contacting surfaces. Ball is loaded in an incremental sequence. Frequency and stroke of the sliding ball can be changed. The friction between the ball and disk results in a torque which is exerted on the disk. Based on the torque, frictional coefficient can be determined. Figure 18 presents the basic schematic and working principle of SRV (Optimol Reciprocating Rig) test method.

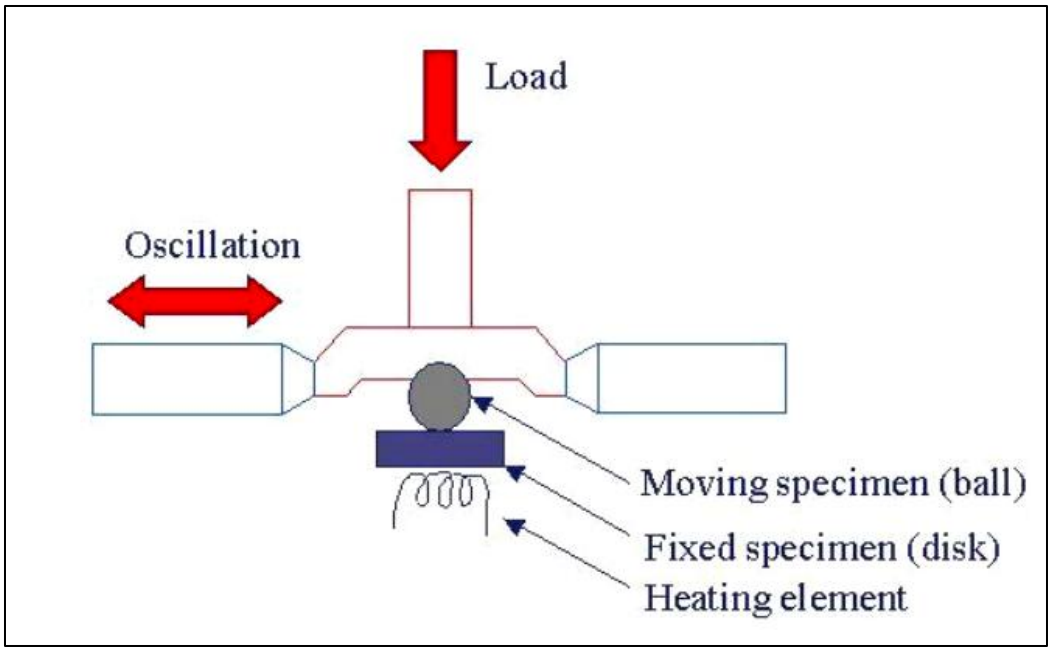

Figure 18: Schematic layout of Optimol SRV machine (Burger, 2006).

Another bench test method is M-ROCEL (Munson Roller in Cylinder Lubricity Evaluator). It employs a crossed roller on cylinder geometry and a data acquisition system. A vertical load is applied on the test roller through the test cylinder under the test fluid lubrication conditions. The wear scar area produced on the roller is determined by using an optical microscope and is approximated by the area formula of an ellipse. The wear scar area stress is also measured and divided by the theoretical Hertzian contact stress and frictional coefficient, to obtain a dimensionless Lubricity Number (LN). This LN is the indication of lubricity of the tested fuel. When LN is greater than 1.0 for the tested fuel, it is considered to have sufficient lubricity. In Figure 19 basic schematics of M-ROCEL (Munson Roller in cylinder Lubricity Evaluator) test method is described.

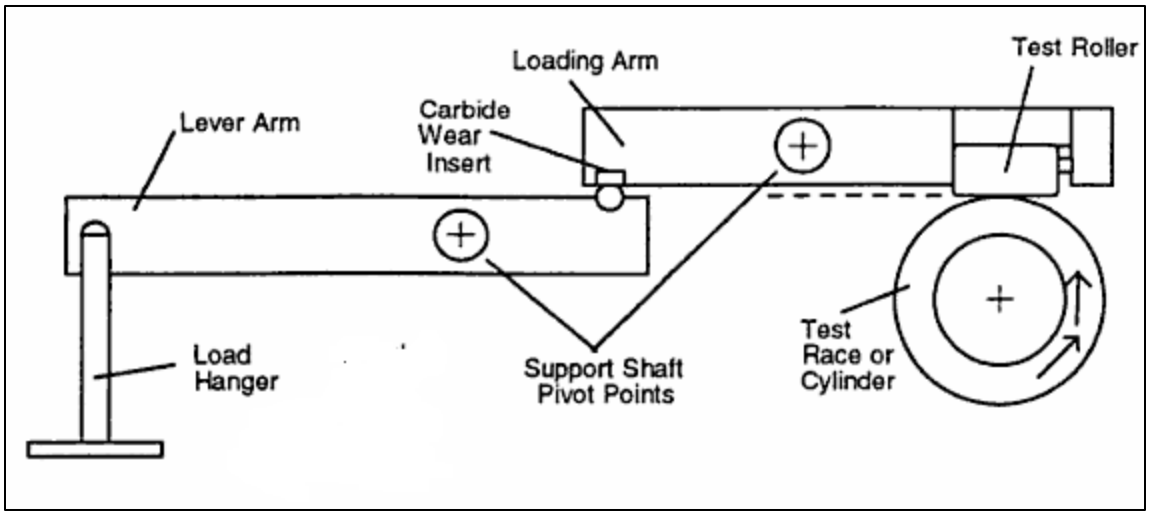

Figure 19: Load unit schematic of M-ROCEL method.(Totten, 2001)

A classical device to measure the friction coefficient under the well defined load is the pin-on-disk tribometer. In this device, a disk is rotating while its surface is scratched by a pin under the test oil lubricating conditions. In this tribometer, the tangential friction force is determined between pin and the rotating disk. Load on the pin is controlled and represents the normal friction force of the friction joint at static condition. The pin is mounted on a stiff lever and tangential frictional force may be determined by the deflection of the lever (Jürgen Butt, Graf, & Kappl, 2003) and deflection of the lever is proportional to tangential friction force at friction couple which is measured by the displacement sensor touched the stiff lever arm. Wear coefficient can be determined after the test by the weight loss of either from pin or of the disk. These two parameters, frictional force and wear are important indications of lubricity of the oil. The research work of this thesis uses a pin-on-disk tribometer to determine the lubricity of biodiesel and mixtures of biodiesel with engine oil. The details of the employed tribometer are described in Chapter 3. Figure 20 presents the basic schematics of pin-on-disk tribometer.

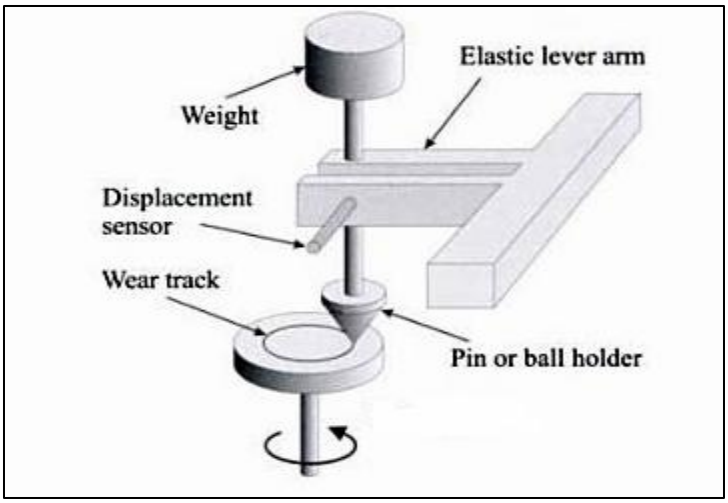

Figure 20: Basic schematics of pin-on-disk tribometer (Jürgen Butt, Graf, & Kappl, 2003)

2.8 Literature Review on Lubrication Property Studies of Biodiesel Due to the Presence of Bio-Components and its Blending with Diesel Fuel

Biodiesel is defined as a mono-alkyl ester of vegetable oil and of animal fat. Among the fuel properties of biodiesel, viscosity and lubricity are the most important to this research work. Lubricity of the biodiesel strongly depends upon the tranesterification process, fatty acid composition and alcohols.

Jianbo Hu and Zexue (Hu & Zexue Du, 2005) made a study on the lubrication properties of biodiesel. In that research, a series of FAME (Fatty Acid Methyl Ester) were synthesized from corn oil, sunflower oil, canola oil, and soybean oil and then they were refined by distillation at reduced pressure and high temperature. In Figure 21 a typical chromatogram of biodiesel is presented. Table 4 presents the percentage of ME (Methyl ester), MG (Monoglycerides), DG (Diglycerides), TG (Triglyceride) and acid value of biodiesel from different vegetable feedstock. Evaluation of the lubrication properties of the refined and unrefined biodiesel was done by measuring the wear scare diameter (WSD) of the HFRR (High Frequency Reciprocating Rig) test. They also find the effects of MG (Monoglycerides), DG (Diglycerides), TG (Triglyceride)

and FFA (Free Fatty acids*)* on the lubricity properties of biodiesel. The result of this research indicates that unrefined biodiesel significantly reduces WSD (Wear scar diameter) when it was used with diesel base oil as compared to refined biodiesel. They concluded that FFA profile was same for both refined and unrefined biodiesel and that MG, DG and TG are the most probable compounds that enhance the lubrication properties of unrefined biodiesel.

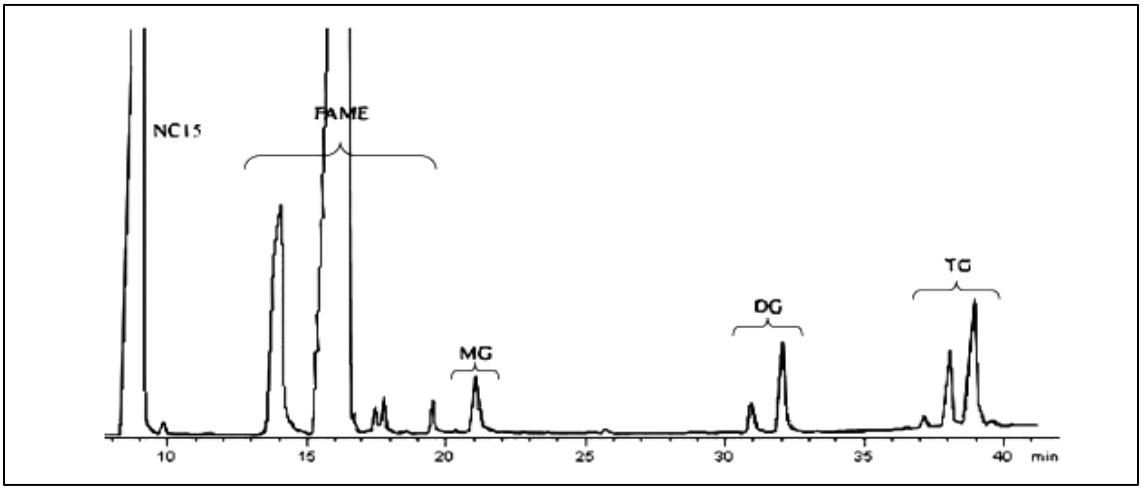

Figure 21: A Typical Chromatogram of Biodiesel.

(Hu & Zexue Du, 2005)

Table 4

Composition and Acid value of Biodiesel

	Refined Canola Biodiesel	**Sunflower Biodiesel**	**Corn Biodiesel**	**Canola Biodiesel**	**Soybean Biodiesel**	**Refined sunflower Biodiesel**
Methyl Esters (w/w%)	96.46	94.88	96.19	96.70	98.00	98.00
Mono-glycerides (w/w%)	0.34	0.27	0.35	0.49	ND	ND
Diglycerides (w/w%)	0.46	0.37	0.20	1.10	ND	ND
Triglyceride (w/w%)	0.44	1.64	0.78	ND	ND	ND
Acid Value (mg KOH/g)	0.14	0.21	0.20	0.18	ND	0.30

(Hu & Zexue Du, 2005)

Kulkarni at el. (Kulkarni, Dalai, & Bakhshi, 2007), investigated the impact of transesterification processes on the lubricity characteristics of biodiesel. In their work they use canola vegetable oil which underwent transesterification with methanol, ethanol and various mixture of methanol/ethanol, keeping the molar ratio of oil to alcohol 1:6, and using KOH as catalyst. They found that the rate of transesterification with mixed alcohols was faster than that for pure methanol and the lubricity of the base oil was better when added 1 %(by vol) of ethyl ester as compared to methyl ester. They also carried out a lubricity test of purified ME (Methyl ester), EE (Ethyl ester), MEE (3:3) (Methyl-ethyl ester obtained by the reaction of vegetable oil with methanol and ethanol by a molar ratio 3:3) and MEE (4.5:1.5) by HFRR and they concluded that lubricity of MEE (3:3) (Methyl ethyl ester with molar ratio 3 to 3) was better than that of pure ME (Methyl ester).

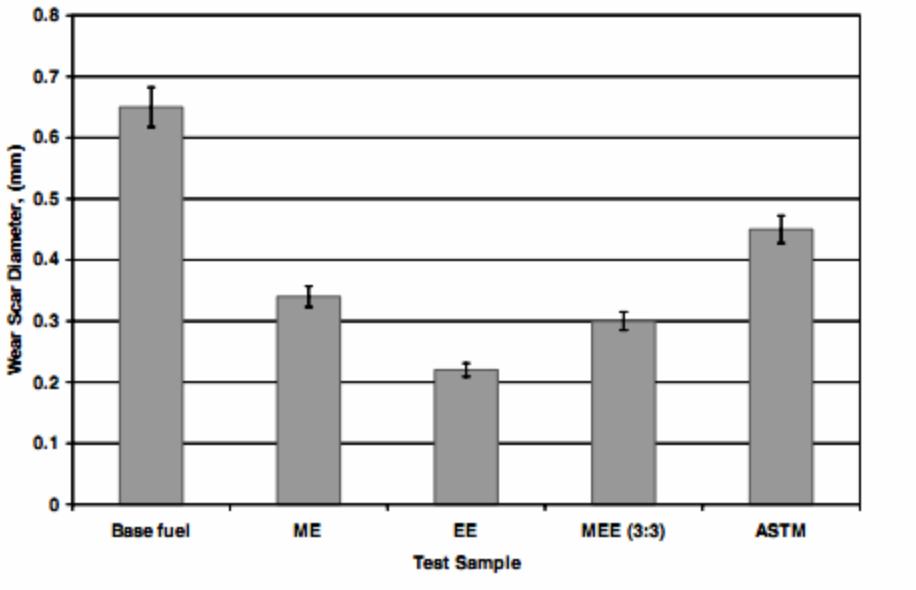

Figure 22: Wear Scar at 1% volume addition of ester to base fuel observed by HFRR.

(Kulkarni, Dalai, & Bakhshi, 2007)

Knothe and Steidley (Knothe & Steidley, Lubricity of Component of Biodiesel and Petrodiesel, 2005) investegated the influence of kinematic viscosity factor in the biodiesel fuel components. In their research they used both straight-chain-ester and branched-esters.They used NMR(Nuclear Magnetic Resonance Spectroscopy) to conform the chain structure of esters, and to determined the kinematic viscosity they used Cannon-Fatenske viscometer.Their results indicate that chain length, position , number,nature of double bonds and nature of oxygenated moieties (oxygenated functional group of the ester molecule) greatly influence the kinematic viscosity fatty acid and it also affects the resulting ester of the biodiesel.

Wadumestheige et al. (Wadumestheige, Ara, Salley, & Simon Ng, 2009) investigated the effect of minor components of biodiesel such as FFA(Free Fatty acids***)***, glycerol, phospholipids and antioxidants. They use ULSD(Ultra Low Sulfur Diesel) and S8 (Synthetic fuel blend) as base oils and the HFRR(High Frequency Reciprocating Rig) method for lubricity test .They also determined the temperature effects on biodiesel lubricity and boundary film formation. Their

results indicated that residues of biodiesel (e.g.unrefined biodiesel) showed better lubricity than those of distilled biodiesel. The presence of minor components such as FFA(Free Fatty acids*)*, glycerol, antioxidant, palmitic acid, tecopherol and asolectin also reduced WSD (Wear scar diameter) by 55% in HFRR(High Frequency Reciprocating Rig.) test, while distilled biodiesel reduced 29% the WSD for the ULSD blend . Figure 23 presents effects of all minor components on HFRR test. For a 2% blend of SBO(Soybean oil biodiesel) in ULSD, Wadumestheige et al. found that WSD increased as the temparature increased up to 70^0C . However, at higher temperature the molecular motion of the polar components would increase enough to distribute them on the metal surfaces and then enhance the lubricity while decreasing WSD. Figure 24 presents effect of the presence of the residue and distilled biodiesel from different sources in ULSD(Ultra Low Sulfur Diesel).

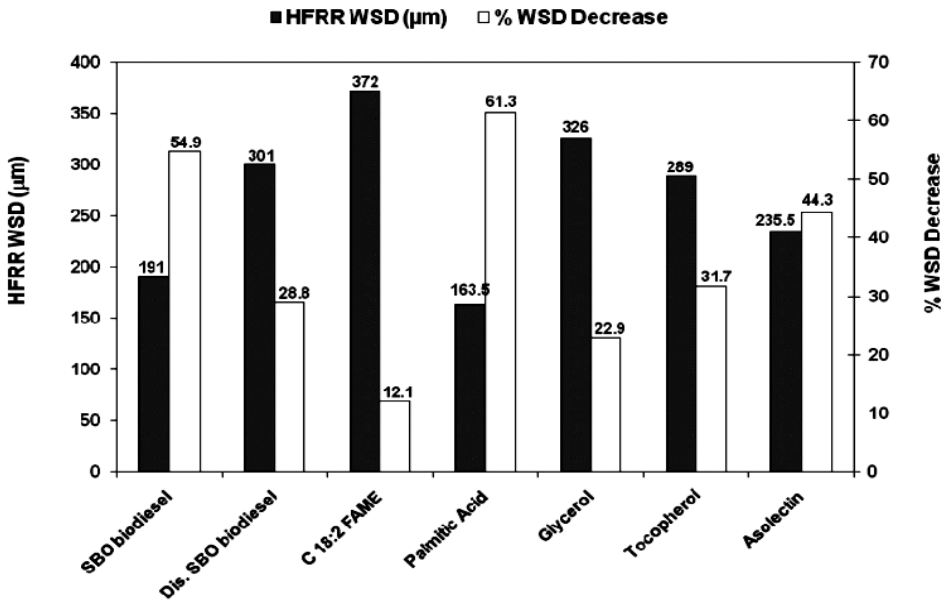

Figure 23: Lubricity effect of different type of minor component.

(Wadumestheige, Ara, Salley, & Simon Ng, 2009)

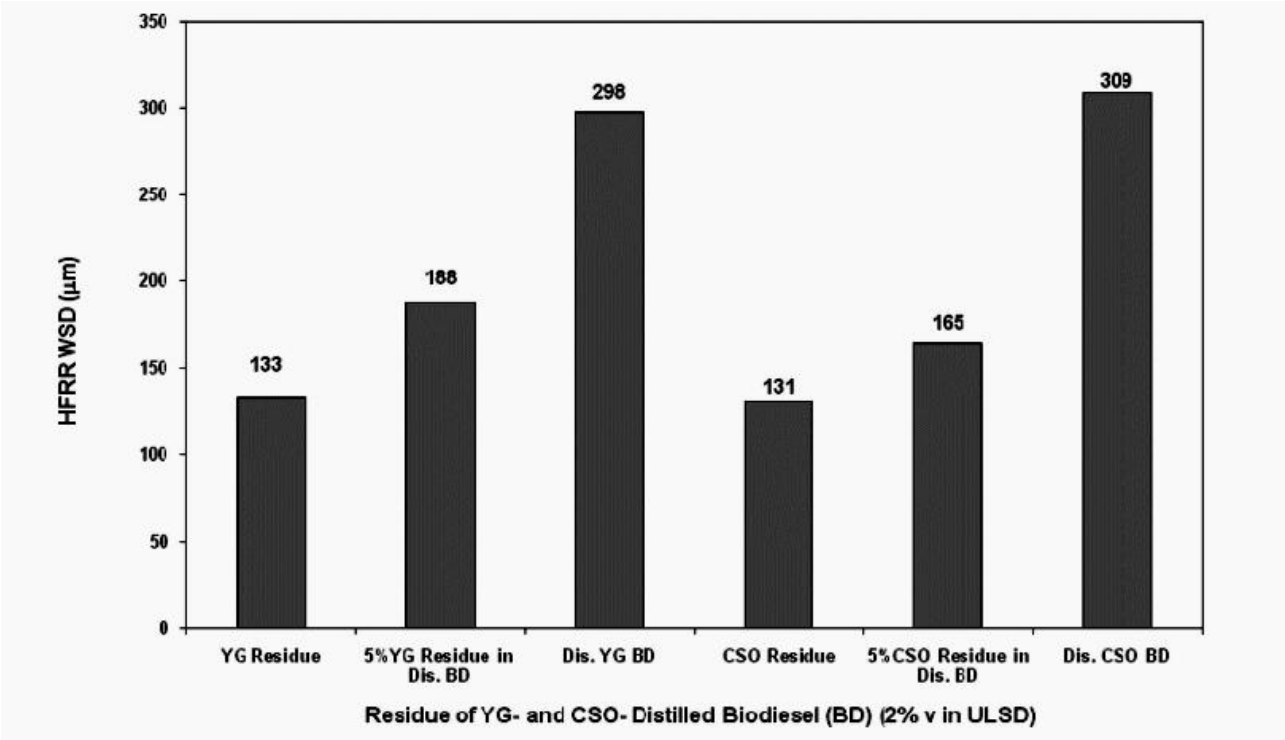

Figure 24: Lubricity of the residue of different distilled biodiesel. (Wadumestheige, Ara, Salley, & Simon Ng, 2009)

Sulek at el. (Sulek, Kulczycki, & Malysa, 2010) made an assessment of tribological properties of the composition of diesel fuel and methyl ester derived from rapeseed oil. That study was carried out for steel-steel pairs with HFRR (High Frequency Reciprocating Rig.) test method. After 75 min tests with a 2N load in presence of 5% methyl ester (%Vol) in diesel oil as base oil they found that friction coefficient decreased by 20%. Their results are presented in Figure 25 and indicate that a further increase of methyl ester content decreases frictional coefficient, and that B100 exhibit a 30% lower friction coefficient than that of diesel fuel. They also characterized wear scar profile by using TOPO L50 profilometer which is presented in Figure 26.

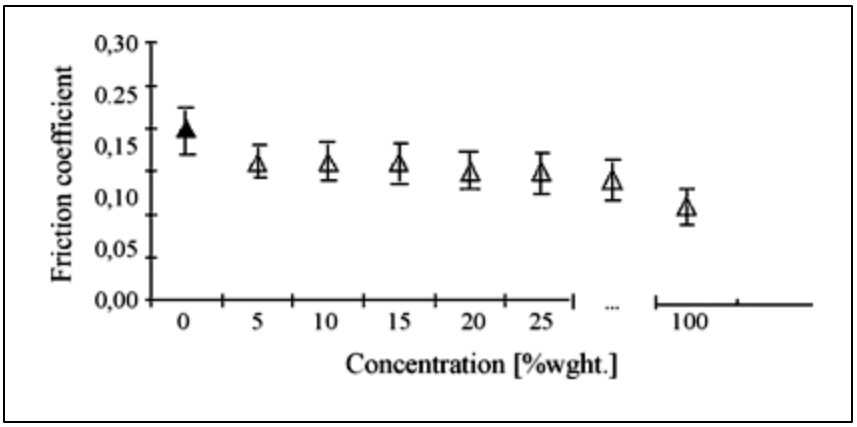

Figure 25: Friction coefficient change with the change of methyl ester concentration in the diesel fuel. (Sulek, Kulczycki, & Malysa, 2010)

.

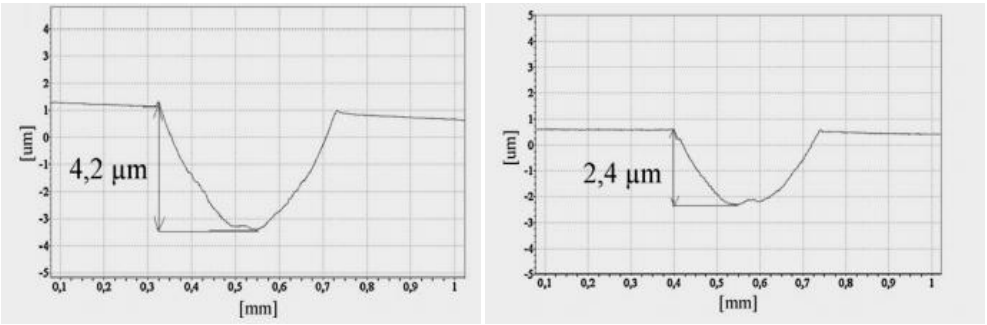

(a) (b)

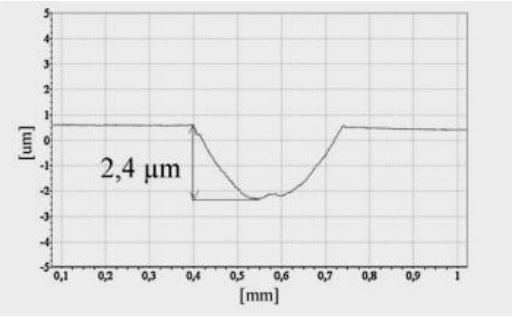

(c)

Figure 26: (a) Depth of Wear Scar by B5. (b) Depth of Wear Scar by B30. (c) Depth of Wear Scar by B100. (Sulek, Kulczycki, & Malysa, 2010)

Sulek at el. also found that 5% (% vol) presence of methyl ester (B5) in diesel oil reduced the depth of wear scar as compared to that of pure diesel fuel oil. After that, an increase of methyl ester concentration caused an increase of depth of wear scar. At 20 %(B20), 25 %(B25), 30% (B30) concentration of methyl ester in the diesel fuel showed the high depth of wear scar than the pure diesel fuel.

2.9 Literature Review on Lubrication Properties of Biodiesel Diluted Engine Oil.

Engine oil dilution effect by biodiesel needs to be investigated. Biodiesel has lower distillation temperature and boiling point and tends to dilute the engine oil even at the small percentage in the fuel. This section reviews previous experimental work from available literature on the effects of biodiesel dilution of engine oil.

A recent research done by Thornton et al. (Thornton, Alleman, Luecke, & McCormick, June, 2009) at the National Renewable Energy Laboratory evaluated the biodiesel fuel blend effect on oil dilution and associate engine performance. A 4 cylinder 2.15L high speed direct injection (HSDI) diesel engine was used as test cell and run by a 20% blend of soy-derived FAME with ultra low sulfur diesel fuel (ULSD). The base engine oil used for the study was CJ-4 oil. After the test run of the engine the engine oil was examined for the presence of FAME and viscosity. Total base number (TBN) and total acid number (TAN) was also determined. Along with engine oil analysis, bearing, piston and PRA were inspected for signs of excessive wear. The result showed that viscosity decreased with increased oil age and increased with fuel dilution. TBN of the engine oil decreased sharply with the increase of oil dilution while TAN increased slightly. Iron content in the oil also increased with the time. The researcher concluded that biodiesel in the engine oil caused oxidation which produced acid and a reduction in TBN. At

the end of test, the engine was disassembled and none of the moving components showed signs of excessive wear or other signs of deterioration.

Agarwal at el. (Agarwal, August, 2006) carried out a detailed investigation to assess the wear effect on engine using biodiesel fuel. They investigated the effects of long term engine operation on engine wear for a 20% blend of LOME (Linseed Oil Methyl Ester). In their research, an engine was run for 32 cycles, each of 16hr of continuous running and engine oil samples were collected after each 128hr of running. After the completion of the test, the engine was disassembled for physical inspection of the wear of moving parts. The results of the investigation, which are presented in Figure 27, 28, and 29, indicated that the lowering of engine oil viscosity was lower in case of biodiesel-fueled system as compared to that of diesel fuel system. Agarwal at el. concluded that for biodiesel fueled engine, oil dilution was lower than that of diesel fueled engine. The quantitative analysis in their research showed that an ash content, which mainly represents the wear debris, was found to be less for biodiesel fueled engine. By use of atomic absorption spectroscopy on the engine oil they found that biodiesel fuel led to lower amount of metallic debris such as Fe, Cu, Zn, Mg, Cr, Pb and Co. This metallic debris originated from various the moving parts of the engine. Figure 29 & 30 presents the amounts of metallic debris in engine oil for both biodiesel and diesel fueled engine. The physical investigation and oil analysis indicated that wear of the various vital parts reduced up to 30% because of the additional lubricity properties of biodiesel.

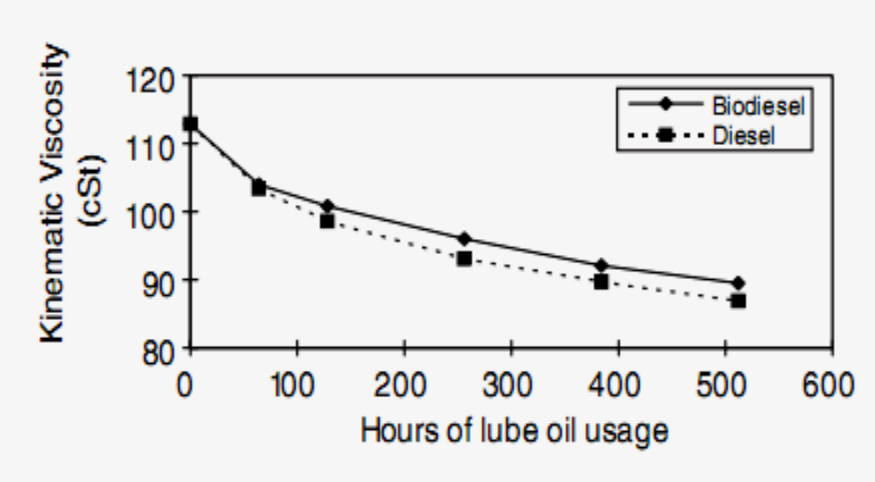

Figure 27: Kinematic Viscosity change of engine oil at 40˚C for B20 and Diesel Fuel. (Agarwal, August, 2006)

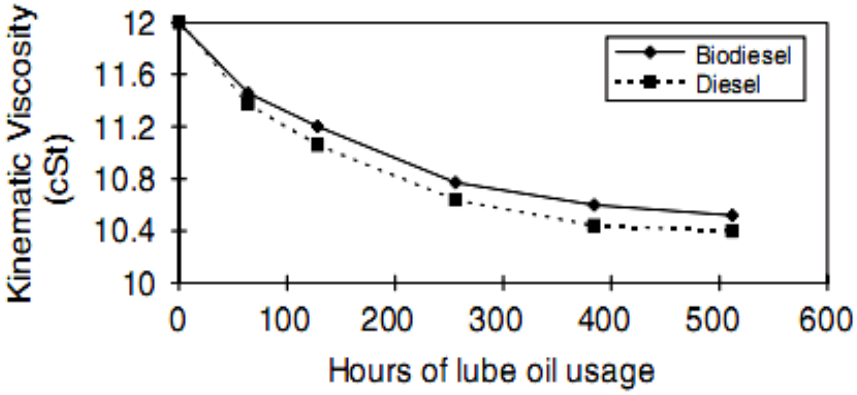

Figure 28: Kinematic Viscosity change of engine oil at 100˚C for B20 and Diesel Fuel. (Agarwal, August, 2006)

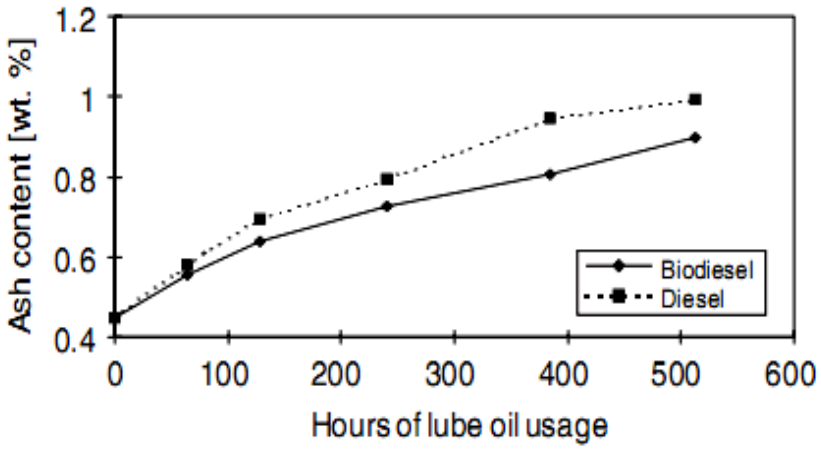

Figure 29: Ash content in the Engine oil for B20 and Diesel Fuel. (Agarwal, August, 2006)

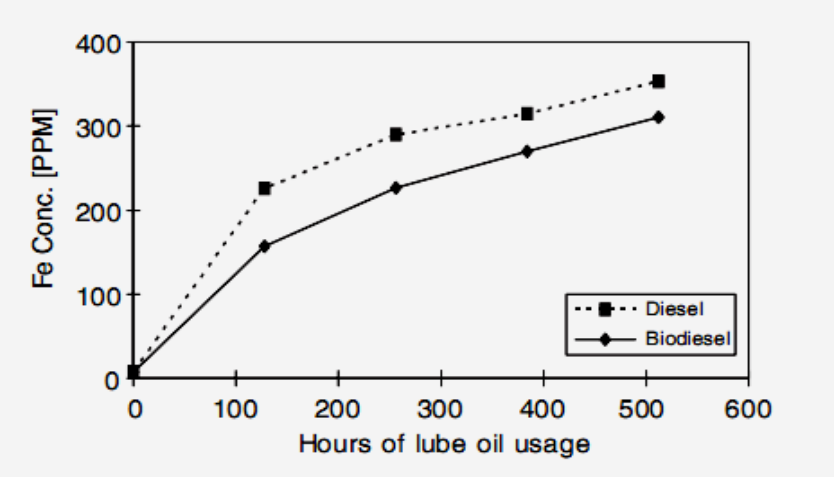

Figure 30: Iron content in the Engine oil for B20 and Diesel Fuel (Agarwal, August, 2006)

Fang and Yamaguchi (Fang, Whitacre, Yamaguchi, & Boons, 2007) carried out an extensive study on a biodiesel contaminated engine oil by Electrical Contact Resistant (ECR), High Frequency Reciprocating Rig(HFRR) and Four-ball test. Their research showed that partially oxidized biodiesel components competed with the typical oil anti-wear additives, mainly with ZDDP (Zinc Dialkyl Dithio Phosphate).They studied a complex formation between oxidized biodiesel component and the ZDDP with FTIR (Fourier Transform InfraRed spectrometer) and P-NMR (Phosphorous 31 Nuclear Magnetic Resonance) techniques. The

result of their study showed that FAME fuel dilution had a negative impact on engine oil performance when methyl esters partially degraded and interacted with the ZDDP anti-wear additives. Even though fresh biodiesel (Fresh methyl ester) may have some potential benefits for engine oil, such as higher intrinsic lubricity and acting as friction modifier. Based on the bench wear test and spectroscopic studies they concluded that engine oil dilution with the aged biodiesel increased wear up to concentration of 5% while fresh biodiesel actually decreased wear.

CHAPTER 3

METHODOLOGY

3.1 Introduction

This chapter presents experimental setup, instruments and data collections methodology. The details of main experimental instruments (pin-on-disk tribometer), its calibration process, and problems associated with data collections and the implemented solutions are discussed. Information about testing parameters, measuring process and measuring equipments are also provided.

3.2 Overview

The research work of this thesis intended to observe the effects of engine oil dilution with biodiesels from canola oil, soybean oil, peanut oil and chicken fat feedstock. Engine oil (15W 40) is diluted with known percentages of biodiesel from these four different feedstock and the changes of dynamic viscosity and lubricity performance of diluted engine oil are being observed. Lubricity is assessed in terms of the frictional force between metal surface contacts, under the diluted engine oil lubricating conditions with a pin-on-disk tribometer.

The effects of the biodiesel diluted engine oil are observed on AISI 1018 steel made rotating disk which is in contact with AISI 316 stainless steel ball. The steel disks are made from a 1” diameter round steel bar, cut by a horizontal lathe. A sequence of polishing stages with files, surface grinder and emery paper are applied on the steel disk to obtain a mirror like polished surface. This polished steel disk is subsequently cleaned in an ultrasonic cleaner bath with a standard cleaning solution. Cleaning procedure is described in section 3.8.

The pin-on-disk tribometer allows testing of friction contacts consisting of a rotating steel disk and a stationary ball, which is placed at the tip of a pin. A 316 stainless-steel bearing grade steel ball of 1/8'' diameter is used as ball material in this work. The relative velocity of the contact is set to 0.15m/s and the sliding distance to 1000m. For the duration of each test run, frictional force and temperature at the frictional joint are being observed. These data are collected with a data acquisition board and interfaced with Labview software for acquisition and storage in a computer. After each test run, steel disk surface is again cleaned, and the specific wear corresponding to the tested engine oil and biodiesel mixture is calculated by using Archard's formula.

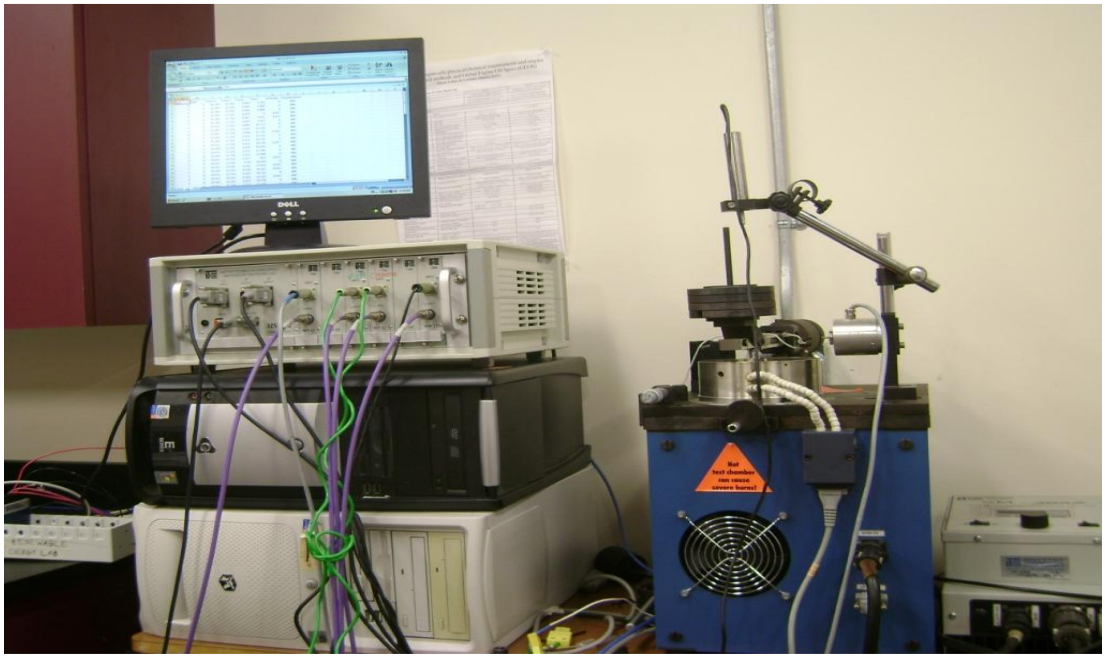

Figure 31: Employed experimental test setup of tribometer and dedicated data acquisition system

Figure 31 presents the experimental setup, which consists of a T-11 pin-on-disk machine, microprocessor aided pin-on-disk machine controller, a microprocessor aided squirrel-case motor

speed controller, data acquisition board and a computer, which is interfaced with both controller and data acquisition board.

3.3 Pin-On-Disk Tribometer

The employed pin-on-disk tribometer can be used to assess tribological properties of lubricants and the engineering materials used for the friction couple in sliding contact. This instrument is specially used to determine the wear factor, specific wear or wear resistance of the tested pair of materials in the presence of different type lubricants, sliding velocity and applied load. The tribometer used in this work is a T-11 pin-on- disk tribometer, designed and manufactured by the Institute for Sustainable Technologies, National Research Institute in Radom, Poland. This tribometer has two units, mechanical unit and measuring or control unit, which are described below.

3.3.1 Mechanical Unit of Pin-On-Disk Tribometer

The mechanical unit of pin-on-disk tribometer consists of the following assemblies:

- Body,
- Table,
- Driving unit,
- Friction couple loading unit,
- Specimens holding assemblies,
- Test chamber,
- Track radius changing mechanism,
- Force Transducer unit, and
- Displacement transducer unit.

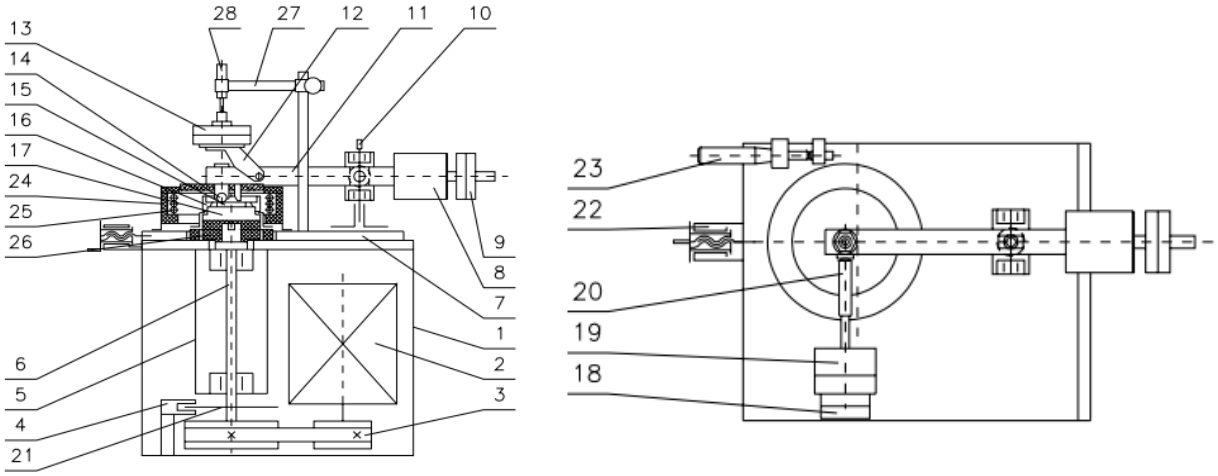

Front View

Top view

1	-	*body*	15	-	*disk*
2	-	*squirrel-cage motor*	16	-	*lock nut*
3	-	*synchronous belt transmission*	17	-	*keep plate*
4	-	*photoelectric speed sensor*	18	-	*force transducer bearer*
5	-	*test shaft tube*	19	-	*force transducer*
6	-	*test shaft*	20	-	*pusher*
7	-	*table*	21	-	*plate with indentations*
8	-	*movable counterweights*	22	-	*table sliding device*
9	-	*stationary counterweight*	23	-	*track radius setting device*
10	-	*lever shaft*	24	-	*test chamber*
11	-	*lever*	25	-	*heater*
12	-	*weight bearer*	26	-	*insulation sleeve*
13	-	*weights*	27	-	*displacement transducer unit*
14	-	*pin/ball*	28	-	*displacement transducer*

Figure 32: Schematics of T-11 Pin-on-disk Tribometer

(Tribology, 1994)

Figure 32 shows all the mechanical units. The main body of the instrument is case shaped and the table, driving unit and photoelectric speed sensor are mounted on the body. The table is able to slide and supports the friction couple unit, pin/ball holding assembly, force transducer unit and displacement transducer unit. The driving unit consists of a squirrel-case motor which is controlled by a sm-303A speed controller. The driving motor and test shaft are

connected with a synchronous belt transmission. The test shaft holds a plate on top and the steel disk is mounted on this plate.

In Figure 32, parts 8 to 13 are components of the friction couple load unit. The friction couple load unit enables free motions of the pin in the vertical and horizontal directions and the pin should be leveled prior to loading. This unit consists of a lever, bearing, lever shaft and horizontal axles. At the rear part of the lever, there is a stationary counterweight and at the front part of the lever, there is a weight bearer. The weights are placed on a pan to exert normal load on the friction couple.

The force transducer unit consists of a frictional force transducer bearer, a fixing plate and a pusher, which are shown in Figure 33. The transducer is mounted on the bearer and the stationary pin exerts force on the pusher while the disk is rotating against it. Therefore, the transducer senses the frictional force at the sliding contact.

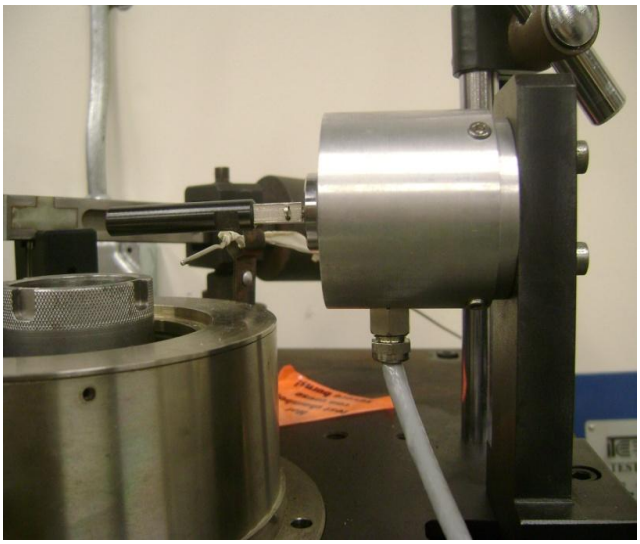

Figure 33: Friction force transducer

The pin holding assembly is located in the front part of the lever of the friction couple load unit. It consists of a holder, which is inserted into a sleeve and fixed by a nut. The disk holding assembly consisting of a keep plate, lock nut and spring ring as shown in Figure 34.

Figure 34: Components of the disk holding assembly

A displacement transducer unit is placed on top of the weight pan of the friction couple unit. This unit consists of a linear variable differential transducer (LVDT) which is held by a clamp and a fixing bolt. In Figure 32 (part 26 and 27) the displacement transducer unit is shown.

3.3.2 Measuring and Controlling Unit:

The Measuring and Controlling system consists of the following parts:

- MST-02 microprocessor aided controller,
- SM-303A motor speed controller,
- Transducers and sensors mounted on the machine, and
- T-11 software for interfacing with the computer.

Figure 35 presents and schematic of the control and data acquisition of the pin-on-disk tribometer, interconnections of working unit and flow of signals. Transducers mounted on the machine receive an analog voltage signal and transfers the voltage signals to the counter unit through a V/F (voltage to frequency) converter. The counter unit measures the frequency signals coming from V/F (voltage to frequency) converter. There is an optical speed sensor which is able to measures rotational speed of the motor shaft.

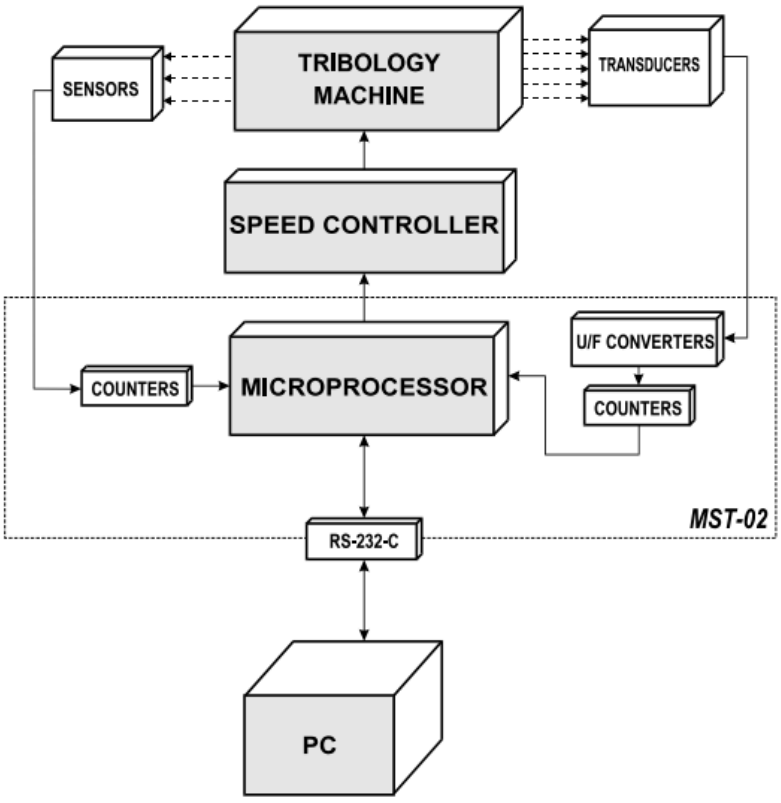

Figure 35: Functional block diagram of computer aided set of control and measurement unit in the pin-on-disk machine. (Tribology, 1994)

A control or data acquisition software (T-11 program) is used to communicate the hardware part of the tribometer with the microprocessor of the MST-02 controller. The SM-303A motor speed controller controls the speed of the motor in the instrument according to the value set in the computer via the microprocessor of the MST -02.

3.3.2.1 MST-02 Microprocessor Aided Controller

The MST-02 microprocessor aided controller controls the I/O (input and output) signals of the tribometer with the help of the T-11 program. It communicates with the computer through a RS-232/24v serial port at a 9600 baud rate. The T-11 program of the computer controls MST-02 and it also stores and convert acquired signals into numeric value. More details about the program will be discussed later in this chapter. Figure 36 presents the I/O (input output) panel of the MST-02 microcontroller.

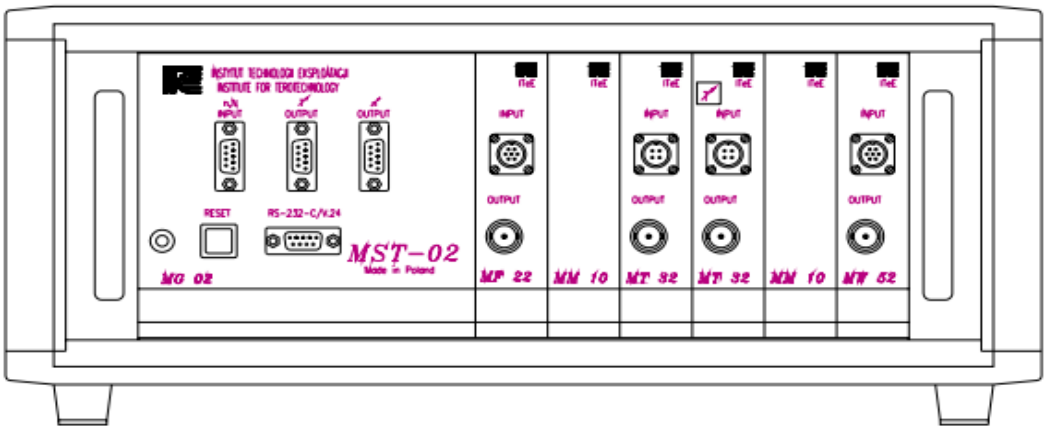

Figure 36: Front view of the MST-02 board (input output unit) (Tribology, 1994)

The MST-02 controller consists of the following unit:

(a) MG-02 Main Board Panel,

(b) MF 22 Board Panel,

(c) MT 32 Board Panel, and

(d) MW 52 Board panel

(a) MG-02 Main Board Panel:

It is an I/O (input output) and control board, which is an interface between computer and measuring boards of the MST-02. The force, temperature, and displacement transducers acquire inputs as analog voltage signals, and the MG-02 converts analog voltage signals into digital frequency signals. The frequency signals are communicated to the computer with a RS-232C serial interface through a DB-9 connector (D-Sub type connector which has 9 pins (for the male connector) or 9 holes (for the female connector)). The MG 02 main board is connected to the following channels output:

- The photo Electric speed sensor,
- The channels for temperature control,
- The SM-303A motor speed controller, and
- The Computer

The MG 02 main board also connects with the following panels through the internal bus (A system which connects all the internal components to the motherboard):

- MF 22 board panels (employed for force measurement)
- MT 32 board panels (employed temperature measurement)
- MW 52 board Panels (employed for vertical displacement measurement)

(b) MF 22 Board Panel:

The MF 22 board panel is designed to measure the frictional force. This panel amplifies and converts a voltage signal coming from a force transducer into frequency (digital) signals using TTL (transistor –transistor logic gate). The converted signals are transferred to the MG 02 main board through an internal bus, where they can be measured by the counters. The MF 22 board panel is connected to the force transducer through the input socket. The output socket of the MF 22, which presented in the Figure 36, provides an amplified voltage signal coming from the force transducer.

(c) MT 32 Board Panel:

This panel is able to measure the temperature. It is connected with the thermocouples by a connecting cable via an input socket. This board amplifies the voltage signals coming from the thermocouples and converts it into digital signals. Conversion of the voltage to frequency is performed by TTL (transistor –transistor logic gate). The frequency signal is further transferred to the MG 02 main board via an internal bus and it can be measured by the counter. The MST 02 contains two MT 32 boards, which are able to measures the temperature of two different thermocouples. There is an output socket in each of the MT 32 board panel. The amplified and conditioned voltage signals of the thermocouples feed out from that socket.

(d) MW 52 board Panels

The MW 52 board panel is designed to measure the vertical displacement of the friction couple. It is connected to the vertical displacement transducer (LVDT). This measurement was not considered in this thesis work.

3.3.2.2 SM-303A Motor Speed Controller

The SM-303A motor speed controller controls the squirrel-cage motor of the main instrument body. The main purpose of this controller is to convert the constant frequency (60 Hz) three phase voltages to a changeable frequency three phase voltage .The rotational speed of the motor is controlled by the changeable frequency or by the pulse width modulation (PWM). Speed change command can be set by a potentiometer knob of the SM-303A controller or by the computer through T-11 program. Motor speed controller is presented in Figure 37.

Figure 37: Motor speed controller

3.3.2.3 Transducers and Sensors Mounted on the Machine

The machine is mounted with three different transducers. They are:

- Frictional force transducer (strain gage),
- K type thermocouple, and
- Displacement transducer (This transducer output was not used in this thesis work)

Frictional force transducer

The transducer senses the tangential frictional force at the sliding contact. In this tribometer, a disk is rotating while its surface is scratched by a pin under a fixed loaded condition and tangential force exerts on the stationery pin. The transducer used in the tribometer is strain gage base transducer. The exerted forced is converted to electrical signal achieved by physical deformation of strain gage attached at the transducer and wired in Wheatstone bridge configuration.

3.3.2.3 T-11 Software and Associated Incompatibility with Available Computer

The T-11 software was written using the Turbo Pascal 6 programming language. This program was primarily written for DOS operating system with 286, 386 or 486 type microprocessor, whose internal clock frequency (speed) must be less than 40 MHz. In this thesis work a Pentium 4 microprocessor and windows XP operating system based computer were used, as the recommended type microprocessor and operating system is obsolete. The internal clock frequency (speed) of the computer used with the tribometer machine is 800 MHz, which is 20 times faster than that of recommended speed. This mismatch causes data or memory over flow during the long experiment duration and T-11 program is crashed. Because of this, the experimental data in this thesis is collected and stored with a separate data acquisition system, which is presented later in this chapter. In the research work of thesis, the T-11 program is only used for the operation of the motor speed controller and for start of the main instrument (pin-on-disk tribometer).

3.4 Modifications of the Pin-On-Disk Tribometer

The reason of software crash of the T-11 program was explained in section 3.3.2.3. To solve this problem a separate data acquisition system was introduced to collect the signals from

friction force transducer and from thermocouples. This data acquisition system was interfaced with the computer via Labview program. A new optical speed sensor was installed due to faulty operation of the previous one.

3.4.1 New Optical Sensor Installation

The optical sensor of the instrument was not working and it was replaced. Figure 38 describes the working principle of the optical sensor. The new optical sensor has different size than that of the OME (original machine equipment). Therefore, a new holder was machined to hold the new sensor. The pictures of optical sensor and holder are shown in the Figure 39.

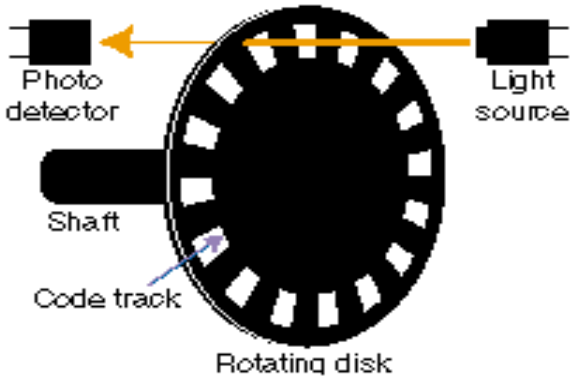

Figure 38: Basic working principle optical sensor (Quadrature Encoder Measurements)

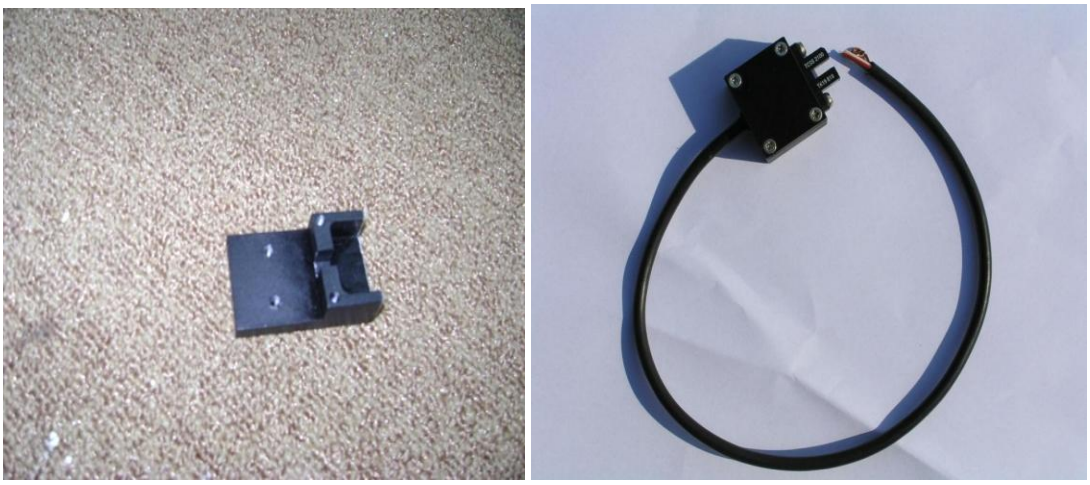

(a) (b)

Figure 39: (a) Optical sensor and (b) Its holder

3.4.2 Data Acquisition System

A new additional data acquisition system was set to acquire signals from friction force transducer and thermocouple used in the instrument. The data acquisition system consists of two NI (National Instruments) modules (NI 9205 and NI 9211) and a legacy chassis NI cDAQ 9171. Figure 40 presents a picture of the modules and Figure 41 presents a picture of the chassis.

The National Instruments 9205 is a C Series module. The NI 9205 is featured with 32 single-ended or 16 differential analog inputs, 16-bit resolution, and a maximum sampling rate (how frequently the analog signal is measured) of 250 kS/s. It has 36-position spring terminal connector for direct connection. Each channel has programmable input ranges of ±200 mV, ±1, ±5, and ±10 V. In this work the ±1V range is used. This module is compatible with the windows operating system and is able to acquire data in real time. Frictional force signal is acquire by this module. The output socket signal of MF 22 board panel is used as the input signal of the module. Out of the 16 differential input channels one channel is in use (+ a_2 and -a_2).This module able to take both the single ended input and differential ended inputs. In this work the differential inputs

are used, where two signal wires coming from each signal sources to the module, one of them goes to the positive input and the other one to the negative input.

The National Instruments NI 9211 thermocouple input module is used to acquire the thermocouple signals. It has 4 differential input channels, 24 bit resolution and 14S/s of sampling rate. This module is able to acquire and decode the thermocouple signals with high-accuracy. This module conditions the signals from two k-type thermocouples, read their signals in mVolts and representing in ^{0}C.

The NI cDAQ-9172 is an eight-slot NI (National Instruments) compact DAQ chassis which can hold up to eight C Series I/O modules. It is connected to the PC with the high speed USB (Universal Serial Bus) port. The NI cDAQ-9172 has two 32-bit counter or timer chips, which are built into the chassis. Module NI 9211 is used for measuring frictional force and module NI 9205 is employed for measuring temperature and both the modules are integrated with the NI cDAQ 9172. Because of this integration, both modules can act as a single device and can outputs all of the collected data through the same bus interface, and it making the Labview programming easier.

3.4.2.1 Labview Program for DAQ System

The NI module and chassis are interfaced with the computer through LabView 2009. The programming language used in LabView (Laboratory Virtual Instrumentation Engineering Workbench) is also referred as G, which is a dataflow type programming language. LabView programs are called virtual instruments (VIs). Each VI has two components: a block diagram and a front panel. During the program run, indicators on the front panel allow monitoring the acquired data.

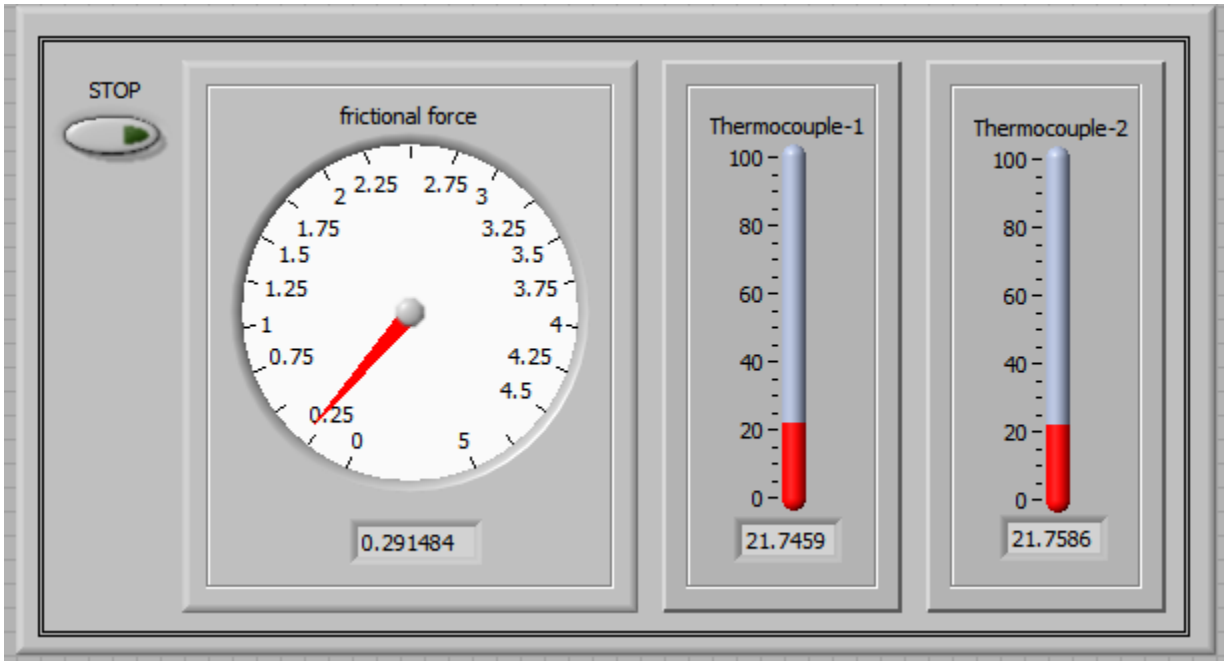

Figure 40: Front panel of the developed LabView VI

The Figure 40 presents the front panel of the LabView program written for this thesis work. The front panel shows the change of frictional force, temperature change of "thermocouple-1"(Inside the hollow pin which holds the ball at its tip) and "thermocouple-2" (temperature change of the friction joint).

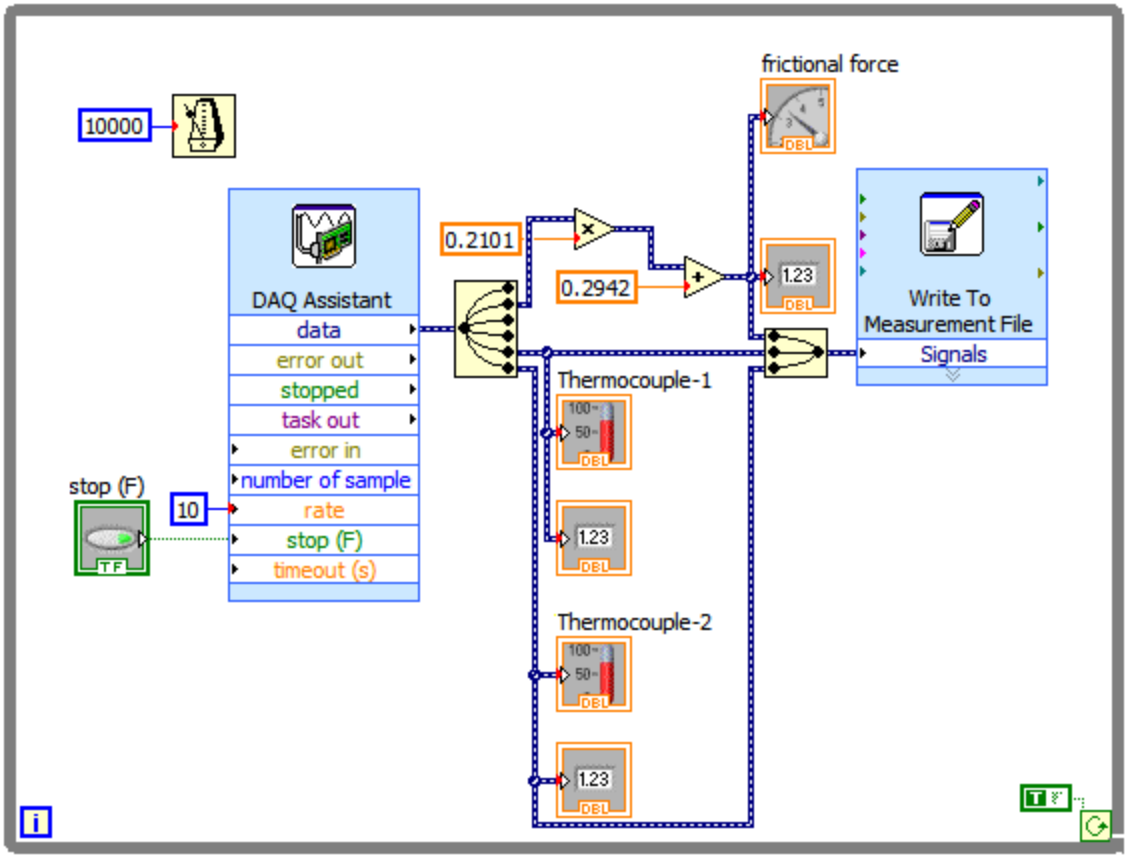

Figure 41: Control panel of the developed LabView VI

Three sets of data (Frictional force, and two k- type thermocouples signal) are taken by the DAQ assistant in the LabView program and are shown in the control panel of VI, presented in Figure 41. For the frictional force signal, data acquisition system reads the change in voltage difference and converts it into kilogram force using the correlation.

$$y=0.2101*x+0.2942$$

Where, y = friction force in kilogram, and

x= friction force signal in mVolt

This correlation was derived from the transducer calibration and it was inserted it in the program to obtain the actual frictional force (in kilogram force) measurements. The NI9211 that

is used for the thermocouple is able to perform the conversion of the voltage signals into temperature. Therefore, no temperature correlation is needed in the LabView program. The program writes the three data pieces into an Excel file at the specified location in the computer, which is set by the program. The front panel also shows the change of data after each 10,000 mseconds or 10 seconds and writes 10 pieces of data per second in the file. After each run (test run duration was 6,700 seconds) this program stores a data file of 67,000 data points. The program can be stopped at anytime by clicking the "stop" button in the front panel.

3.5 Pin-On-Disk Tribometer Calibration

Before using the tribometer each of the sensors and transducers needs to be calibrated. The MST-02 controller and SM 303A speed controller do not need calibration as they are relying on factory settings. The T-11 program calibration command consists of the following menu options:

- Frictional force calibration,
- Rotational speed calibration,
- Pin/ball temperature calibration,
- Chamber temperature calibration, and
- Displacement calibration.

Displacement sensors output is not used in this thesis work and the thermocouple signals are alternatively conditioned and measured by the NI9205 module. The frictional force transducers signals are conditioned by the MST 02 controller but measured by NI 9211 module. For these reasons, frictional force transducer and rotational speed of the motor are calibrated through the T-11 program.

3.5.1 Frictional Force Calibration

The frictional force transducer must be unscrewed from the main body of the machine for its calibration. The pusher rod is also removed and the transducer is placed on a flat surface for calibration. A calibration pan of weight is 0.093 gm was placed on the transducer according to Figure 42. The load was gradually applied on the calibration pan ranged in a range of 0 to 5 kg. When the frictional force calibration option is chosen in the calibration menu, the dialog box presented in Figure 43 appears and the applied load must be correctly entered in the dialog box presented in Figure 44. Once the calibration was completed, the plot of Figure 45 was displayed on the computer screen. This plot was an indication of correct calibration of the frictional force transducer.

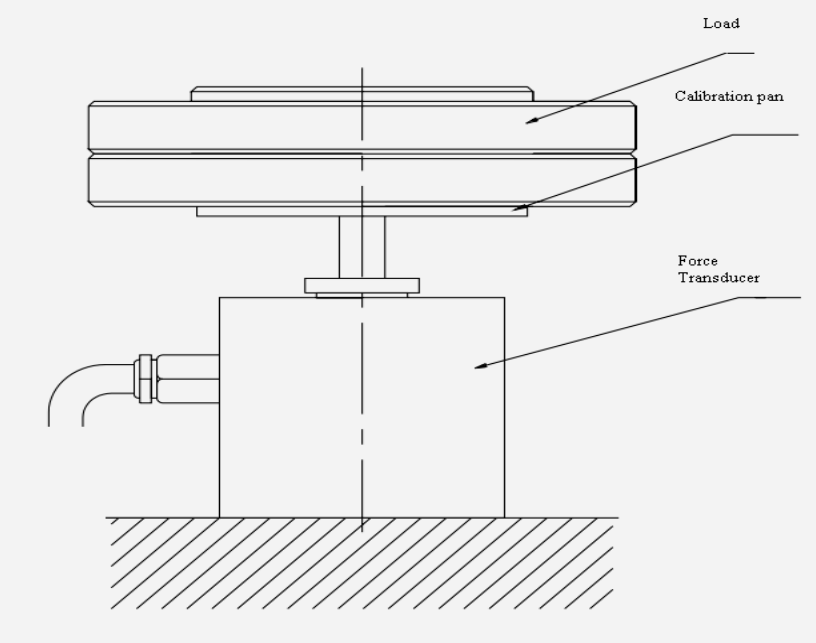

Figure 42: Schematic of the calibration of frictional force transducer

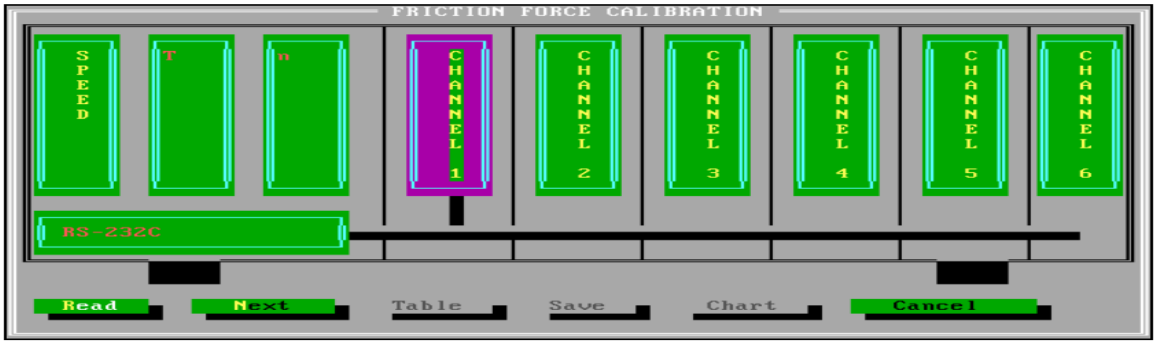

Figure 43: Frictional force calibration dialog box in T-11 program (Tribology, 1994)

Figure 44: Dialog box of entering current load value for frictional force calibration with T-11 program. (Tribology, 1994)

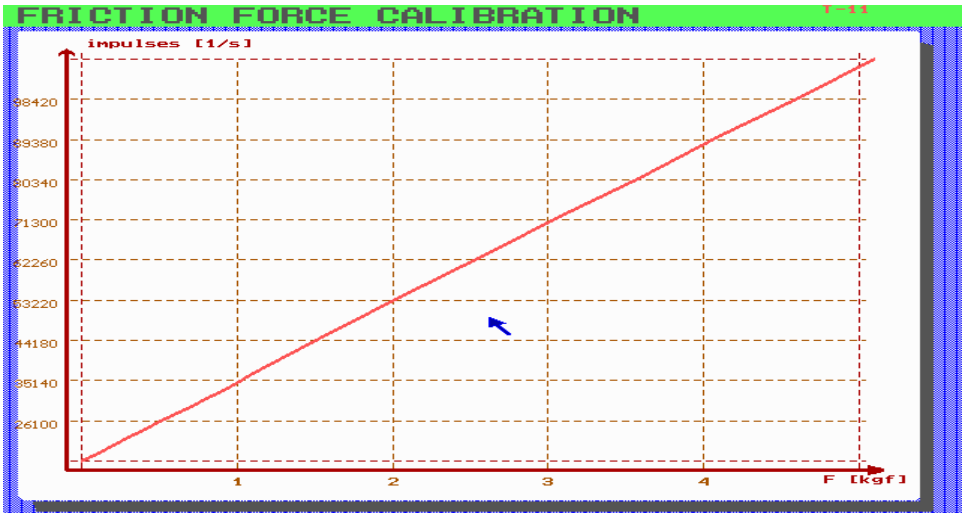

Figure 45: Correct frictional force calibration characteristic obtained by T-11 program. (Tribology, 1994)

3.5.2 Rotational Speed Calibration

The rotational speed calibration is carried out automatically by the T-11 program when the rotational speed calibration command is chosen from the calibration menu of the T-11 program. In this automatic calibration process, rotational speed is changed from lowest (0 rps) to highest value (16 rps) and the instant speed (rps) appears in the dialog box like Figure 46. Before starting the rotational speed calibration, the SM 303A speed controller was set in start mode. After a successful calibration, a characteristic plot as that of Figure 47 appears on the screen, and it is the indication of correct performance of optical speed sensors and the motor.

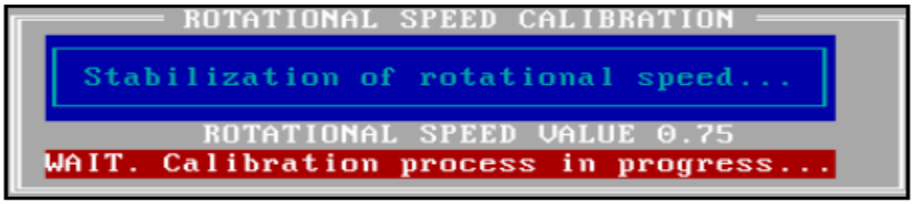

Figure 46: Calibration progress window in T-11 program (Tribology, 1994)

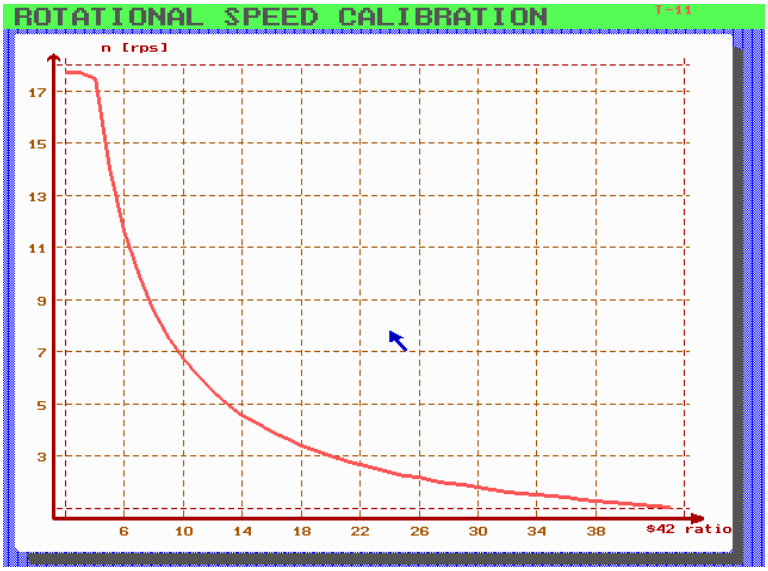

Figure 47: Rotational speed characteristic of the motor during calibration using T-11 program. (Tribology, 1994)

3.6 Disk and Ball Materials of the Tested Friction Couple

The ASTM G 99 standard describes the test method for wear testing with a pin-on-disk (tribometer) apparatus. According to this standard, significant wear can be assumed either in disk material and/or in the ball material and the pair of ball and disk materials should be chosen according this assumption. AISI 1018 is a low carbon steel and has a better machinability characteristic than high carbon ones. Machinability properties are important characteristic in this

thesis work, as disks are made from 1" diameter round bar through several steps. The density of AISI 1018 is 7.87g/cm^3 and its hardness (in Rockwell B scale) is 71. The 316 stainless-steel is the standard molybdenum-bearing grade austenitic stainless steels and its density is 8.00 g/cm^3 and its hardness (in Rockwell B scale) is 95.

In this thesis work, it is assumed that significant wear would happen only for the disk material. AISI 1018 steel is used as disk material and bearing grade 316 stainless-steel is used as the ball material, the latter being much harder than the disk material. In summary because of typical hardness of the materials, the assumption is made that the wear happens on the softer surface of the AISI 1018 steel disk.

3.7 Disk Cutting and Polishing Process

The tribological experiments with the pin-on-disk tribometer are carried out on a 25.4 mm (1") diameter disk, with a width 6 ±1 mm. This disk is made from the 1" diameter round bar by a standard parting operation with a horizontal lathe machine. This process yields a disk with unfinished rough surface. This rough disk is polished in a sequence with files, grinding wheels and finally with emery paper to obtain a mirror like polished surface. The detail of disk polishing process will be discussed elaborately in Appendix C

3.8 Surface Cleaning Process

After polishing, the disk surface was cleaned in ultrasonic bath. A Cole-Parmer 8848 ultrasonic cleaner was used for the ultrasonic cleaning of the disk. The employed ultrasonic cleaner is presented in the Figure 48.

Figure 48: Ultrasonic bath of the disk with indirect method

Surface cleaning is critical before and after each test run according to ASTM G99 test standard. Before each of the experiments, the disk was cleaned in ultrasonic bath for 20 minutes with Cole-Parmer Micro-90 Cleaning Solution. Cole-Parmer Micro-90 Cleaning Solution removes oil, grease, wax, particulates, stains and biological debris from the metal disk surface. Indirect method for ultrasonic cleaning was used in cleaning the disk, which means the disk is not placed inside the ultrasonic cleaner directly. The tray inside the ultrasonic cleaner is filled with water. A beaker is filled with warm water and Cole-Parmer Micro-90 Cleaning Solution in a volume ratio of 50:1. The disk is placed inside the beaker.

The surface cleaning process is repeated after the completion of test run in order to obtain an accurate weight of metal removed from the disk surface due to wear. This wear estimation operation is described in the chapter 4.

3.9 Biodiesel and Engine Oil Used in this Thesis Work

The US Army, Navy, Air Force and Marines all use standard B20, a mixture of 20% biodiesel and 80% diesel throughout the country (National Biodiesel Board , 2003). A recent report reveals the military efforts to use sustainable biofuels across all their operations (Military Biofuel Applications, 2010). 15W 40 engine oil is one of the military's widely used lubricating oils (Masoner, Erck, & Ajayi, 2009) and this was the reason to choose 15w 40 as the test lubricating or engine oil in this work.

Biodiesel from different feedstock contains different types and fractions of fatty acid. Therefore, biodiesel dilution effects on the performance of engine oil (15w 40) may vary based upon the employed biodiesel feedstock. In this thesis work, biodiesel from four types feedstock is used, three of them are from vegetable feedstock (canola, peanut and soybean oil biodiesel) and one of them is from animal source (chicken fat biodiesel).

15W-40 mineral oil is a heavy duty engine oil, and it is primarily recommended for use in winter climate where temperatures never fall below 15^0 F (-9^0 C). (Dixon, 2008). In this work partially synthetic SAE 15W 40 Mobil engine oil is used, with a 30% synthetic base stock. This engine oil satisfies the SAE 40 viscosity grade. Table 5 presents the typical properties of the employed 15W-40 engine oil.

Table 5
Typical properties of 15W-40 mineral oil

SAE Grade	15W-40
Viscosity, ASTM D 445 cSt @ 40ºC cSt @ 100ºC	 111 15.2
Viscosity Index, ASTM D 2270	140
Sulfated Ash, wt%, ASTM D 874	0.9
Total Base Number, mg KOH/g, ASTM D 2896	10.7
Pour Point, ºC, ASTM D 97	-36
Flash Point, ºC, ASTM D 92	241
Density @15 ºC kg/l, ASMT D 4052	0.872

(Mobil Delvac Elite 15W-40)

Chicken Fat Biodiesel (CFB):

Animal fats are attractive feedstock for biodiesel because they may cost less than vegetable oil. Animal fat feedstock can be made into a high-quality biodiesel which meets the ASTM specifications for biodiesel. Animal fats are highly saturated and solidify at a relatively high temperature; this allows the use of animal fat biodiesel in warm climates. The saturated fatty acids in animal fats should contribute to better oxidative stability for biodiesel (Stuckey, 1972). The fatty acid types are defined by the number of carbon atoms and the number of double bonds in the molecule. Animal fats contain very little polyunsaturated fatty acids, such as linoleic acid and linolenic acid, which are responsible for chemical decomposition of fat. In this work, animal fat biodiesel from chicken fat feedstock is used, collected from “Down To Earth Energy” company, a biodiesel producer in Georgia. Table 6 presents the different fatty acids percentage of chicken fat.

Table 6

Fatty acid percentages in chicken fats

Fatty acid	Percentage (%)
Myristic acid 14:0	1
Palmitic acid16:0	25
Palmitoleic acid 16:1	8
Stearic acid 18:0	6
Oleic acid 18:1	41
Linoleic acid 18:2	18

(Gerpen, 2010)

Vegetable Feedstock Biodiesel:

In this thesis, biodiesels employed are from three type's vegetable feedstock: canola, soybean and peanut oil are used. These biodiesels are produced in the Renewable Energy Lab of the Dept. of Electrical and Mechanical Engineering of Georgia Southern University. Table 7 presents general fatty acid components of vegetable oil feedstock. The Renewable Energy Lab produced these biodiesel from canola, soybean and peanut oil according to the ASTM standard. Table 8 presents a comparative fatty acid percentage of all the four different feedstock used in this work.

Table 7
Fatty acid percentages in typical vegetable fat

Fatty acid	Percentage (%)
Palmitic acid 16:0	15
Palmitoleic acid 16:1	8
Stearic acid 18:0	5
Oleic acid 18:1	25-30
Linoleic acid 18:2	45-50

(chemicalland21, 2008)

Table 8
Fatty acid percentages in different feedstock

Fatty acid	Chicken fat (%)	Soybean oil (%)	Peanut oil (%)	Canola oil (%)
Palmitic acid 16:0	25	6-10	8-9	ND(no data)
Stearic acid 18:0	6	2-5	2-3	7
Oleic acid 18:1	41	20-30	50-65	54
Linoleic acid 18:2	18	50-60	20-30	30
Linolenic acid 18:3	ND	5-11	ND	7

(Rick, 2010)

3.11 Preparation of Biodiesel Diluted Engine Oil

In this work, the employed engine oil (15W 40) was diluted by the four different source of biodiesel (e.g. peanut oil, Canola oil, Soybean oil and Chicken Fat). Engine oil dilutions by

the biodiesel were prepared for four different percentage, they were 5%, 10%, 20% and 30%. A total 40ml mixture of engine oil and biodiesel was prepared for each of the percentages mixtures of biodiesel. The volume fraction of engine oil and biodiesel oil was changed according to the percentage in each 40 ml mixture. For 5% diluted engine oil, 38ml of engine oil and 2ml of biodiesel were mixed together. For 10% diluted engine oil, 36ml of engine oil and 4 ml of biodiesel were mixed together. For 20% diluted engine oil, 32ml of engine oil and 8 ml of biodiesel were mixed together. For 30% diluted engine oil, 28ml of engine oil and 12 ml of biodiesel were mixed together. To maintain the exact volumes of engine oil and biodiesel in the mixture, a micropipette (United Scientific Supplies, Inc.) was used, with a 1-1000µl oil capacity with 98.9% accuracy. After making the mixtures of engine oil and the biodiesel, a magnetic stirrer was used for the homogeneous mixing of engine oil and biodiesel. Figure 49 presents picture of the volume measurements of oil by micropipette and of the magnetic stirrer.

(a) (b)

Figure 49: (a) Volume measurements of oil by micropipette. (b) Magnetic stirrer for making homogeneous mixture of engine oil and biodiesels.

3.12 Viscosity Measurement

Viscosity of the engine oil is an important characteristic of engine oils in engineering applications. The dynamic viscosity of the diluted engine oil was measured with a Brookfield Rotational Viscometers. This instrument measures the shearing stress on a spindle rotating at a constant speed while it is immersed in the sample oil. The degree of spindle lag is indicated on a rotating dial. This reading multiplied by a conversion factor, which is based on spindle size and rotational speed, gives a value for viscosity in centipoises. The LCD display of the viscometer shows dynamic viscosity reading of centipoises (cp) or milipascal seconds (mPaS), as well as percent of torque, and speed.

After each of the experiments a mixture of engine oil and biodiesel is remains on the surface of the disk. The amount of this leftover oil is very small to be measured the viscosity with the available viscometer. Because of this problem an alternate method was followed in this research work. After each test run the disk with the leftover oil was dipped in the corresponding 40ml mixture of engine oil and biodiesel and the viscosity was measured.

Viscosity of mixture after test run:

It is assumed that both the engine oil and the biodiesels are organic substance. When two organic solution of different viscosity mixed together, following relationship is exist (Kern, 1965).

$$\frac{1}{U} = \frac{W1}{U1} + \frac{W2}{U2}$$

Where,

U = Viscosity of the mixture of leftover (used) diluted engine oil on the disk (after test run) and the diluted engine oil(fresh)

U_1 = Viscosity of biodiesel diluted engine oil (fresh)

W_1 = Weight fraction of diluted engine oil (fresh)

U_2 = Viscosity of leftover (used) diluted engine oil on the disk (after test run)

W_2 = Weight fraction of leftover (used) diluted engine oil on the disk (after test run)

For this thesis work, it is assumed

$W_1 = 0.999$

$W_2 = 0.001$

3.13 Specific Wear Calculation

Sliding wear is commonly treated in terms of material loss, which is a function of hardness of the material, sliding distance and normal load applied on the object. Frictional coefficient (or frictional force) between the sliding components, which is also related to the lubricity of lubricant, may greatly affect the wear rate. In this work, the dimensional wear coefficient or specific wear is calculated with Archard's Equation:

$$W_s = \frac{V}{FL}$$

Where,

W_s = specific wear (in mm^3/Nm)

V= wear volume (in mm^3)

In this work,

$$V = \frac{m * 1000}{\rho}$$

m= mass loss (in grams)

ρ=density (in g/cm^3)

For AISI 1018 steel,

$\rho = 7.87 g/cm^3$

Specific wear can be varies, depending upon contact material, load, environment and lubricants (Kholi & Mittal, 2008). As contacted material, load and environment are kept unchanged, specific wear can be correlated with the lubricants (i.e. biodiesel diluted engine oil).

CHAPTER 4

RESULTS AND DISCUSSIONS

4.1 Introduction

In this chapter, the experimental results are presented of the lubricity testing of biodiesel diluted engine oil, of the dilution effects on the viscosity properties of mixture and of the surface interactions of biodiesel diluted engine oil at the frictional surfaces. Specific wear for the different feedstock-diluted engine oils are also presented and the observations of temperature change at the frictional joint are also included.

4.2 Experimental Results of Biodiesel Diluted Engine Oil

Lube oil or engine oil is required to maintain a high viscosity index, a good thermal and oxidative stability and a good lubricity. The overall lubricity quality of the oil should control the wear rate and frictional force between the moving surfaces. In this work wear rate, frictional force, viscosity changes are measured, and oxidative stability are observed to evaluate the lubricity of the biodiesel diluted engine oils. Each experiment is conducted under the following constant test -controlled parameters:

Relative sliding velocity of disk and ball = 0.15m/s,

Total sliding distance = 1 km,

Duration of each experiment = 6667 seconds or 1 Hr 52 minutes,

Normal load applied on the ball = 2kg or 19.62N,

Room temperature = 17^0 C to 19^0C,

Relative humidity = 55% -60% (Data according to Physical Plant of GSU), and

Surface roughness of steel disk = Maintained between 1μin to 10μin (presented in Appendix C)

4.2.1 Canola Oil Biodiesel Diluted Engine Oil

Canola oil biodiesel (COB) is made from vegetable feedstock. Its major fatty acid components are stearic acid (7-9%), oleic acid (54%), linoleic acid (30%) and linolenic (7%).The engine oil was diluted with the canola oil biodiesel at 5%, 10%, 20% and 30%. The effect of dilution on the dynamic viscosity change of the freshly prepared diluted engine oil was observed. Along with this, viscosity change of this diluted engine oil after the experiment also was determined. Dynamic viscosity measurement was carried out at 24^0C. Figure 50 presents the measured change of dynamic viscosity for the tested percentages of oil dilutions when they were freshly prepared. The relation between the diluted engine oil viscosity and the percentage of canola oil biodiesel in the engine oil (EO) fits a quadratic adjustment, which is presented below.

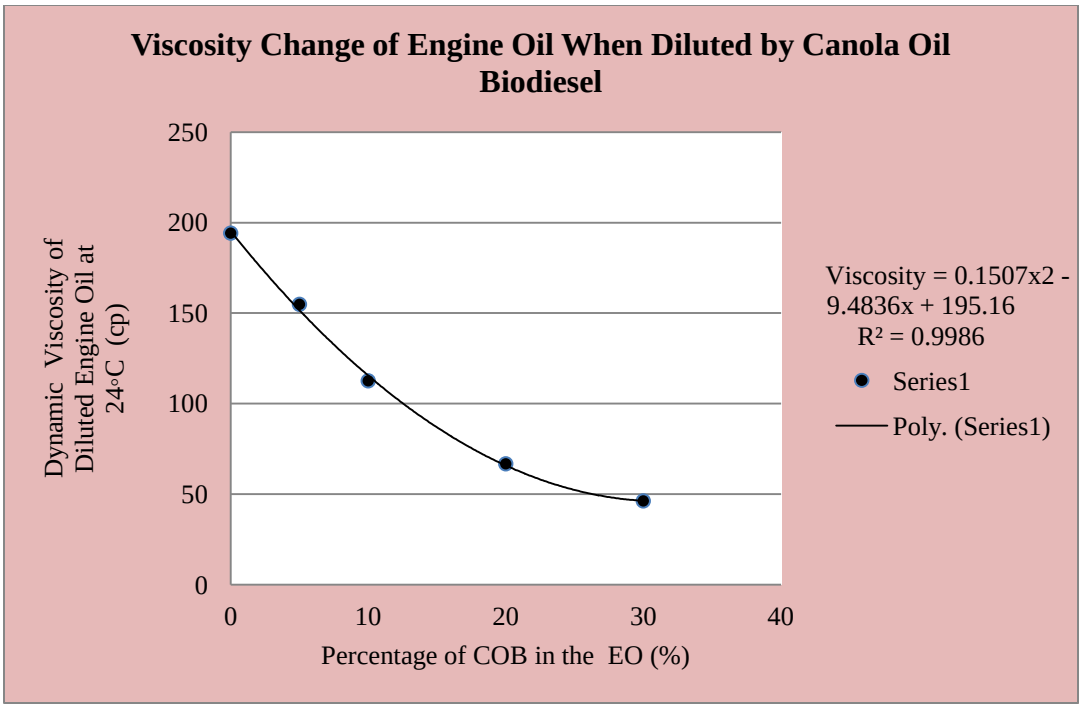

Figure 50: Viscosity change of EO when diluted by COB

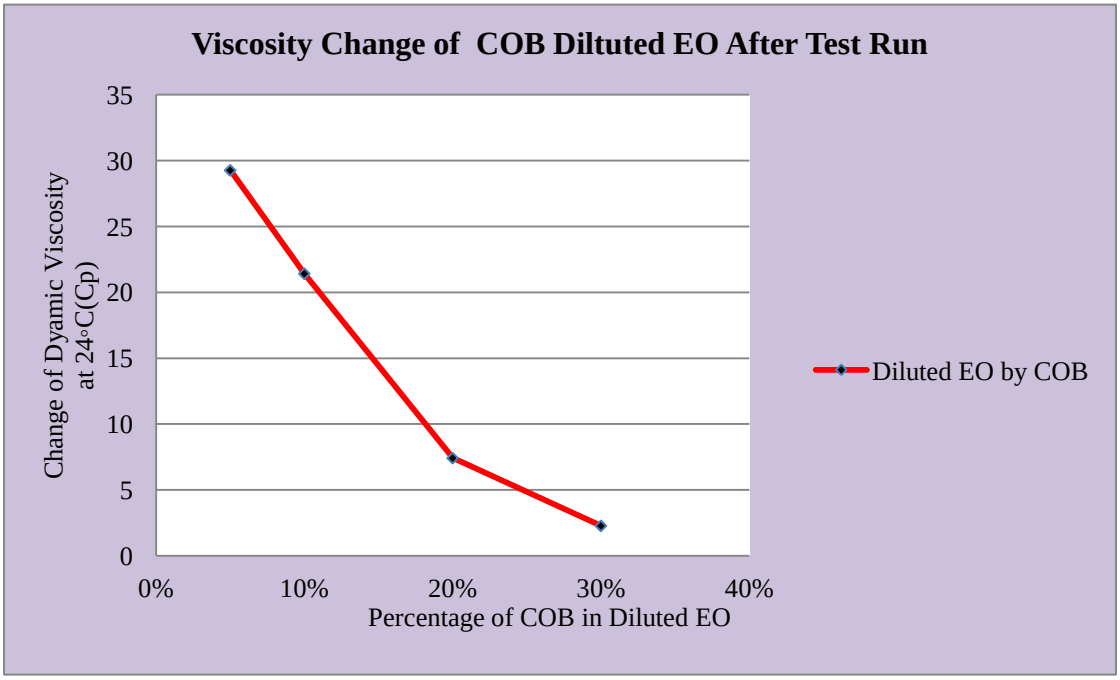

Figure 51: Viscosity change of COB diluted EO after the experiment.

Figure 51 presents the dynamic viscosity change of the diluted EO after the experiments. It shows that increasing percentages COB, the dynamic viscosity sharply decreased, which is not desirable in a good lubricant. This may happen due to local heat generation due to friction and the tribo-chemical reactions of the COB components under friction

Specific wear was measured for the different dilution percentages of engine oil by CBO (canola oil biodiesel), as presented in Figure 52. The 0% dilution represents the pure engine oil (EO). The plot shows that for the 10 % dilution the measured specific wear was the lowest, and that for the 20% dilution measured specific wear was the highest. This observed result could be because of the interactions with the engine oil anti-wear additives ZDDP (Zinc Dialkyl Dithio Phosphate), which usually bonds to the metallic surfaces to form a protective layer against wear. The polar components in biodiesel (e.g. fatty acid methyl ester), may also attracts the ZDDP molecules. Therefore, when ZDDP is not fully attracted to the surface or is less available to give protection to surface, wear rates may increase.

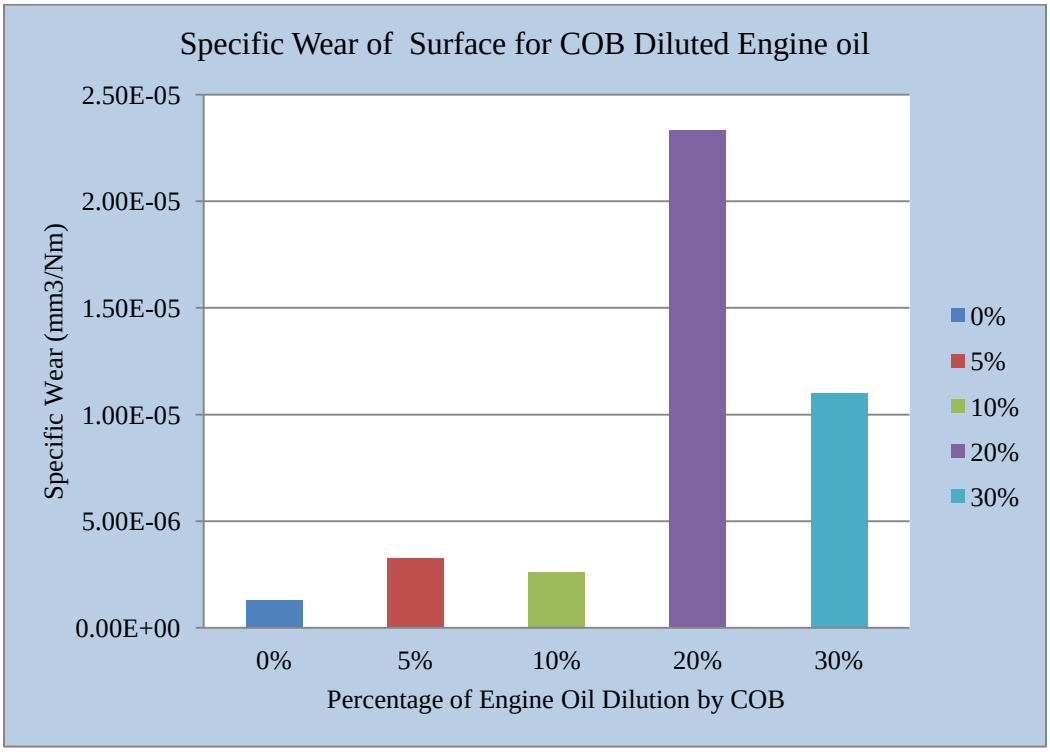

Figure 52: Specific wear amount of the surface in presence of COB diluted EO.

The in-process friction force between the contact surfaces is presented in Figure 53 which shows that friction force remained stable and the COB (Canola Oil Biodiesel) diluted engine oil (EO) seemed able to provide an antifriction layer on the surface. For all the four dilution percentages, frictional force did not significantly increased during test time. This means that no lubrication failure occurred in the 1 km sliding contact (or in equivalent 1 hour 51 minutes, or 6667 sec). But for all tested four dilution percentages it takes about 1,000 second to build up an adequate friction reducing layer on the surface. Figure 54 presents the variation of average friction force during the test for different dilution percentages. After testing with COB diluted engine oil for the four dilution percentage, an oxidized layer of oil was observed as left on the surface which is presents in Figure 55 and this phenomenon was observed for all the four tested percentages; it may be an indication of some reduced oxidative stability of engine oil when it is diluted by COB.

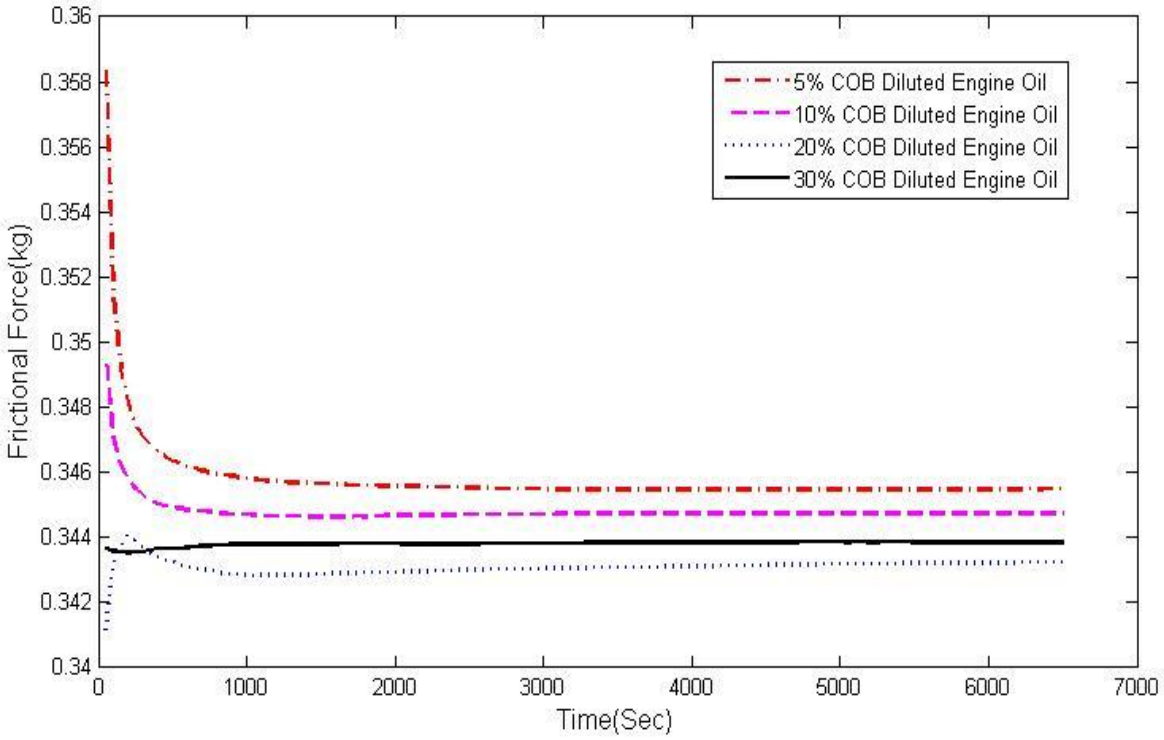

Figure 53: In process friction force with the time for COB diluted EO

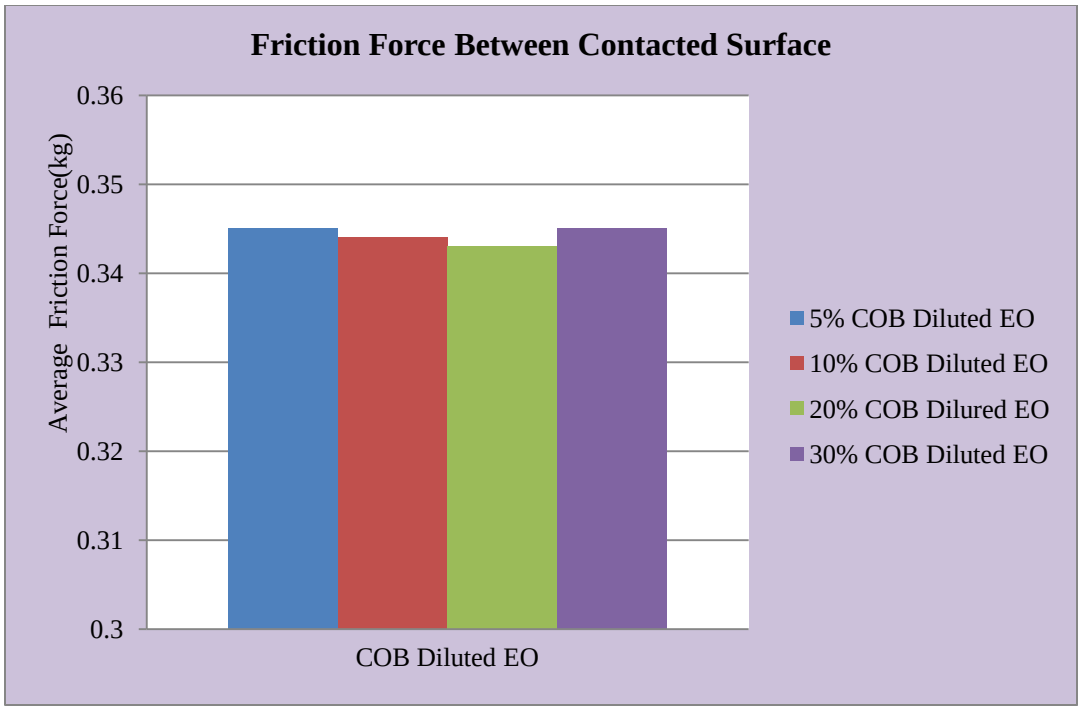

Figure 54: Average friction force between the contacted surfaces for COB diluted EO.

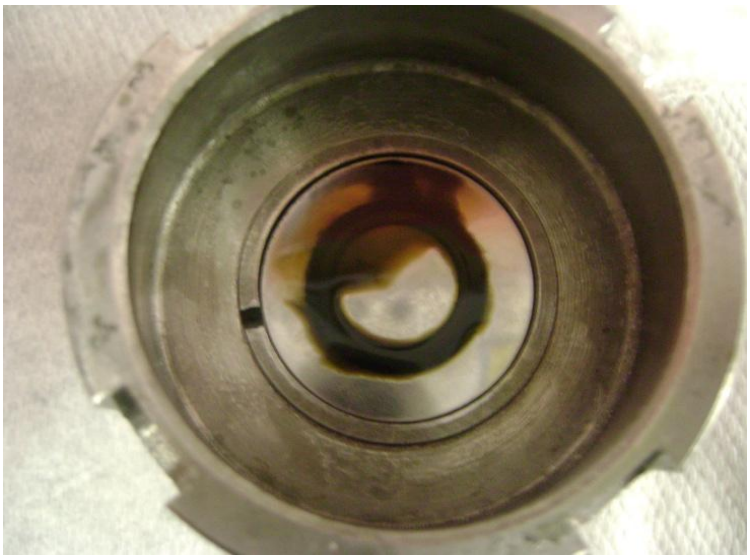

Figure 55: The left over oxidized oil after a test run with a typical COB diluted EO.

4.2.2 Peanut Oil Biodiesel Diluted Engine Oil

Peanut oil Biodiesel (POB) is another promising vegetable feedstock for biodiesel. Its major fatty acid components are palmitic acid (8-9%), oleic acid (50-65%), and linoleic acid (30-40%). This oil also contains some 6-8% (total) of arachidic acid, arachidonic acid, behenic acid, lignoceric acid and smaller amount of other fatty acids. The engine oil (EO) is diluted with the peanut oil biodiesel (POB) at 5%, 10%, 20% and 30%. Figure 56 presents the change of dynamic viscosity with these percentages of engine oil (EO) dilution. The relation between the diluted engine oil viscosity and the percentage of peanut oil biodiesel (POB) in the engine oil (EO) fits a quadratic adjustment as presented in the Figure 56. Figure 57 presents the dynamic viscosity change of the diluted EO after the tests.

Figure 58 shows the specific wear at the tested surfaces for the different dilution percentages of engine oil by POB. This plot indicates that at a 10% dilution of EO (engine oil) the measured specific wear amount is the lowest for the tested interval.

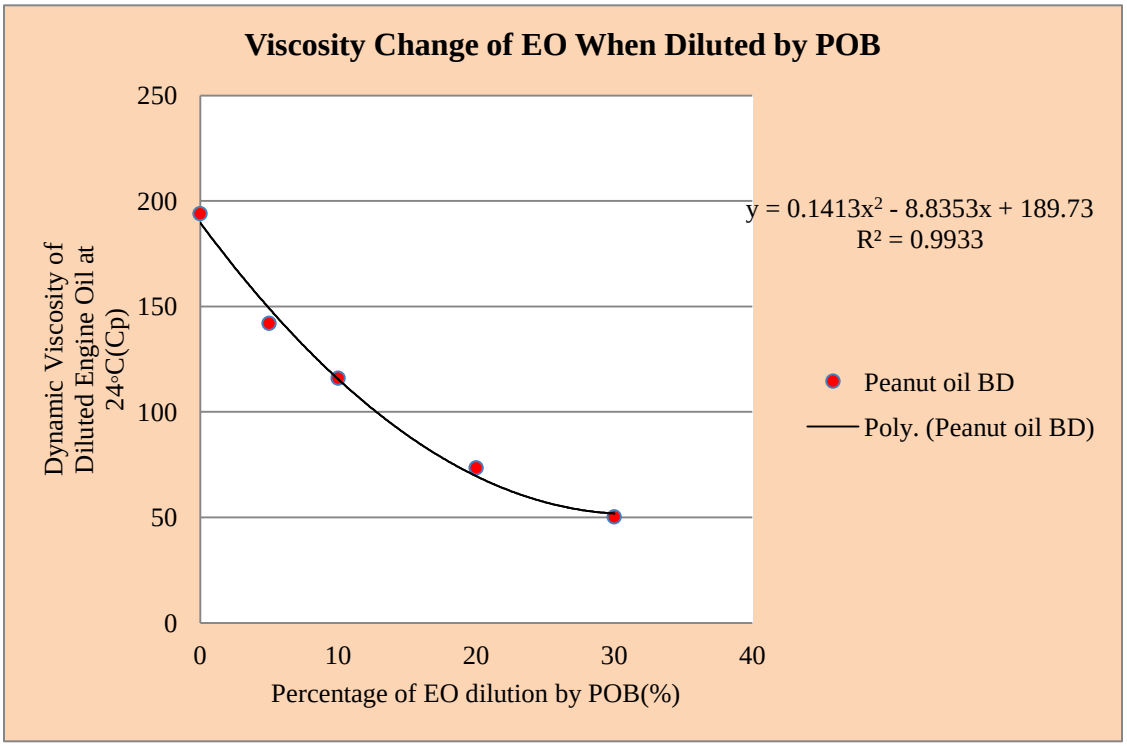

Figure 56: Viscosity change of EO when diluted by POB

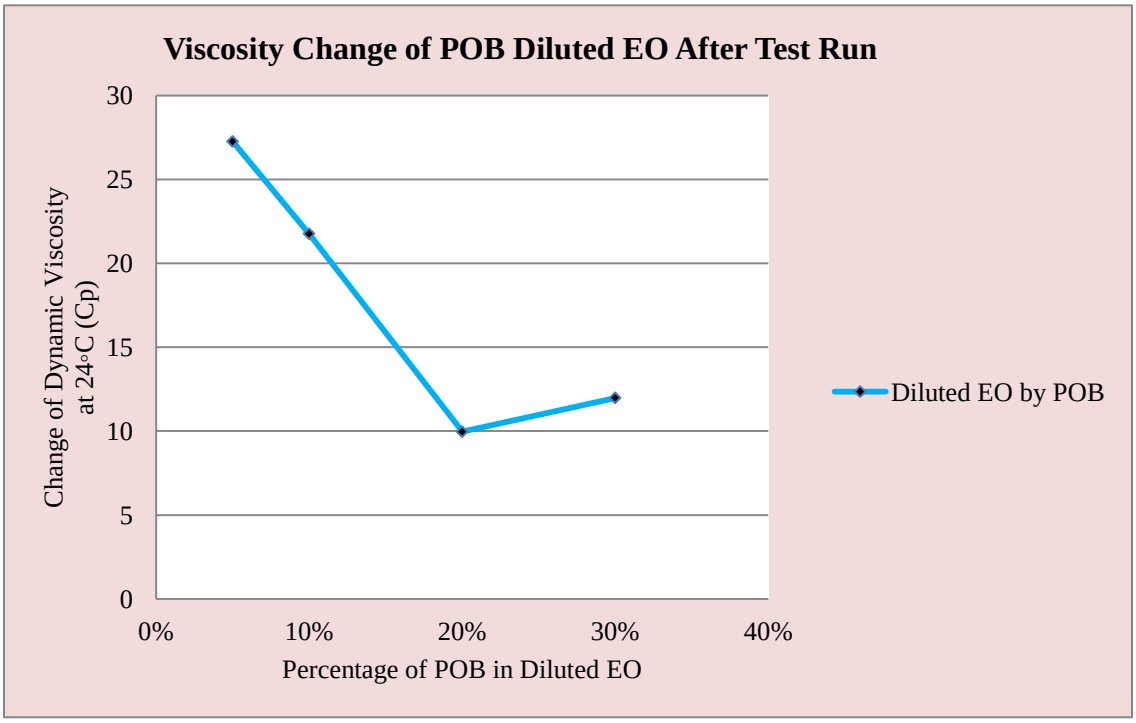

Figure 57: Viscosity change of POB diluted EO after the experiment.

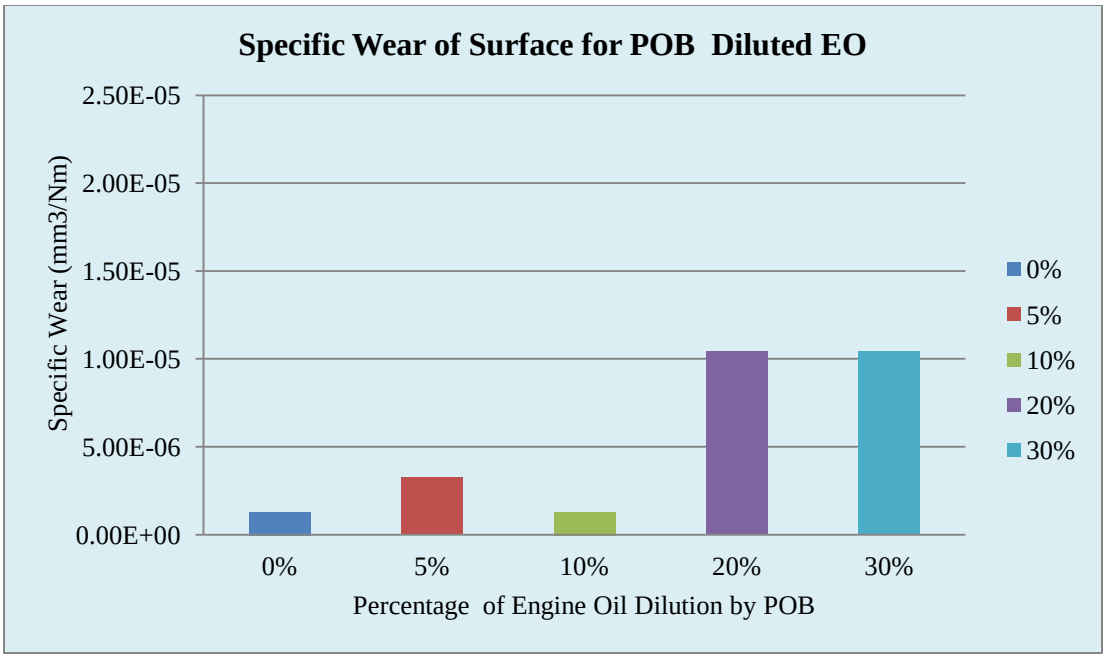

Figure 58: Specific wear amount of the surface in presence of POB diluted EO.

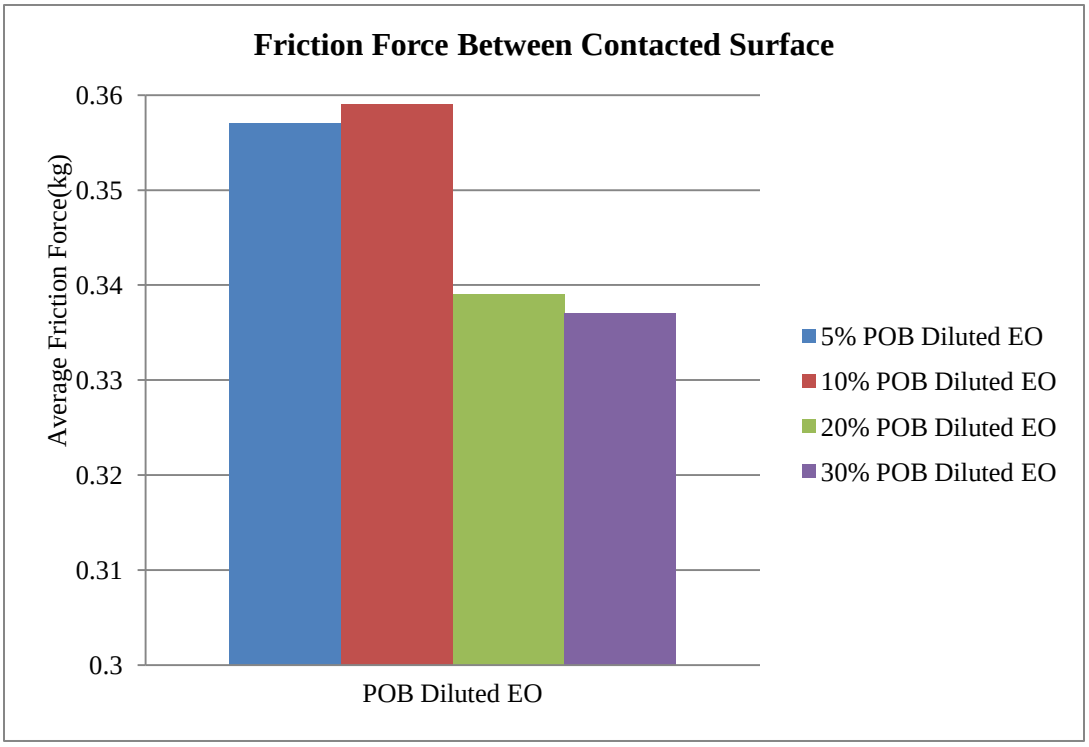

Figure 59: Average friction force between the contacted surfaces for POB diluted engine oil

Average friction force is presented in Figure 59 and the measured value was the lowest for the 30% dilution of EO by POB. The in-process friction force presented in Figure 60 shows that an anti- friction layer was formed on the surface in a short time. For the 20% and 30% POB (Peanut oil biodiesel) diluted EO (engine oil), the measured friction force is lower than that of 5% and 10%. This may be due to some unknown tribo-chemical reaction of diluted EO which may enhance lubricity property of the engine oil.

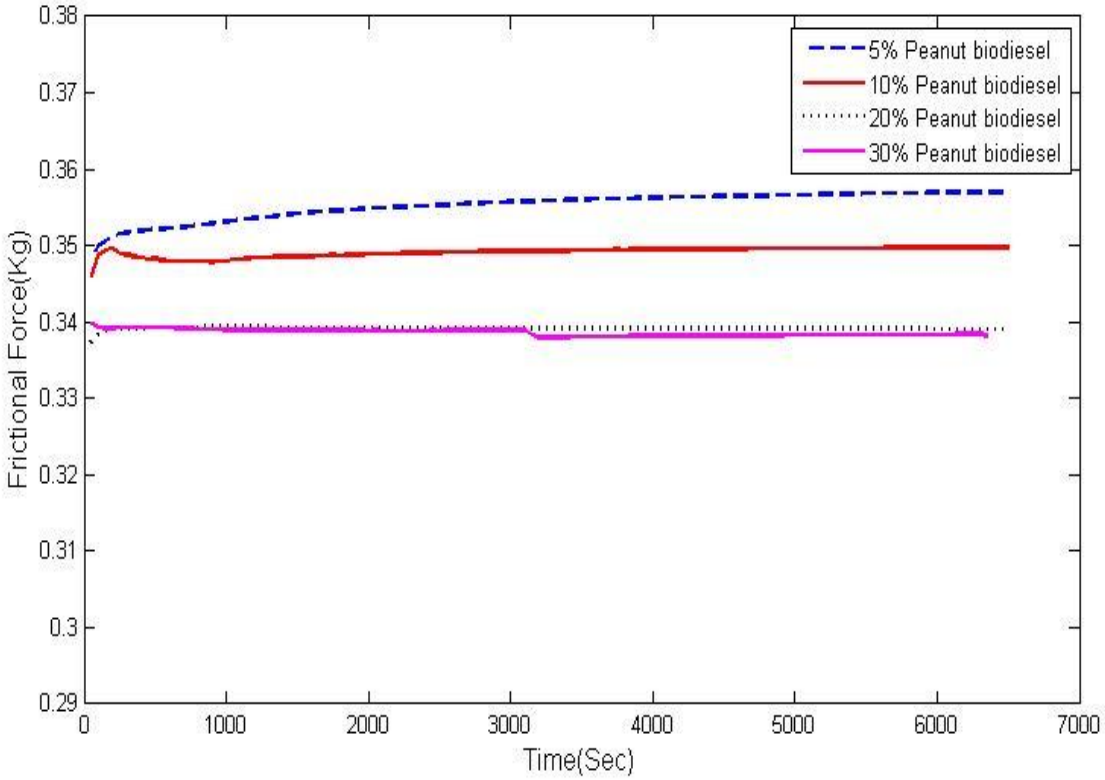

Figure 60: In process friction force Vs the time for POB diluted EO

Figure 61 presents the temperature change during the test runs for the four different mixture percentages. In the figure, T1 represents the temperature measured by the thermocouple (Thermocouple-1 of Figure 43) which was inserted in the hollow space of the pin, while the pin holds the ball at its tip; T2 represents the temperature measured by the thermocouple (Thermocouple -2 of Figure 43) which was placed near the friction couple joint. In this work, test chamber was not insulated and heat produced by the friction was left to dissipate. After the test runs the color of diluted engine oil also was observed and is presented in Figure 62; it was noticed a small degree of color change. That small change suggested that the diluted engine oil does not significantly lose its stability through oxidation for the tested condition.

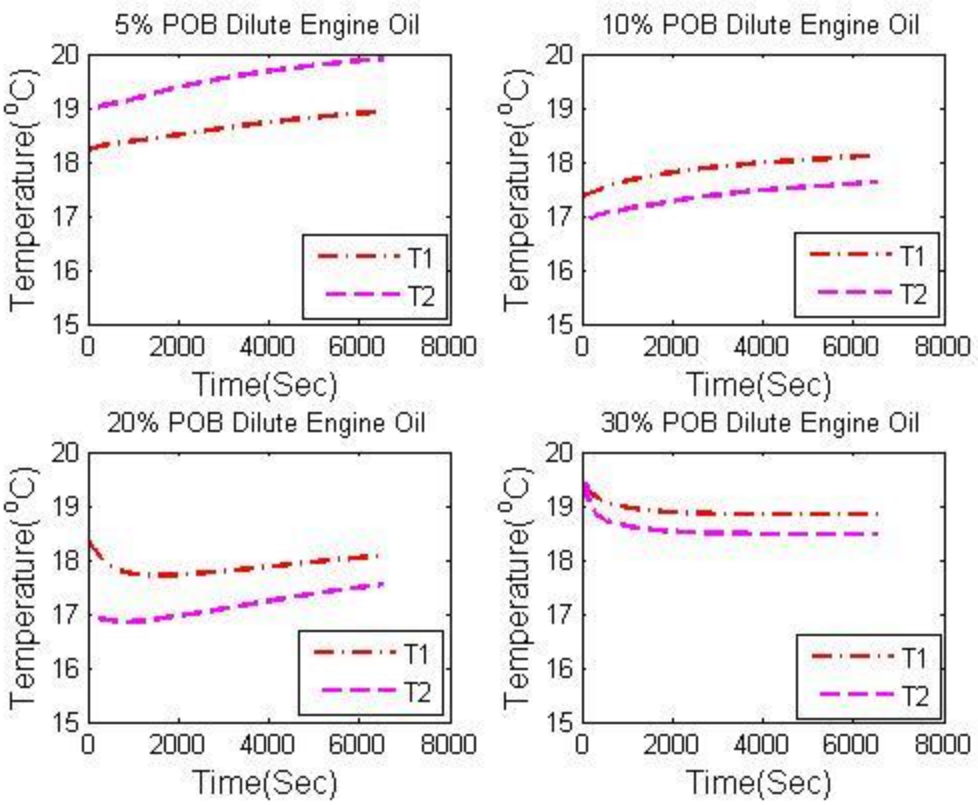

Figure 61: In process temperature profiles of ball and test chamber vs. time for POB diluted EO.

Figure 62: The left over oxidized oil after a test run with a typical POB diluted EO

4.2.3 Soybean Oil Biodiesel Diluted Engine Oil

Soybean oil Biodiesel (SOB) is a vegetable feedstock biodiesel. Their major fatty acid components are palmitic acid (6-10%), oleic acid (20-30%), linoleic acid (50-60%) and stearic acid (2-5%). The engine oil (EO) was diluted with soybean oil biodiesel (SOB) at 5%, 10%, 20% and 30%. Figure 63 presents the measured dynamic viscosity for the tested percentage of freshly prepared diluted engine oil (EO). The relation between the diluted engine oil viscosity and the percentage of soybean oil biodiesel (SOB) in the engine oil (EO) fits a quadratic adjustment, which is included in Figure 63. Figure 64 presents the dynamic viscosity change of the diluted EO after the tests.

Figure 65 shows the measured specific wear amount from the worn surface at different dilution percentages of engine oil by SOB. This plot also shows that for the 10% dilution of EO the specific wear amount was minimum.

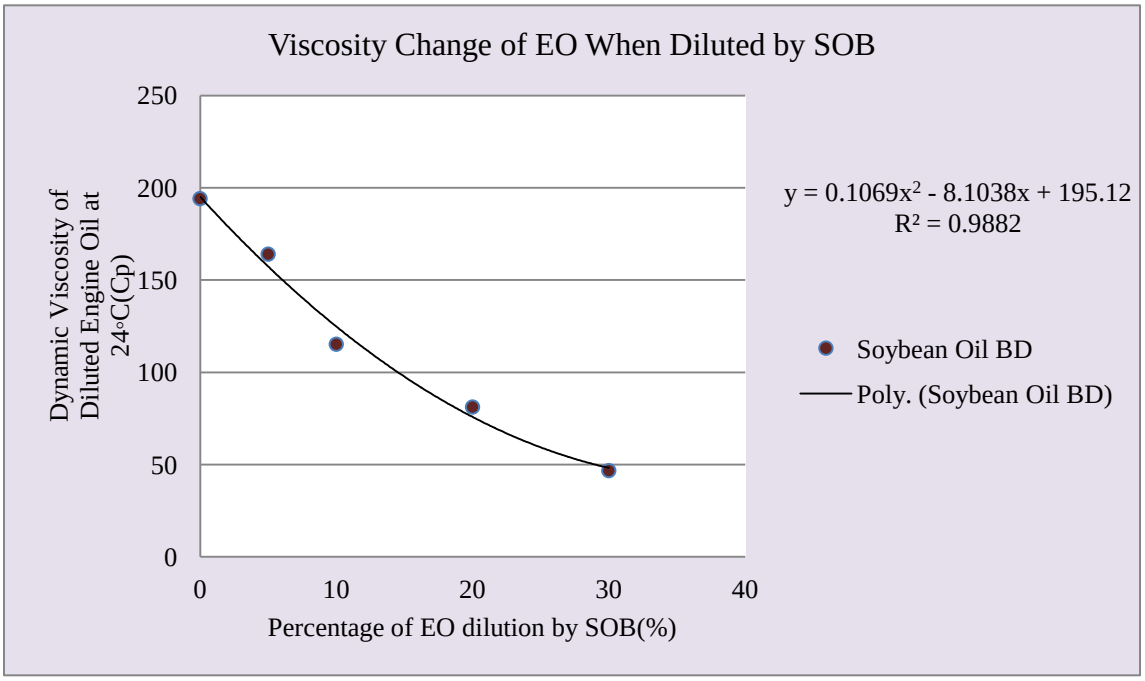

Figure 63: Measured viscosity of EO when diluted by SOB

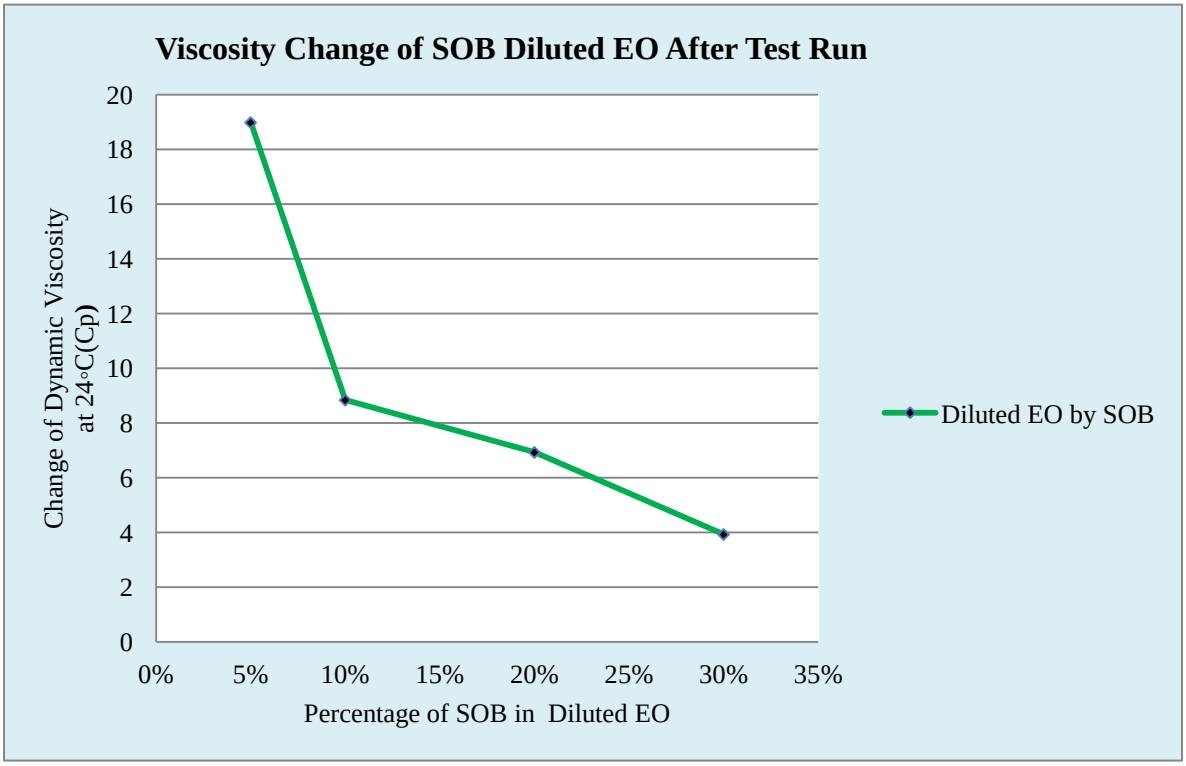

Figure 64: Viscosity change of SOB diluted EO after the experiment.

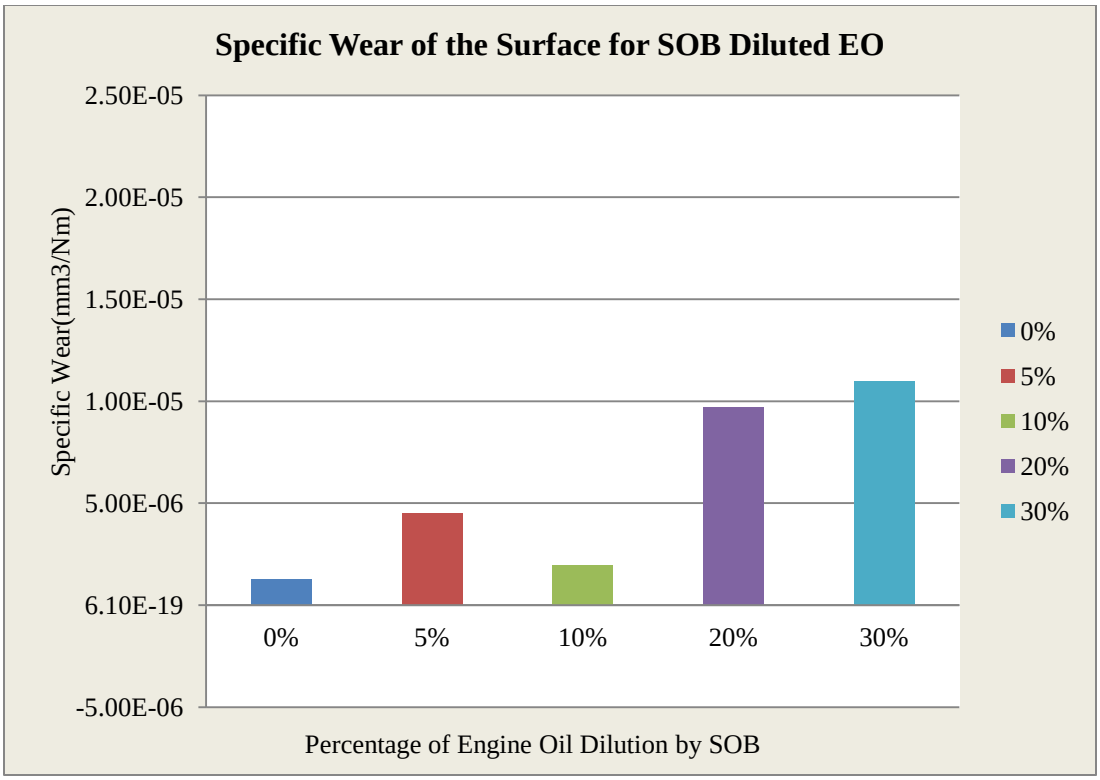

Figure 65: Specific wear amount of the surface in presence of SOB diluted EO.

Average friction force was measured minimum for the 30% dilution of EO by SOB, as it presented in Figure 66. Figure 67 shows that in-process friction force reached a stable value after a 2,000 seconds run, and that indicating that for diluted EO it would take about 2,000 seconds of run to form a low friction layer on the surface. Figure 67 shows that for the 30% SOB dilution the friction force tends to slightly increase with time. After the test the color of the diluted engine oil was also observed, and is presented in Figure 68. It was observed that for all the tested percentage the diluted oil became darker after the test.

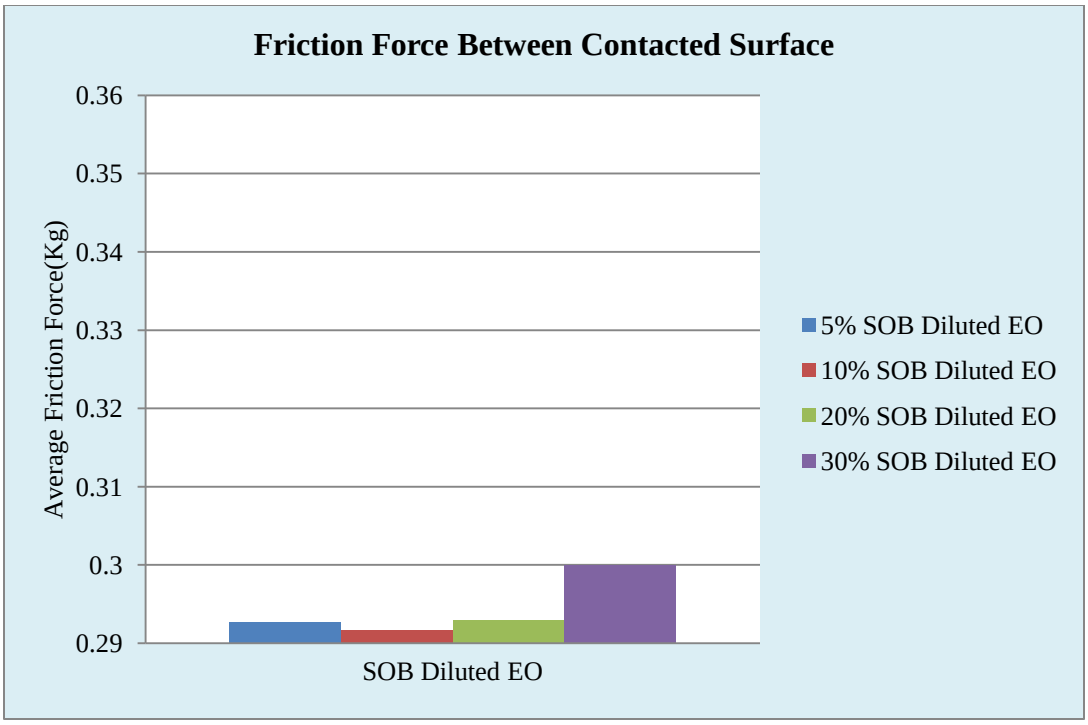

Figure 66: Average friction force between the contacted surfaces for SOB Diluted engine oil.

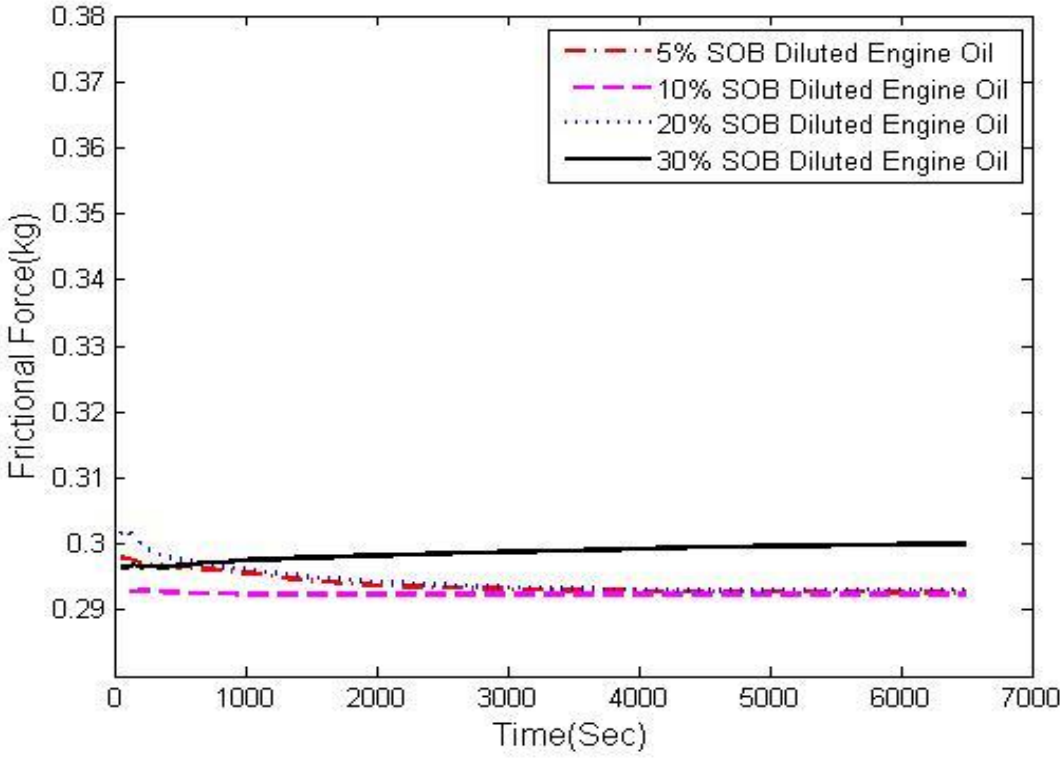

Figure 67: In process friction force with the time for SOB diluted EO

Figure 68: The left over oxidized oil after a test run with a typical SOB diluted EO

4.2.4 Chicken Fat Biodiesel Diluted Engine Oil

Animal fats are attractive feedstock for biodiesel, and Chicken Fat Biodiesel (CFB) is one of the animal feedstock biodiesels that contains saturated fatty acids. Its major components are palmitic acid (25%), oleic acid (41%), linoleic acid (18%) and stearic acid (6%). It contains smaller amounts of some saturated fatty acids, such as linoleic acid, than those of vegetable feedstock biodiesels.

Figure 69 presents the measured dynamic viscosity for the different tested percentages of engine oil (EO) dilution. The relation between the diluted engine oil viscosity and the percentage of chicken fat biodiesel (CFB) in the engine oil (EO) fits quadratic adjustments, which included in Figure 69. Figure 70 presents the dynamic viscosity change of the diluted EO after the tests.

Figure 71 shows the measured specific wear amount for the tested worn disk surface at different dilution percentages of engine oil (EO) by CFB. This plot shows that at a 10% dilution of EO the specific wear amount was measured to be minimum.

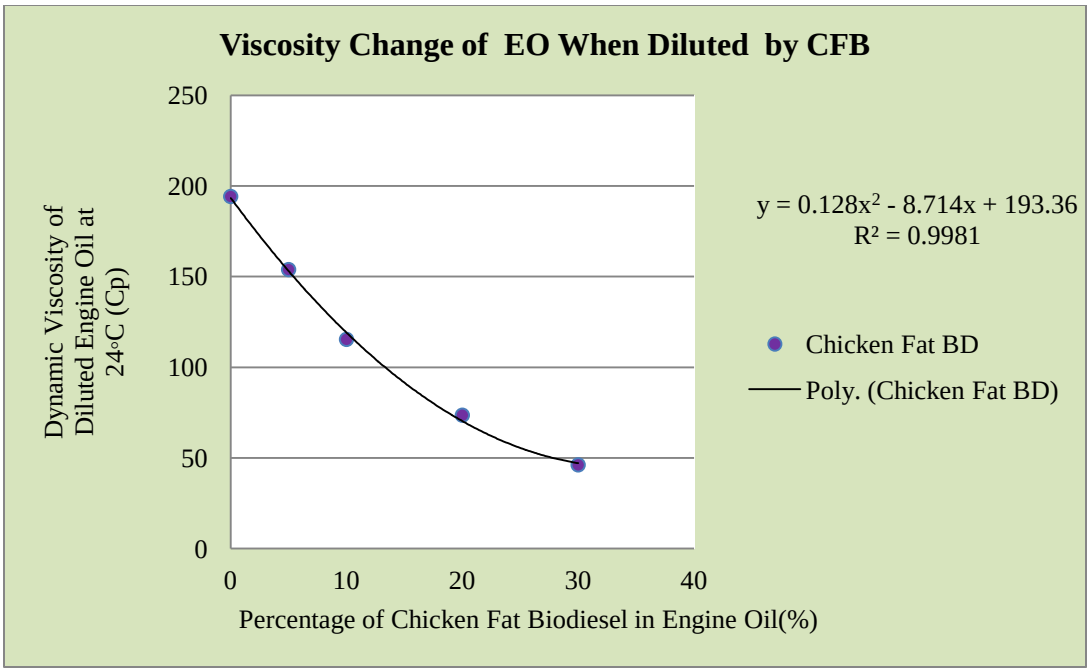

Figure 69: Viscosity change of EO when diluted by CFB

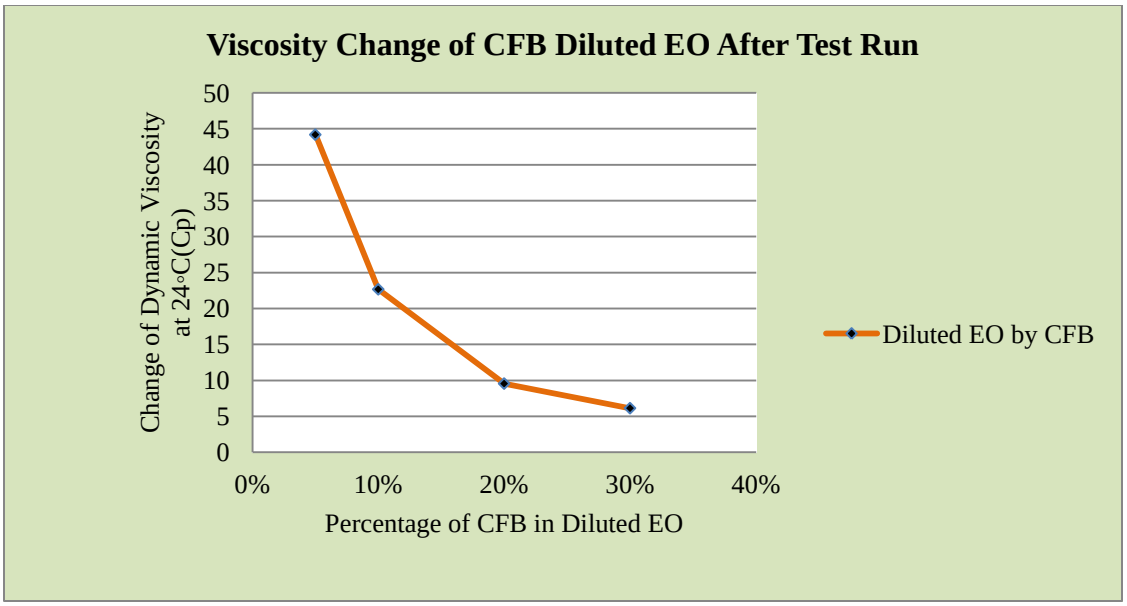

Figure 70: Viscosity change of CFB diluted EO after the experiment

The measured average friction force was found minimum for the 30% dilution of EO by CFB as presented in Figure 72. During the test, the friction force reached a stable value after a 3000 seconds run. Figure 73 presents the in-process friction force for all percentage of CFB diluted EO.

After each test run no significant color change of the engine oil mixture was observed, which is an indication of good oxidative stability. Typical leftover oil after a test run is presented in Figure 74.

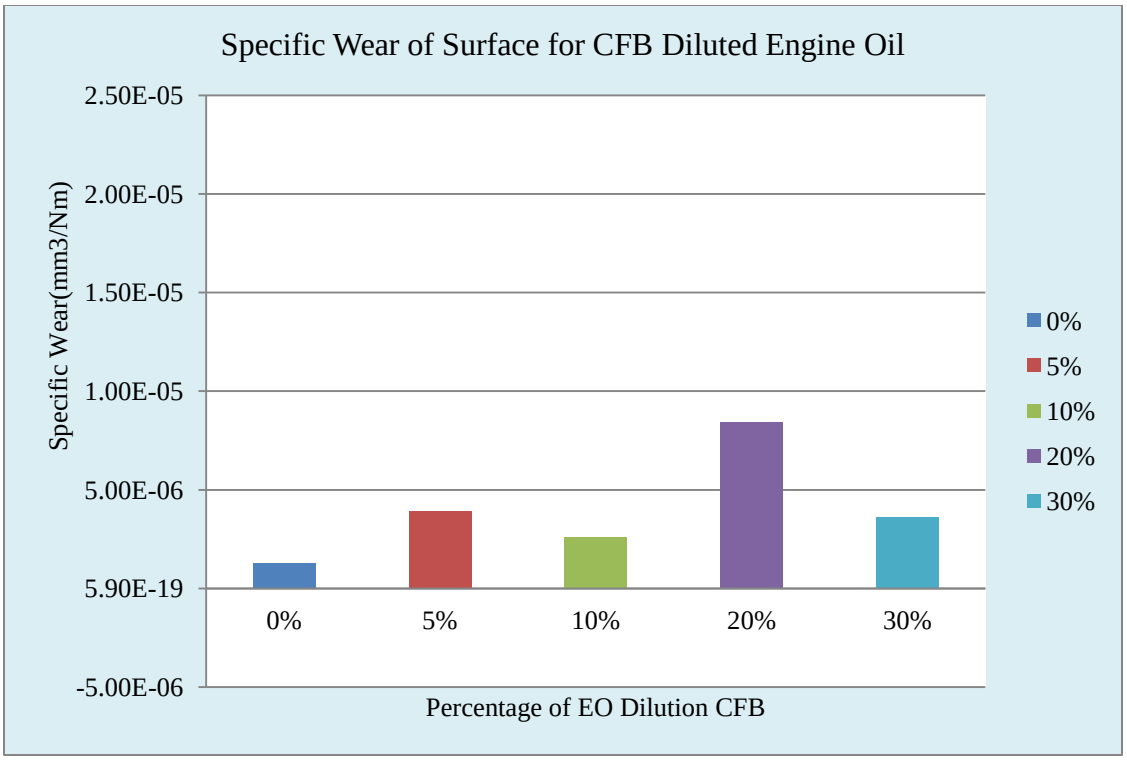

Figure 71: Specific wear amount of the surface in presence of CFB diluted EO.

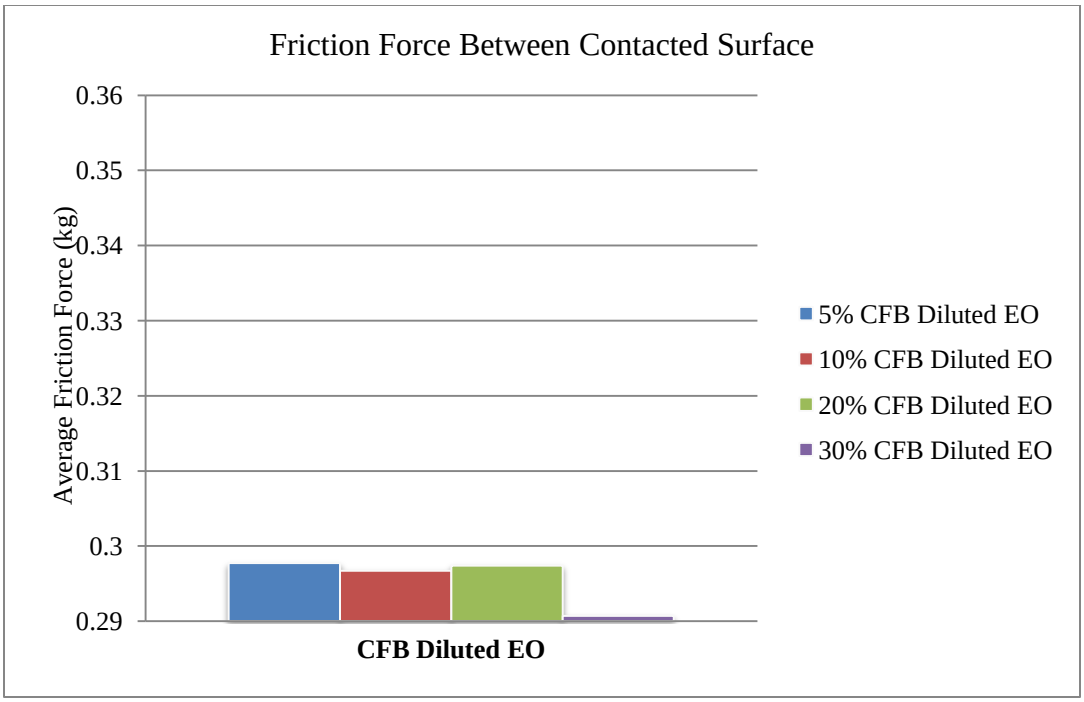

Figure 72: Average friction force between the contacted surfaces for CFB diluted engine oil(EO).

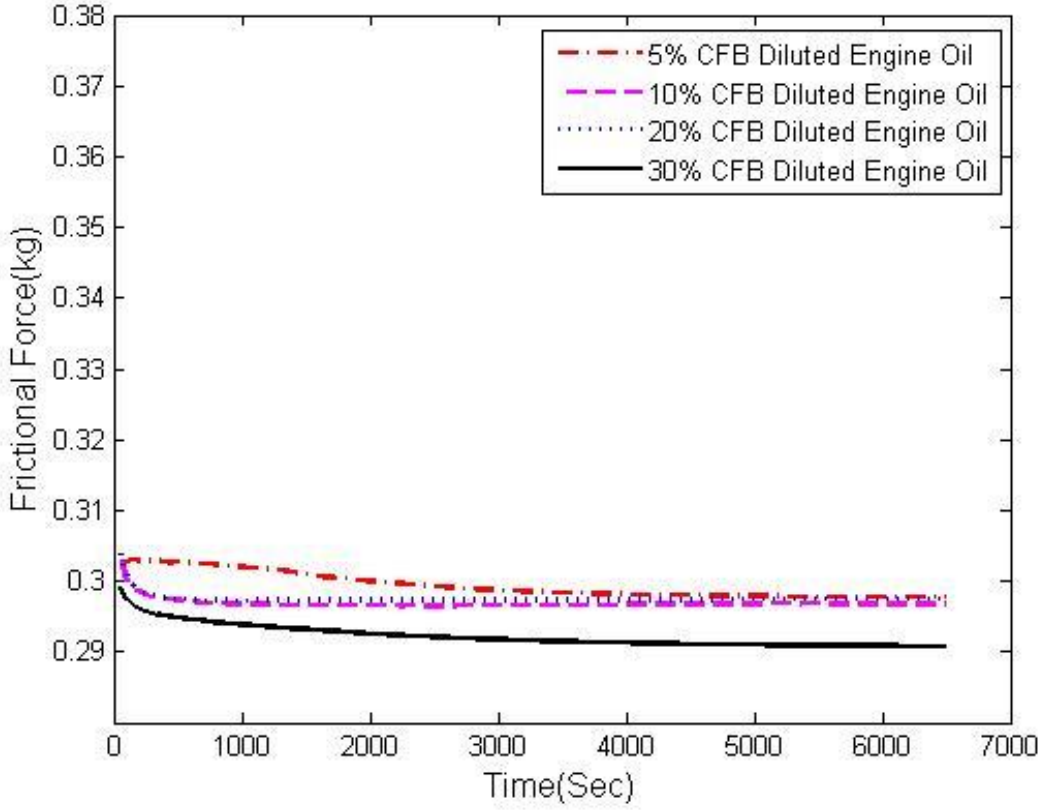

Figure 73: In process friction force with the time for CFB diluted EO

Figure 74 : The left over oxidized oil after a test run with a typical CFB diluted EO

4.3 Friction and Wear Test for Pure Biodiesel

Friction force and wear in the presence of all the four employed B100 or pure biodiesel (B100: 100% biodiesel) were tested, and the measured friction forces for pure engine oil (15W 40) were used as reference for comparison. Figure 75 presents in-process friction for the B100 of COB, POB, SOB and CFB. The results indicate that B100 from CFB yields a similar friction force (or lubricity performance) than that of EO (15W 40). The POB (peanut oil biodiesel) friction force became similar to that of EO after a 3,000 seconds run. The friction forces for COB and SOB are comparatively higher than those of EO, POB and CFB.

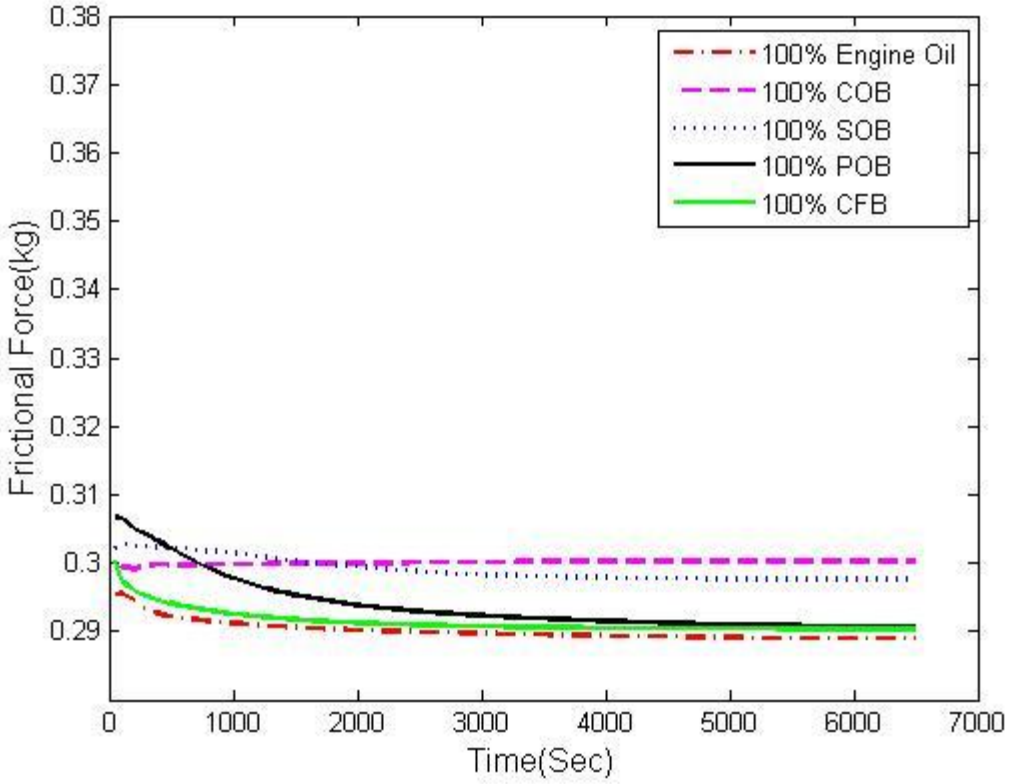

Figure 75: In process friction force with the time for B100 for the four tested biodiesel and EO

Specific wear of the surface as measured for all the four types B100 are presented in Figure 90. The animal fat feedstock biodiesel (chicken fat biodiesel) yielded the minimum amount of specific wear. Among the vegetable feedstock biodiesels POB yielded the minimum amount of specific wear. The SOB and COB produce comparatively higher specific wear than those of the CFB and POB. Specific wear of the surface for pure 15W 40 was also determined and it is shown in Figure 76 as reference. Although POB and CFB produced lower specific wear, it was five times greater than that of 15W 40.

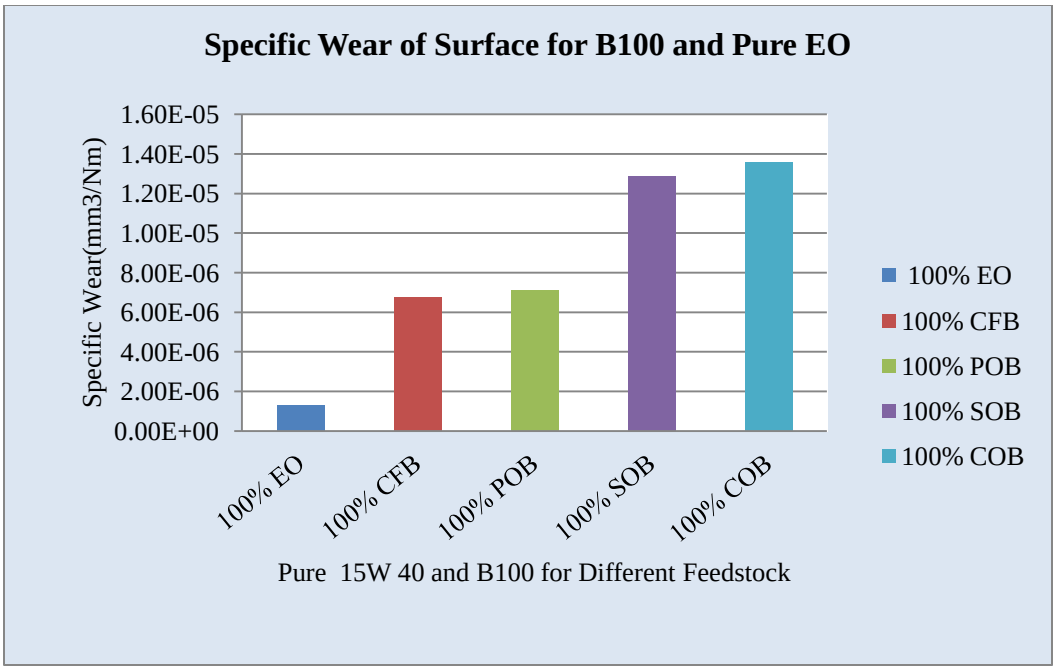

Figure 76: Specific wear amount of the surface in presence of all four types B100 and pure EO

4.4 Overall Comparison of Results

Dynamic viscosity changes patterns are similar for all the four test percentages and types of biodiesel and they can be adjusted by a quadratic fits as presented in Figure 77. After test run, the measured dynamic viscosity changes are presents in Figure 78. This figure shows that in the 5% to 20% interval for SOB diluted EO dynamic viscosity significantly dropped as compared to the other three. In the 20% to 30% SOB and COB diluted EO exhibit almost same pattern. In the entire tested interval CFB and POB shows the lowest dynamic viscosity drop.

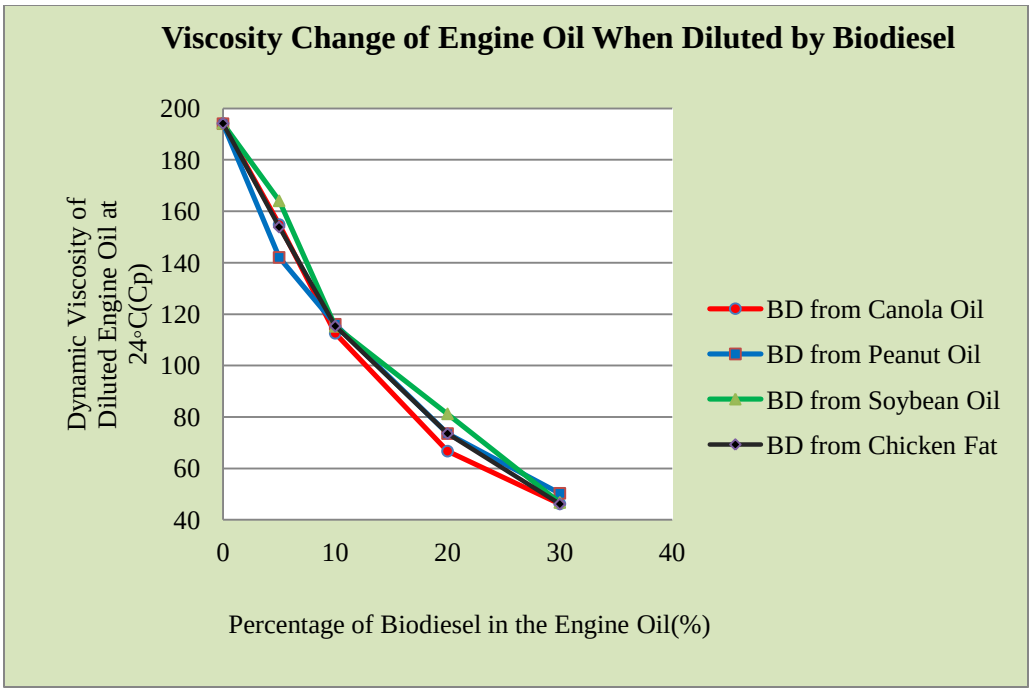

Figure 77: Viscosity change of EO when diluted by Biodiesel

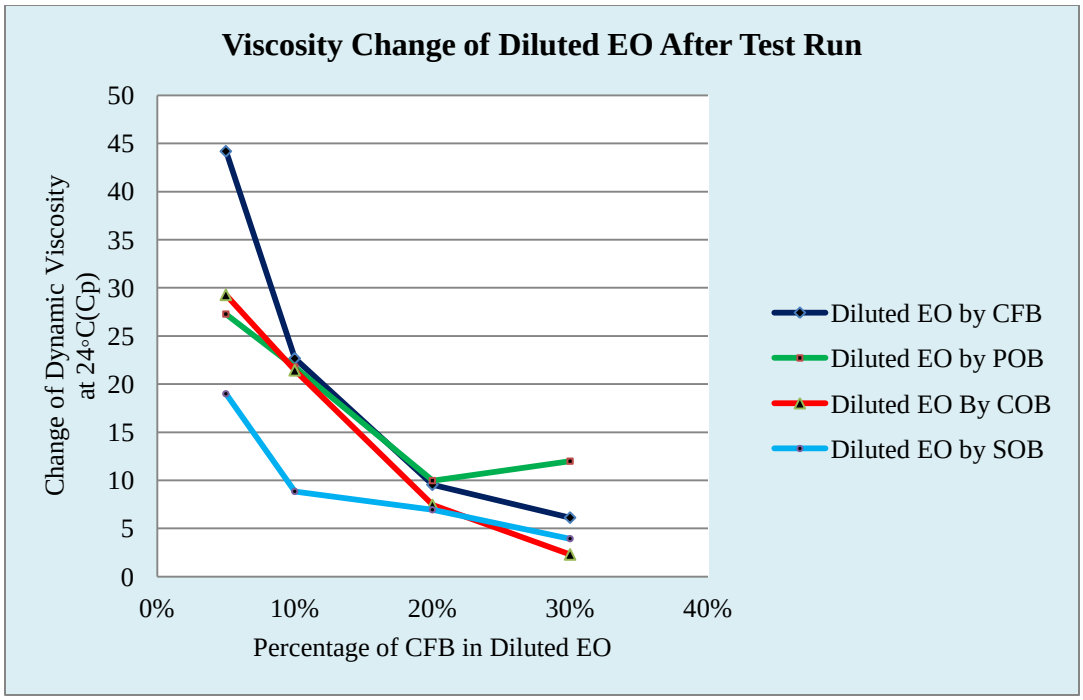

Figure 78: Viscosity change of diluted EO after the experiment

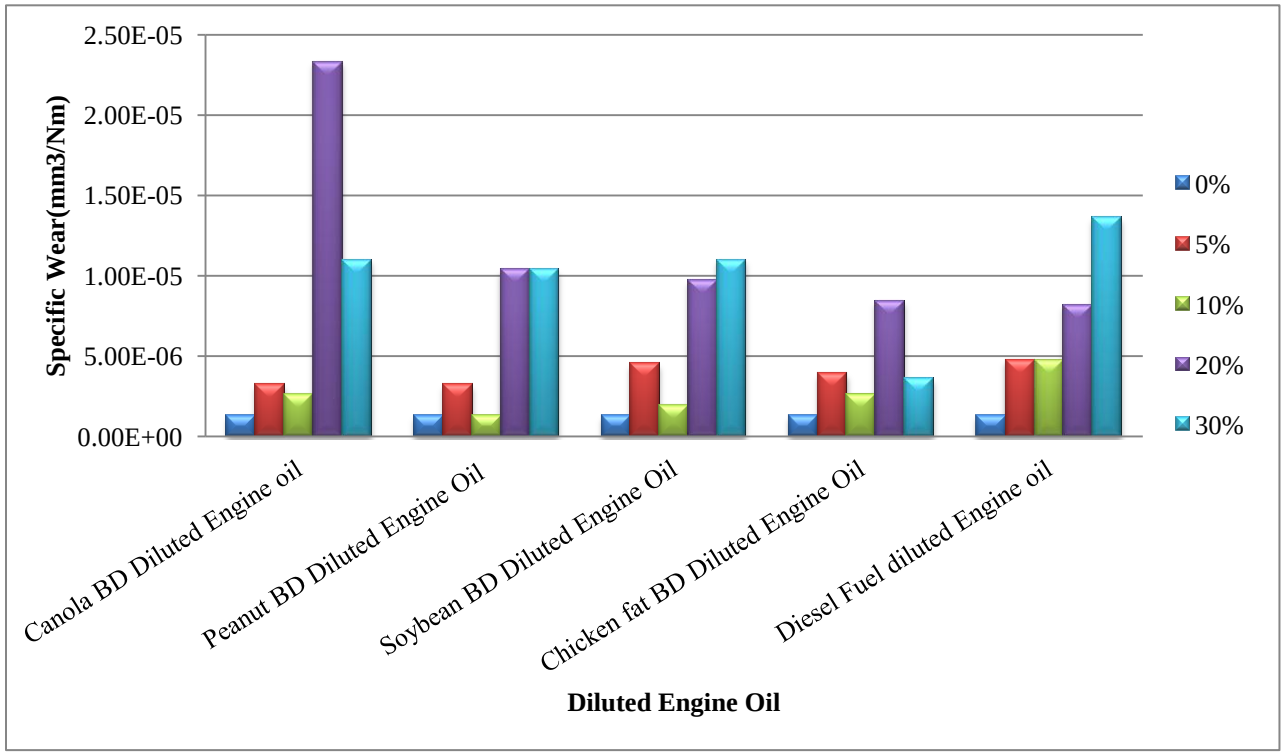

Figure 79: Specific wear amount of the surface in presence of all four types Biodiesel and Diesel oil diluted Engine oil.

Figure 79 presents the summary of measured wear for all mixtures of the four tested biodiesel on SAE 15W40 oil, as compared with those from fossil diesel in engine oil mixtures. The employed engine oil (SAE 15W 40) also was diluted with fossil diesel, as a set of reference mixtures, for the same 5%, 10%, 20% and 30% volume ratios, and pin-on-disk tests were carried out for each mixtures for the same test conditions than those of biodiesel mixtures. For 20% and 30% dilution, the specific wear amount seems to increase as compared to those of 5% and 10% dilution for the SOB, COB and POB diluted EO; the specific wear amount was higher than that for CFB diluted EO. The summery of the figure 79 also shows that for the four biodiesels, any degree of mineral-oil dilution by the tested biodiesels reduces the wear protection performance of the engine oil in the investigated intervals, even at small amounts, such as the tested 5% dilution. However, the measured levels of wear for all four biodiesel mixtures, are not substantially different than corresponding wear values for mixtures of fossil-diesel in same SAE15W40 engine oil.

CHAPTER 5

CONCLUSIONS AND RECOMMENDATIONS FOR FUTURE WORK

Literature review of this thesis work revealed that engine oil contamination can be one of the main reasons of early engine oil degradation and of eventual engine cessation. Oil can be become contaminated when unburned or incomplete burnt fuel blows by through the piston rings and ends up in the crankcase. Although some limited engine oil dilution by diesel engine fuel is acceptable but when the engine is fueled by biodiesel or biodiesel blend then engine oil dilution rate and it effects can be different than those from the regular diesel fuel. This is mainly because of the penetrating, solvencies, and lower distillation temperature of biodiesel than that of diesel fuel.

Research shows that biodiesel or FAME fuel dilution had a negative impact on engine oil performance when methyl esters of biodiesel partially degraded and interacted with the ZDDP anti-wear additives. Biodiesel in the engine oil caused oxidation which produced acid components and a reduction in TBN (Total Base Number). The effects are influenced by the FAME properties of biodiesel and it depends upon the feedstock and employed transesterification process. Feedstock are responsible for various chain length, position , number and nature of double bonds or various types acid content in FAME and FAME acid contents are usually identified as an important viscosity factor in the biodiesel. Recent research suggested that various types acid contents in FAME such as, FFA, glycerol, antioxidant, palmitic acid, tecopherol , asolectin helps to reduced WSD or surface wear where as some other FAME

components, such as linoleic acid plays a role to interact with the ZDDP anti-wear additives and increse wear rate on the surface .

In this thesis work the employed pin-on-disk tribometer was refurbished with an updated data acquisition system. The new data acquisition system acquires and stores in-process friction force and temperature at the friction joint. This research work showed the feasibility of employing a pin-on-disk tribometer for testing wear and friction force changes for the mixtures of biodiesel and engine oil on selected metal surfaces of AISI 1018 steel. All the data collected during the experiment are compared and some conclusions are drawn about effects of biodiesel dilution in engine oil.

In this work, specific wear was measured for the different dilution percentages of engine oil by CBO (canola oil biodiesel). The result shows that for the 10 % dilution the measured specific wear was the lowest and that for the 20% dilution was the highest. These observed results could be because of the interactions with the engine oil anti-wear additives ZDDP (Zinc Dialkyl Dithio Phosphate), which usually bonds to the metallic surfaces to form a protective layer against wear. The polar components in biodiesel (e.g. fatty acid methyl ester), may also attracts the ZDDP molecules. Therefore, when ZDDP is not fully attracted to the surface or is less available to give protection to surface and wear rates may increase. After testing with COB diluted engine oil for the four dilution percentage, an oxidized layer of oil was observed as left on the surface and this is observed for all the four tested percentages and it may be an indication of some reduced oxidative stability of engine oil when it is diluted by COB.

For the 30% dilution of EO by POB, measured average friction force value was the lowest. The in-process friction force shows that an anti- friction layer was formed on the surface in a short time. Also for the 20% and 30% POB (Peanut oil biodiesel) diluted EO (engine oil), the measured friction force is almost steady in the entire 6000s experimental duration. This may

be due to some unknown chemical reaction of diluted EO and the contact materials. Small changes of leftover oil suggested that the POB diluted engine oil does not significantly lose its stability through oxidation.

For the 30% dilution of EO by SOB, average friction force was measured minimum and in-process friction force reached a stable value after a 2,000 seconds run, and that indicates that for diluted EO it would take about 2000 seconds of run to form a low friction layer on the surface but for the 30% SOB dilution the friction force tends to slightly increases with time. For all the tested percentage the diluted oil became darker after the test, indicating reduced oxidation stability for SOB diluted engine oil

For the 30% dilution of EO by CFB, the measured average friction force was found minimum and during the test, the friction force reached a stable value after a 3,000 seconds run for all percentage of CFB diluted EO. After each test run no significant color change of the engine oil mixture was observed, which is an indication of good oxidative stability for the CFB diluted EO.

Specific wear amounts of the surface measured for all the four types B100 and the animal fat feedstock biodiesel (chicken fat biodiesel) yielded the minimum amount of specific wear. Among the vegetable feedstock biodiesels the POB yielded the minimum amount of specific wear. The SOB and COB produces comparatively higher specific wear than those of the CFB and POB. Specific wear of the surface for pure 15W 40 was also determined as reference. Although POB and CFB produced lower specific wear, it was five times greater than that of SAE15W 40 engine oil.

Dynamic viscosity change patterns are similar for all the four test percentages and types of biodiesel. After the test run, measured dynamic viscosity of the leftover oil on the surface shows that in the 5% to 20% interval for SOB diluted EO dynamic viscosity significantly

dropped as compared to the other three. In the 20% to 30% SOB and COB diluted EO exhibit almost same pattern. In the entire tested interval CFB and POB shows the less dynamic viscosity dropping.

From all the results of this work some general conclusions can also be drawn. The most important overall conclusion is that, any degree of engine oil dilution by biodiesel reduces the performance of engine oils even at small amount, such as the tested 5%. For all the tested biodiesel feedstock dilution at 10% yielded the lowest amounts of surface wear. A probable reason is may be at the 10% dilution, polor components of biodiesel may exert a little attraction to the ZDDP of engine oil and ZDDP additives can provide a good wear protection on the surface.

The overall performance of the tested animal fat feedstock biodiesel diluted engine oil is better than that of vegetable feedstock biodiesel dilution. Animal fat feedstock biodiesel contains around 25% of palmitic acid, being higher than that of the vegetable feedstock biodiesel. Animal fat biodiesel also contains smaller amount of linoleic acid than that of vegetable feedstock biodiesel. This observation suggest that higher amounts of palmitic acid and lower amounts of linoleic acid may play an important role in reducing the tested engine oil dilution effects by biodiesel.

It was also found that among the tested vegetable feedstock biodiesel, peanut oil biodiesel yields lower surface wear but also higher friction force at the friction joint as compare to those measured for soybean oil biodiesel and canola oil biodiesel. Peanut oil biodiesel was also found to yield a better lubricity than the other two vegetable feedstock biodiesels and this may be due to lower linoleic acid content than for soybean and canola oil biodiesel. It was also observed that canola oil biodiesel and soybean oil biodiesel diluted engine oil may be prone to faster oxidize in presence of air and for small increases of temperature as compared to chicken fat biodiesel

diluted and peanut oil biodiesel diluted engine oils. The latter could be as stable as pure engine oil.

The results are suggested that, this sliding contact tribometer exhibit a realistic and a reproducible result over a wide range of testing condition. So the outcome of this bench test type research work exhibit a good prediction of biodiesel dilution effect in engine oil and it can be used as a reference for the future field test.

Remarks for Future Research

With the existing facilities linoeic acid and palmitic acid diluted engine oil can be tested to observe their direct effect on surface wear and friction properties. A research with the similar methodology can be performed with the second generation biodiesel i.e. biodiesel from non-food feedstock. For future research, the existing pin-on-disk instrument should be employed with a temperature controller of heater for allowing high temperature test and iron alloy can be used as disk materials to represents the typical contact pairs of engine. Such research can be conducted for the engine crankcase material at the elevated temperature and it can mimic the real engine operating condition. A Profilometer can be employed to obtain the worn surface profile and SEM techniques should be used to observe the surface microstructure change and wear pattern resulting from the biodiesel diluted engine oil as lubricant. A more advance study of the effects of biodiesel in engine oil should include by identification and quantification of the by-products left on surface by using analysis techniques as FTIR and Raman spectroscopy.

REFERENCES

Agarwal, A. K. (August, 2006). Biofuels(alcohols and biodiesel) Application as Fuel for Internal Combustion Engines. *Energy and Combustion Science* , 233-271.

Bennett, S. (2009). *Modern Diesel Technology: Diesel Engines.* New York: Delmar,Cengage Learning.

Biodiesel-b100 Retrieved July 8, 2010, from Biodieselkit.co.uk: http://www.biodieselkits.co.uk/biodiesel-b100/

Booser, E. R. (1994). *CRC Handbook of Lubrication: Monitoring, materials, synthetic lubricants* (Vol. 3). Denver , MA, USA: CRC Press.

Brookfield. 2005. Retrieved Octobar 27, 2010, from http://www.brookfield.co.uk: http://www.brookfield.co.uk/uk/products/viscometers/laboratory-dv-ii.asp

Burger, N. D. (2006). *University of Petroria* . Retrieved July 2010, from upetd.up.ac.za/thesis/available/etd-12142006.../07back.pdf

Chasen, D., & Fasano, P. (2009). A Study of Biodiesel Fuel Impact on Lubricant. *STLE* .

Chemicalland21. (2008). *Fatty Acid, Vegetable Oil*. Retrieved October 2010, from chemicalland21 website: http://www.chemicalland21.com/industrialchem/iuh/fatty%20acids,%20vegetable-oil.htm

Cole-Parmer Technical Library . (2009). Retrieved October 26, 2010, from Cole-Parmer website: http://www.coleparmer.com

Comfort, A. (2003). An Introduction to Heavy Duty Diesel Engine Frictional Losses and Lubricant Properties Affecting Fuel Economy-Part 1. *SAE International.*

Dardalis, D. (2004). *Rotating Linear Engine:A New Approach to Reduce Engine Friction and Increase Fuel Economy in Heavy Duty Engines.* RLE Technologies, Inc., Austin, Texas.

Delphi Diesel System, S. A. (June, 2000). *Fuels for Diesel Engines-Diesel Fuel Injection Equipment Manufacturar Common Position Statement.*

Dixon, J. (2008). *Modern Diesel Technology: Preventive Maintenance and Inspection.* NY: Cengage Learning.

Duffield, J., Shapouri, H., Graboski, M., McCormick, R., & Wilson, R. (1998). *U.S Biodiesel development:New Markets for Conventional and Genetically Modified Agricultural Products.* Economic Research Service, USAD, Washington, DC.

Edwards, D. (2009). *Energy Trading and Investing.* McGraw-Hill.

EPA. (1999). *In-Use Marine Diesel Fuel.* Fairfax ,VA.

F. D. Gunstone, J. L. (2007). *The Lipid Handbook* (Third edition). FL: CRC press.

Fang, H. L., Whitacre, S. D., Yamaguchi, E. S., & Boons, M. (2007). Biodiesel Impact on wear protection of Engine oil. *Powertrain & Fluid Systems Conference and Exhibition.* Chicago, IL.

Fitch, J. (2007, May). Four Lethel Diesel Engine Oil Contaminants. *Machinery Lubrication* .

Fuel Fact Sheet Retrieved July 26, 2010, from National Biodiesel Board website: https://docs.google.com/viewer?url=http://www.biodiesel.org/pdf_files/fuelfactsheets/Lubricity.PDF

Garpen, J. V. (2004). *Business Management for Biodiesel Producer.* Oak Ridge: NREL.

Gerpen, J. V. (2010, October). *Farm Energy*. Retrieved October 2010, from Animal Fats for Biodiesel Production : http://www.extension.org/pages/Animal_Fats_for_Biodiesel_Production#Fatty_Acid_Content_of_Animal_Fats

Gili, F., Igartua, A., Luther, R., & Woydt, M. (January 2010). The Impact of Biofuels on Engine oil performance. *TAE Esslingen, 17th Int. Colloquium Tribology.* Germany.

Graboski, M. S.; McCormick, R. L.; J.D. Ross. (1996). Transient Emission from No.2 Diesel and Biodiesel Blends in a DDC Series 60 Engines. *Society of Automobile Engine Technology.*

Heywood, J. (1988). *Internal Combustion Engine Fundamentals.* New York: McGraw-Hill.

Hu, J., & Zexue Du, C. L. (2005). Study of Lubrication properties of Biodiesel as Fuel Lubricity Enhancers. *Fule ,Volume 84, Issues 12-13* , 1601-1606.

Jürgen Butt, H., Graf, K., & Kappl, M. (2003). *Physics and Chemistry of Interface.* Berlin: Wiley-VCH.

Kern, D. Q. (1965). *Process Heat Transfer.* London: McGRAW-Hill.

Kholi, R., & Mittal, K. (2008). *Developments in Surface Contamination and Cleaning.* Norwich, NY, US: William Andrew Inc.

Knothe, G., & Steidley, K. R. (2005). Kinematic Viscosity of Biodiesel Fuel Components and Related Compounds.Infuence of Compound structure and Comparision to petrodiesel Fuel Components. *Fuel.* Elsivier Ltd.

Knothe, G., & Steidley, K. R. (2005). Lubricity of Component of Biodiesel and Petrodiesel. *Energy and Fuels , 19*, 1192-1200.

Knothe, G., Gerpen, J. V., & Krahl, J. (2005). *The Biodiesel Handbook.* AOCS Publishing.

Kulkarni, M. G., Dalai, A., & Bakhshi, N. (2007). Transesterification of Canola Oil in Mixed Methanol/Ethanol system and Use of Ester as Lubricity Additive. *Biosource Technology* , 2027-2033.

Macartchouk, A. (2002). *Diesel Engine Engineering.* New York, NY: Mareel Dekker,Inc.

Masoner, A., Erck, R., & Ajayi, O. (2009). Lubrication Properties of a 15W-40 Diesel Engine Oil and Its Base Stock with Additives. *Tribology and Lubrication Technology* .

(2010). *Military Biofuel Applications.* Energy Business Reports.

Mobil Delvac Elite 15W-40. (2001). Retrieved October 2010, from http://www.mobil.com: http://www.mobil.com/USA-English/Lubes/PDS/GLXXENCVLMOMobil_Delvac_Elite_15W-40.aspx

Munson, J., & Hetz, P. (1999). *Seasonal Diesel Fuel and Fuel Additive Lubricity Survey Using the" Munson ROCLE" bench test.* Saskatchewan Canola Development Commission, SK, Canada.

National Biodiesel Board . (2003, July). Retrieved Octobar 2010, from http://www.biodiesel.org: http://www.biodiesel.org/resources/pressreleases/fle/20030616_military_users.pdf

Pavesi, L., & Fauchet, P. M. (2008). *Biophotonics.* Heidelberg, German: Springer.

Quadrature Encoder Measurements. Retrieved from http://zone.ni.com.

Rick. (2010, January). *Biodiesel Feedstock Oils*. Retrieved October 2010, from make-biodiese website:http://www.make-biodiesel.org/index.php?option=com_content&view=article&id=69&Itemid=88

Sappok, A. G., & Wong, V. W. (April 2009). Impact of Biodiesel on Ash Emissions and Lubricant Properties Affecting Fuel Economy and Engine Wear: Comparison with Conventional Diesel Fuel. *SAE International Journal of Fuels and Lubricants , vol. 1 no. 1*, 731-747.

Schwaller, A. E. (2005). *Total Automotive Technology* (4th Edition ed.). New York: Thomson Delmar Learning.

Scott, D. (2009, December). *The National Biodiesel Board (NBB)*. Retrieved Octobar 25, 2010, from http://www.biodiesel.org/

Stuckey, B. N. (1972). *Handbook of Food Additives* (2nd edition ed.). (T. Furia, Ed.) Cleveland, OH: CRC Press.

Sulek, M., Kulczycki, A., & Malysa, A. (2010). Assessment of the Lubricity of Compositions od Fuel oil with Biocomponents Derived from Rape-seed. *Wear 268* , 104-108.

Thornton, M., Alleman, T., Luecke, J., & McCormick, R. (June, 2009). Impact of Biodiesel Fuel Blends Oil Dilution on Light-Duty Diesel Engine Operation. *2009 SAE International Powertrain,Fuels and Lubricants Meeting.* Florence, Italy.

Totten, G. E. (2001). *Bench Testing of Industrial Fluid Lubrication and Wear properties Used in machinary Application.* . Danvers, MA: ASTM.

Tribology,(1994). *Instructional Manual: T-11 High Temparature Pin-on-Disk Machine* . Poland.

U.S Oilchek. (2007). Retrieved August 8, 2010, from http://www.usoilcheck.com/oilchek/used+oil+analysis/tutorial/fuel+dilution.asp

Van Garpen, J. (September, 1996). Cetane Number Testing of Biodiesel. *Liquid Fuels and Industrial Products from Renewable Sources.* Nashville, Tennessee.

Wadumestheige, K., Ara, M., Salley, S. O., & Simon Ng, K. (2009). Investigation of Lubricity Characteristics of Biodiesel in Petroleum Synthetic fuel. *Energy and Fuels* , *23*, 2229-2234.

Weiksner, J. M., Crump, S. L., & White, T. L. *Understading Biodiesel Fuel Quality and Performence.* U.S Department of Energy.

APPENDIX A

Rest of the Temperature Change and In-Process Frictional Force Plot

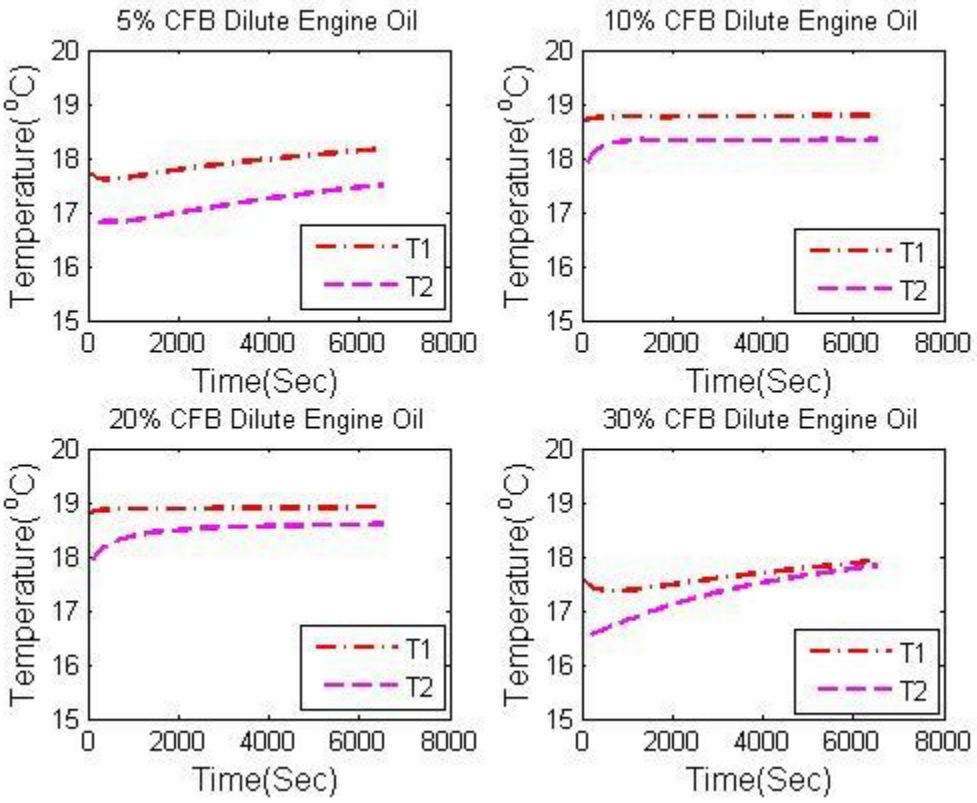

Figure A1: In-process temperature profiles of ball and test chamber vs. time for CFB diluted EO

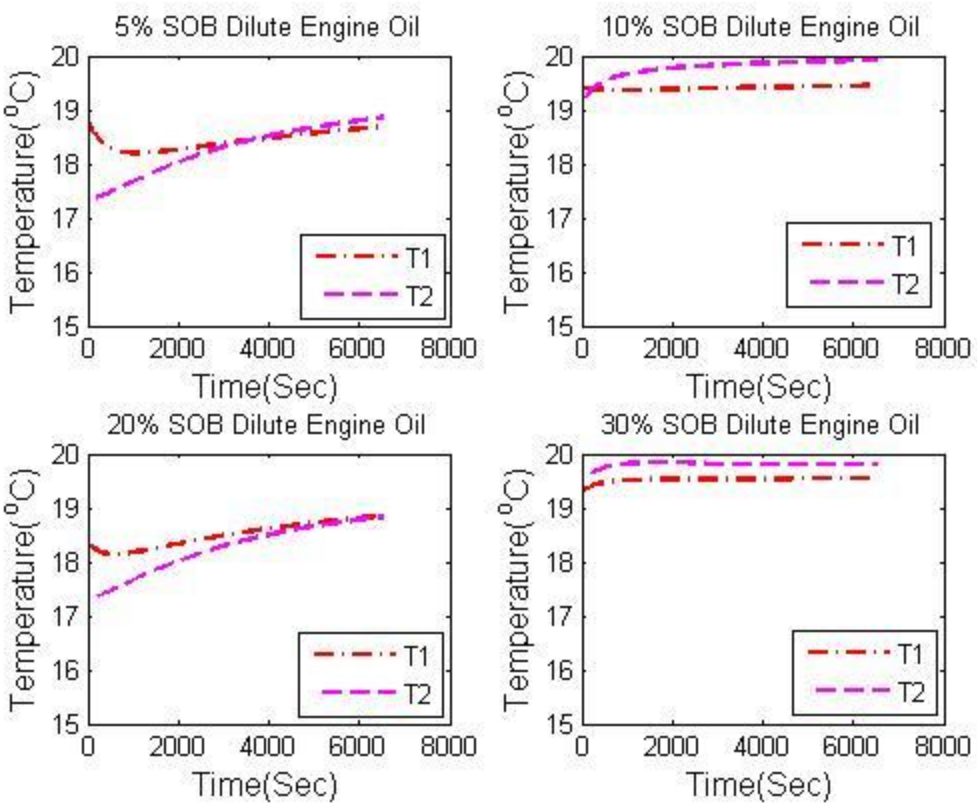

Figure A2: In-process temperature profiles of ball and test chamber vs. time for CFB diluted EO

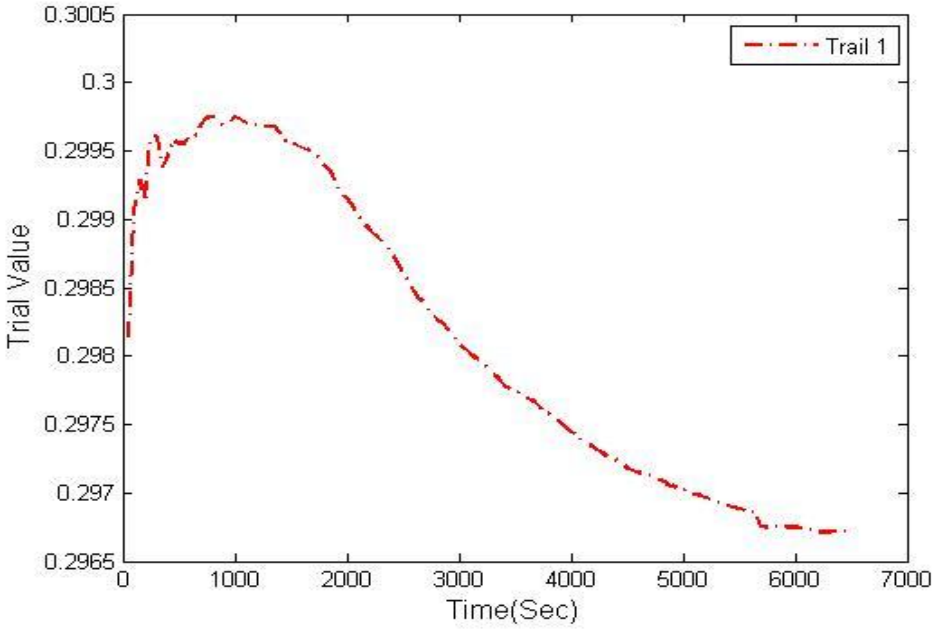

Figure A3: Change of friction force for 30% CFB diluted EO for trial 1.

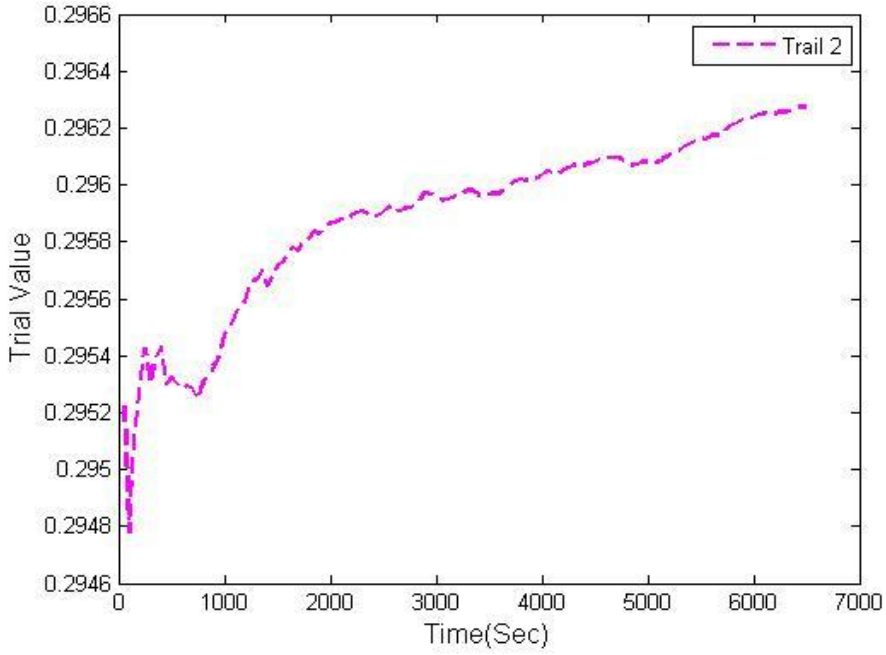

Figure A4: Change of friction force for 30% CFB diluted EO for trial 2.

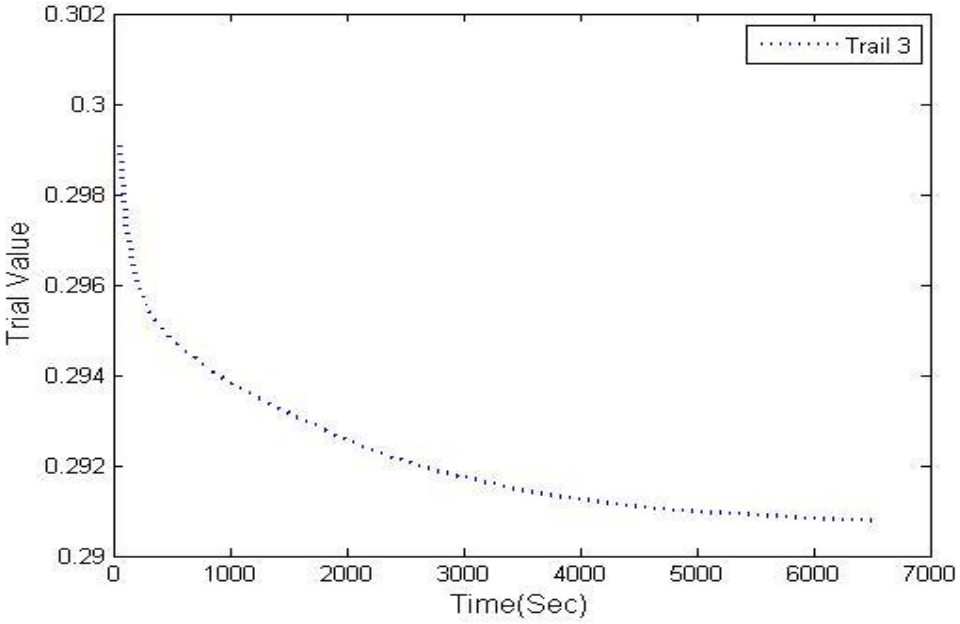

Figure A5: Change of friction force for 30% CFB diluted EO for trial 3.

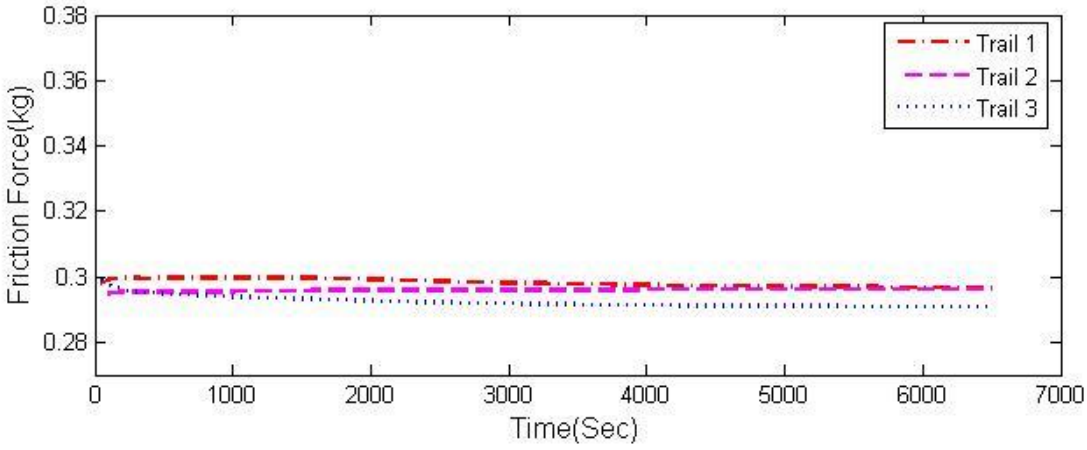

Figure A6: Change of friction force for 30% CFB diluted EO for three trials.

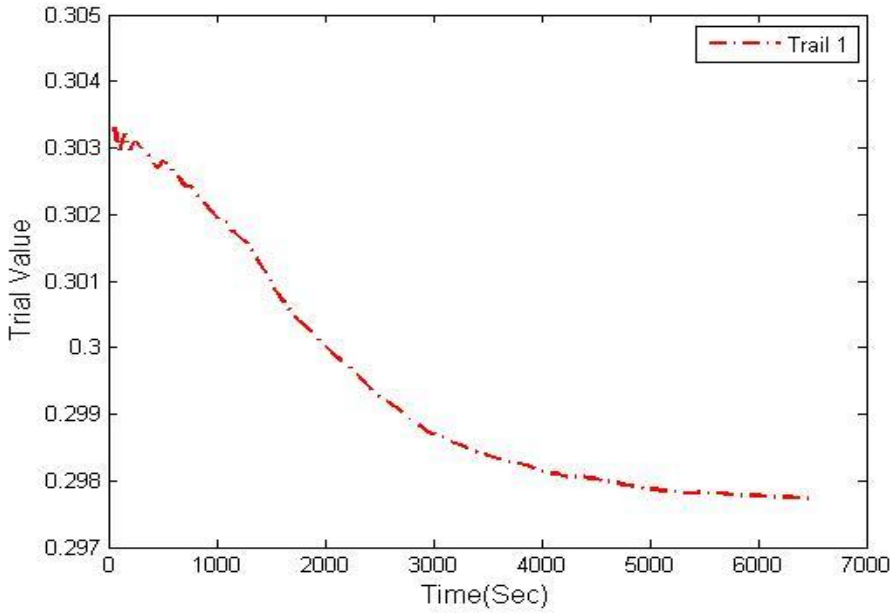

Figure A7: Change of friction force for 5% CFB diluted EO for trial 1.

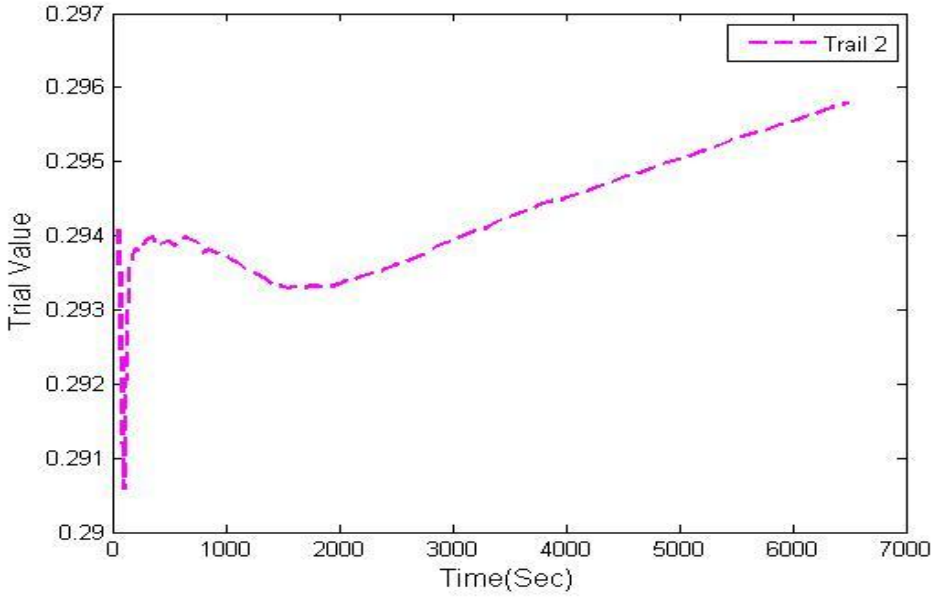

Figure A8: Change of friction force for 5% CFB diluted EO for trial 2.

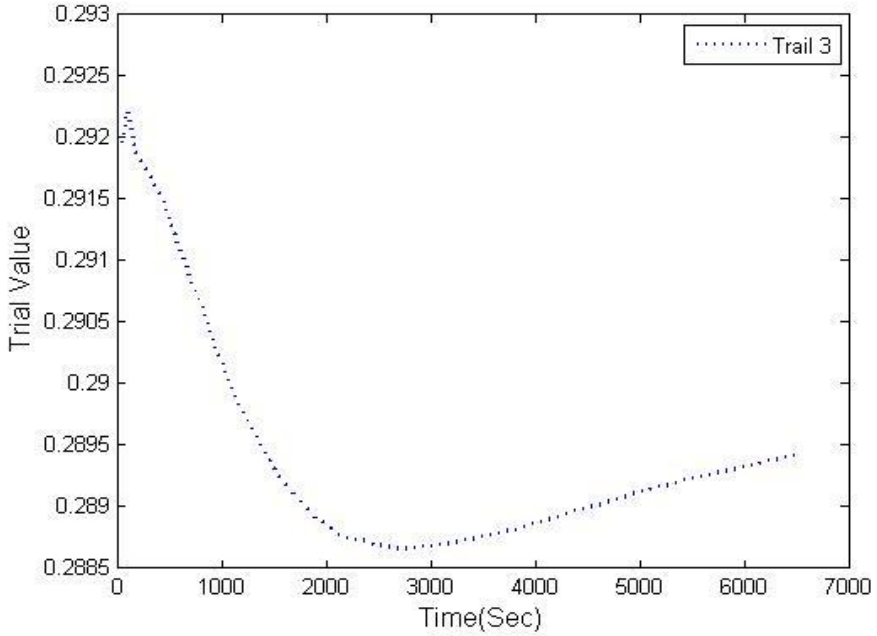

Figure A9: Change of friction force for 5% CFB diluted EO for trial 3

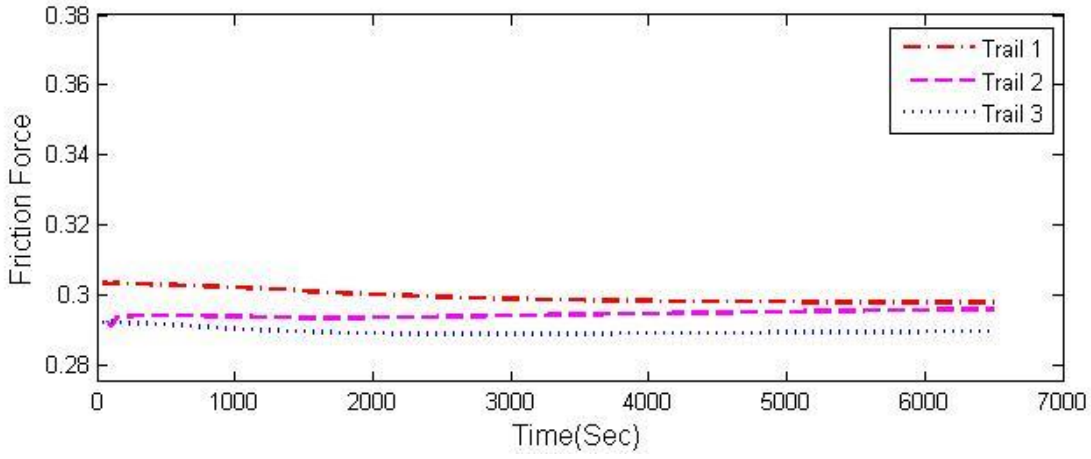

Figure A10: Change of friction force for 5% CFB diluted EO for three different trials

APPENDIX B

Developed MatLab Code for the Data Analysis

```
% this progarm will take data from xlsx sheet and draw plots
close all;
clear all;
a=1;
b=500;
%% Reading data from xls file
data=xlsread('canola data.xlsx'); % reading data from the Excel data sheet

% Making avergae every 500 data and then storing then a
for i=1:1:130  % storing data every 100 intervel and storing
    for p=a:1:b;
        can5(p)=(data(p,2));
        can10(p)=(data(p,3));
        can20(p)=(data(p,4));
        can30(p)=(data(p,5));
    end;
    a=b+1;
    b=a+499;

    canola5(i)=mean(can5);
    canola10(i)=mean(can10);
    canola20(i)=mean(can20);
    canola30(i)=mean(can30);
end;
%% getting time to plot
for i=1:1:130  % storing data every 100 intervel and storing
    p=i*500;
    time(i)=data(p,1);

end;
%% Plotting
figure(1),plot(time,canola5,'-.r','linewidth',1.8); % ploting
hold on; plot(time,canola10,'--m','linewidth',1.8);
         plot(time,canola20,':b','linewidth',1.8);
         plot(time,canola30,'-k','linewidth',1.8);
         ylim([0.28 0.38]); % setting y limit
          xlabel('Time(Sec)','Fontsize',12);
          ylabel('Frictional Force(kg)','Fontsize',12);
          legend('5% COB Diluted Engine Oil','10% COB Diluted Engine Oil',...
                 '20% COB Diluted Engine Oil','30% COB Diluted Engine Oil');
```

```
% this progarm will take data from xlsx sheet and draw plots
close all;
clear all;
a=1;
b=500;
%% Reading data from xls file
data=xlsread('chicken fat.xlsx'); % reading data from the Excel data sheet

% Making avergae every 500 data and then storing then a
for i=1:1:130  % storing data every 100 intervel and storing
    for p=a:1:b;
        cfb5(p)=(data(p,2));
        cfb10(p)=(data(p,3));
        cfb20(p)=(data(p,4));
        cfb30(p)=(data(p,5));
    end;
    a=b+1;
    b=a+499;

    chickenfat5(i)=mean(cfb5);
    chickenfat10(i)=mean(cfb10);
    chickenfat20(i)=mean(cfb20);
    chickenfat30(i)=mean(cfb30);
end;
%% getting time to plot
for i=1:1:130  % storing data every 100 intervel and storing
    p=i*500;
    time(i)=data(p,1);

end;
%% Plotting
figure(1),plot(time, chickenfat 5,'-.r','linewidth',1.8); % ploting
hold on; plot(time, chickenfat 10,'--m','linewidth',1.8);
         plot(time, chickenfat 20,':b','linewidth',1.8);
         plot(time, chickenfat 30,'-k','linewidth',1.8);
         ylim([0.28 0.38]); % setting y limit
          xlabel('Time(Sec)','Fontsize',12);
          ylabel('Frictional Force( ^{o}C','Fontsize',12);
          legend('5% CFB Diluted Engine Oil','10% CFB Diluted Engine Oil',...
                 '20% CFB Diluted Engine Oil','30% CFB Diluted Engine Oil');


% this progarm will take data from xlsx sheet and draw plots
close all;
clear all;
a=1;
b=500;
%% Reading data from xls file
data=xlsread('peanut.xlsx'); % reading data from the Excel data sheet

% Making avergae every 500 data and then storing then a
for i=1:1:130  % storing data every 100 intervel and storing
    for p=a:1:b;
        pob5(p)=((data(p,2));
        pob10(p)=(data(p,3));
        pob20(p)=(data(p,4));
```

```
        pob30(p)=(data(p,5));
    end;
    a=b+1;
    b=a+499;

    peanut5(i)=mean(pob5);
    peanut 10(i)=mean(pob10);
    peanut 20(i)=mean(pob20);
    peanut 30(i)=mean(pob30);
end;
%% getting time to plot
for i=1:1:130  % storing data every 100 intervel and storing
    p=i*500;
    time(i)=data(p,1);

end;
%% Plotting
figure(1),plot(time, peanut5,'-.r','linewidth',1.8); % ploting
hold on; plot(time, peanut 10,'--m','linewidth',1.8);
         plot(time, peanut 20,':b','linewidth',1.8);
         plot(time, peanut 30,'-k','linewidth',1.8);
         ylim([0.28 0.38]); % setting y limit
          xlabel('Time(Sec)','Fontsize',12);
          ylabel('Frictional Force(kg)','Fontsize',12);
          legend('5% POB Diluted Engine Oil','10% POB Diluted Engine Oil',...
                 '20% POB Diluted Engine Oil','30% POB Diluted Engine Oil');
```

```
% this progarm will take data from xlsx sheet and draw plots
close all;
clear all;
a=1;
b=500;
%% Reading data from xls file
data=xlsread('soybean.xlsx'); % reading data from the Excel data sheet

% Making avergae every 500 data and then storing then a
for i=1:1:130  % storing data every 100 intervel and storing
    for p=a:1:b;
        sob5(p)=(data(p,2));
        sob10(p)=(data(p,3));
        sob20(p)=(data(p,4));
        sob30(p)=(data(p,5));
    end;
    a=b+1;
    b=a+499;

    soybean5(i)=mean(can5);
    soybean 10(i)=mean(can10);
    soybean 20(i)=mean(can20);
    soybean 30(i)=mean(can30);
end;
```

```
%% getting time to plot
for i=1:1:130  % storing data every 100 intervel and storing
    p=i*500;
    time(i)=data(p,1);

end;
%% Plotting
figure(1),plot(time, soybean 5,'-.r','linewidth',1.8); % ploting
hold on; plot(time, soybean 10,'--m','linewidth',1.8);
         plot(time, soybean 20,':b','linewidth',1.8);
         plot(time, soybean 30,'-k','linewidth',1.8);
         ylim([0.28 0.38]); % setting y limit
          xlabel('Time(Sec)','Fontsize',12);
          ylabel('Frictional Force(kg)','Fontsize',12);
          legend('5% SOB Diluted Engine Oil','10% SOB Diluted Engine Oil',...
                 '20% SOB Diluted Engine Oil','30% SOB Diluted Engine Oil');
```

```
% this progarm will take data from xlsx sheet and draw plots
close all;
clear all;
a=2;
b=500;
%% Reading data from xls file
data=xlsread('chicken fat.xlsx'); % reading data from the Excel data sheet

% Making avergae every 500 data and then storing then a
for i=1:1:130  % storing data every 100 intervel and storing
    for p=a:1:b;
        T105(p)=((data(p,9)));
        T205(p)=(data(p,10));

        T110(p)=((data(p,11)));
        T210(p)=(data(p,12));

        T120(p)=((data(p,13)));
        T220(p)=(data(p,14));

        T130(p)=((data(p,15)));
        T230(p)=(data(p,16));
    end;
    a=b+1;
    b=a+499;

    mT105(i)=mean(T105);
    mT205(i)=mean(T205);

    mT110(i)=mean(T110);
    mT210(i)=mean(T210);

    mT120(i)=mean(T120);
    mT220(i)=mean(T220);
```

```
    mT130(i)=mean(T130);
    mT230(i)=mean(T230);

end;
%% getting time to plot
for i=1:1:130  % storing data every 100 intervel and storing
    p=i*500;
    time(i)=data(p,1);

end;
%% Plotting
figure(1),plot(time,mT105,'-.r','linewidth',1.8); % ploting
hold on; plot(time,mT205,'--m','linewidth',1.8);
         ylim([15 20]);
          xlabel('Time(Sec)','Fontsize',12);
          ylabel('Temperature( ^{o}C)','Fontsize',12);
          legend('T1','T2');

figure(2),plot(time,mT110,'-.r','linewidth',1.8); % ploting
           hold on; plot(time,mT210,'--m','linewidth',1.8);
            ylim([15 20]);
          xlabel('Time(Sec)','Fontsize',12);
          ylabel('Temperature( ^{o}C)','Fontsize',12);
          legend('T1','T2');

figure(3),plot(time,mT120,'-.r','linewidth',1.8); % ploting
          hold on; plot(time,mT220,'--m','linewidth',1.8);
           ylim([15 20]);
          xlabel('Time(Sec)','Fontsize',12);
          ylabel('Temperature( ^{o}C)','Fontsize',12);
          legend('T1','T2');

figure(4),plot(time,mT130,'-.r','linewidth',1.8); % ploting
        ylim([15 20]);
          hold on; plot(time,mT230,'--m','linewidth',1.8);
          xlabel('Time(Sec)','Fontsize',12);
          ylabel('Temperature( ^{o}C)','Fontsize',12);
          legend('T1','T2');


figure(5), subplot(2,2,1),plot(time,mT105,'-.r','linewidth',1.8); % ploting
          hold on; plot(time,mT205,'--m','linewidth',1.8);
           ylim([15 20]);
          xlabel('Time(Sec)','Fontsize',12);
          ylabel('Temperature( ^{o}C)','Fontsize',12);
          legend('T1','T2');
          title (['5% CFB Dilute Engine Oil'])

           subplot(2,2,2),plot(time,mT110,'-.r','linewidth',1.8); % ploting
           hold on; plot(time,mT210,'--m','linewidth',1.8);
            ylim([15 20]);
          xlabel('Time(Sec)','Fontsize',12);
          ylabel('Temperature( ^{o}C)','Fontsize',12);
          legend('T1','T2');
```

```
title (['10% CFB Dilute Engine Oil'])

 subplot(2,2,3),plot(time,mT120,'-.r','linewidth',1.8); % ploting
hold on; plot(time,mT220,'--m','linewidth',1.8);
 ylim([15 20]);
xlabel('Time(Sec)','Fontsize',12);
ylabel('Temperature( ^{o}C)','Fontsize',12);
legend('T1','T2');
title (['20% CFB Dilute Engine Oil'])

 subplot(2,2,4),plot(time,mT130,'-.r','linewidth',1.8); % ploting
hold on; plot(time,mT230,'--m','linewidth',1.8);
 ylim([15 20]);
xlabel('Time(Sec)','Fontsize',12);
ylabel('Temperature( ^{o}C)','Fontsize',12);
legend('T1','T2');
title (['30% CFB Dilute Engine Oi
```

```
% this progarm will take data from xlsx sheet and draw plots
close all;
clear all;
a=2;
b=500;
%% Reading data from xls file
data=xlsread('peanut.xlsx'); % reading data from the Excel data sheet

% Making avergae every 500 data and then storing then a
for i=1:1:130  % storing data every 100 intervel and storing
    for p=a:1:b;
        T105(p)=((data(p,9)));
        T205(p)=(data(p,10));

        T110(p)=((data(p,11)));
        T210(p)=(data(p,12));

        T120(p)=((data(p,13)));
        T220(p)=(data(p,14));

        T130(p)=((data(p,15)));
        T230(p)=(data(p,16));
    end;
    a=b+1;
    b=a+499;

    mT105(i)=mean(T105);
    mT205(i)=mean(T205);

    mT110(i)=mean(T110);
    mT210(i)=mean(T210);
```

```
    mT120(i)=mean(T120);
    mT220(i)=mean(T220);

    mT130(i)=mean(T130);
    mT230(i)=mean(T230);

end;
%% getting time to plot
for i=1:1:130  % storing data every 100 intervel and storing
    p=i*500;
    time(i)=data(p,1);

end;
%% Plotting
figure(1),plot(time,mT105,'-.r','linewidth',1.8); % ploting
hold on; plot(time,mT205,'--m','linewidth',1.8);
         ylim([15 20]);
          xlabel('Time(Sec)','Fontsize',12);
          ylabel('Temperature( ^{o}C)','Fontsize',12);
          legend('T1','T2');

figure(2),plot(time,mT110,'-.r','linewidth',1.8); % ploting
           hold on; plot(time,mT210,'--m','linewidth',1.8);
            ylim([15 20]);
          xlabel('Time(Sec)','Fontsize',12);
          ylabel('Temperature( ^{o}C)','Fontsize',12);
          legend('T1','T2');

figure(3),plot(time,mT120,'-.r','linewidth',1.8); % ploting
          hold on; plot(time,mT220,'--m','linewidth',1.8);
           ylim([15 20]);
          xlabel('Time(Sec)','Fontsize',12);
          ylabel('Temperature( ^{o}C)','Fontsize',12);
          legend('T1','T2');

figure(4),plot(time,mT130,'-.r','linewidth',1.8); % ploting
        ylim([15 20]);
          hold on; plot(time,mT230,'--m','linewidth',1.8);
          xlabel('Time(Sec)','Fontsize',12);
          ylabel('Temperature( ^{o}C)','Fontsize',12);
          legend('T1','T2');


figure(5), subplot(2,2,1),plot(time,mT105,'-.r','linewidth',1.8); % ploting
          hold on; plot(time,mT205,'--m','linewidth',1.8);
           ylim([15 20]);
          xlabel('Time(Sec)','Fontsize',12);
          ylabel('Temperature( ^{o}C)','Fontsize',12);
          legend('T1','T2');
          title (['5% POB Dilute Engine Oil'])

           subplot(2,2,2),plot(time,mT110,'-.r','linewidth',1.8); % ploting
           hold on; plot(time,mT210,'--m','linewidth',1.8);
            ylim([15 20]);
```

```
            xlabel('Time(Sec)','Fontsize',12);
            ylabel('Temperature( ^{o}C)','Fontsize',12);
            legend('T1','T2');
            title (['10% POB Dilute Engine Oil'])

             subplot(2,2,3),plot(time,mT120,'-.r','linewidth',1.8); % ploting
            hold on; plot(time,mT220,'--m','linewidth',1.8);
             ylim([15 20]);
            xlabel('Time(Sec)','Fontsize',12);
            ylabel('Temperature( ^{o}C)','Fontsize',12);
            legend('T1','T2');
            title (['20% POB Dilute Engine Oil'])

             subplot(2,2,4),plot(time,mT130,'-.r','linewidth',1.8); % ploting
            hold on; plot(time,mT230,'--m','linewidth',1.8);
             ylim([15 20]);
            xlabel('Time(Sec)','Fontsize',12);
            ylabel('Temperature( ^{o}C)','Fontsize',12);
            legend('T1','T2');
            title (['30% POB Dilute Engine Oil'])


% this progarm will take data from xlsx sheet and draw plots
close all;
clear all;
a=2;
b=500;
%% Reading data from xls file
data=xlsread('soybean.xlsx'); % reading data from the Excel data sheet

% Making avergae every 500 data and then storing then a
for i=1:1:130  % storing data every 100 intervel and storing
    for p=a:1:b;
        T105(p)=((data(p,9)));
        T205(p)=(data(p,10));

        T110(p)=((data(p,11)));
        T210(p)=(data(p,12));

        T120(p)=((data(p,13)));
        T220(p)=(data(p,14));

        T130(p)=((data(p,15)));
        T230(p)=(data(p,16));
    end;
    a=b+1;
    b=a+499;

    mT105(i)=mean(T105);
    mT205(i)=mean(T205);

    mT110(i)=mean(T110);
    mT210(i)=mean(T210);

    mT120(i)=mean(T120);
```

```
    mT220(i)=mean(T220);

    mT130(i)=mean(T130);
    mT230(i)=mean(T230);

end;
%% getting time to plot
for i=1:1:130  % storing data every 100 intervel and storing
    p=i*500;
    time(i)=data(p,1);

end;
%% Plotting
figure(1),plot(time,mT105,'-.r','linewidth',1.8); % ploting
hold on; plot(time,mT205,'--m','linewidth',1.8);
         ylim([15 20]);
          xlabel('Time(Sec)','Fontsize',12);
          ylabel('Temperature( ^{o}C)','Fontsize',12);
          legend('T1','T2');

figure(2),plot(time,mT110,'-.r','linewidth',1.8); % ploting
           hold on; plot(time,mT210,'--m','linewidth',1.8);
            ylim([15 20]);
          xlabel('Time(Sec)','Fontsize',12);
          ylabel('Temperature( ^{o}C)','Fontsize',12);
          legend('T1','T2');

figure(3),plot(time,mT120,'-.r','linewidth',1.8); % ploting
          hold on; plot(time,mT220,'--m','linewidth',1.8);
           ylim([15 20]);
          xlabel('Time(Sec)','Fontsize',12);
          ylabel('Temperature( ^{o}C)','Fontsize',12);
          legend('T1','T2');

figure(4),plot(time,mT130,'-.r','linewidth',1.8); % ploting
        ylim([15 20]);
          hold on; plot(time,mT230,'--m','linewidth',1.8);
          xlabel('Time(Sec)','Fontsize',12);
          ylabel('Temperature( ^{o}C)','Fontsize',12);
          legend('T1','T2');


figure(5), subplot(2,2,1),plot(time,mT105,'-.r','linewidth',1.8); % ploting
          hold on; plot(time,mT205,'--m','linewidth',1.8);
           ylim([15 20]);
          xlabel('Time(Sec)','Fontsize',12);
          ylabel('Temperature( ^{o}C)','Fontsize',12);
          legend('T1','T2');
          title (['5% SOB Dilute Engine Oil'])

           subplot(2,2,2),plot(time,mT110,'-.r','linewidth',1.8); % ploting
           hold on; plot(time,mT210,'--m','linewidth',1.8);
            ylim([15 20]);
          xlabel('Time(Sec)','Fontsize',12);
          ylabel('Temperature( ^{o}C)','Fontsize',12);
```

```
legend('T1','T2');
title (['10% SOB Dilute Engine Oil'])

 subplot(2,2,3),plot(time,mT120,'-.r','linewidth',1.8); % ploting
hold on; plot(time,mT220,'--m','linewidth',1.8);
 ylim([15 20]);
xlabel('Time(Sec)','Fontsize',12);
ylabel('Temperature( ^{o}C)','Fontsize',12);
legend('T1','T2');
title (['20% SOB Dilute Engine Oil'])

 subplot(2,2,4),plot(time,mT130,'-.r','linewidth',1.8); % ploting
hold on; plot(time,mT230,'--m','linewidth',1.8);
 ylim([15 20]);
xlabel('Time(Sec)','Fontsize',12);
ylabel('Temperature( ^{o}C)','Fontsize',12);
legend('T1','T2');
title (['30% SOB Dilute Engine Oil'])
```

APPENDIX C
SAMPLE PREPARATION

Sample Steel Disk Cutting Process: Parting Operation by Horizontal Lathe

The 25.4 mm diameter steel disk with the width 6 ±1 mm were made by a G 0554 Grizzy gear head floor type horizontal lathe machine. A picture of the lathe used in this work is presented in Figure C1. The round steel bar or the work piece is hold by the three-jaw self centering chuck with the help of a rotating clamp, which is presented in Figure C2. Parting operation of the lathe is applied to slice the round bar, and in this operation of lathe a blade-like cutting tool, which is shown in Figure C3, is plunged directly into the work piece to cut it off.

Figure C1: Lathe used for making disks in the thesis work

The Figure C4 presents the work pieces rotational direction and cutting tools direction of the parting operation of lathe. The parting operation requires low speed of the spindle; in this work a 200-250 rpm was maintained to cut the disk. At the end of the cutting process a rough surface with a protruding part from the center of the disk was obtained. Figure C5 presents the surface profile of the disk after sliced with the lathe

Figure C2: The chuck holding the round bar in the parting operation.

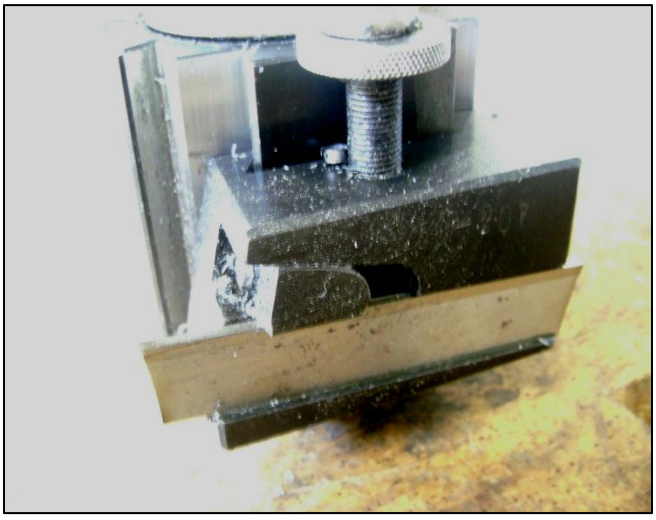

Figure C3: Carbide cutting tool used for parting operation

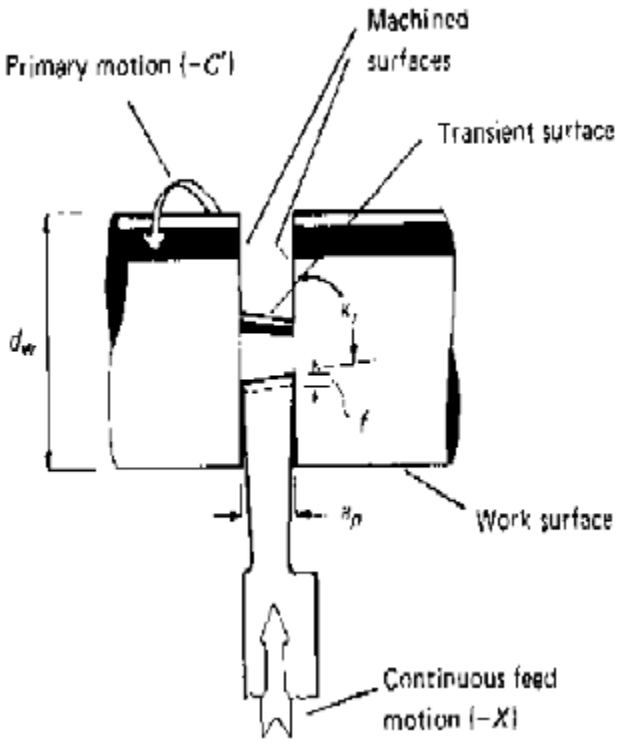

Figure C4: Basic schematics of parting operation

Figure C5: Surface profile of the disk after parting operation

Parting operation also leaves a sharp edge at the end of the work piece. A file was used to chamfer the edge to avoid hazard. For chamfering the edge, the lathe was running at low speed (below 100rpm) and a smooth cut file was placed at the edge of work piece at a 45 degree angle. This yielded a filing edge which is presented in Figure C6.

Figure C6: Chamfering the work- piece edges with file.

Polishing of Steel Disk with the File

The rough disk surface which was presented in Figure C5 is polished with the double cut flat file to remove the protruding surface. After that a bastard file, a second cut file and a smooth file are sequentially used. After this polishing with the files, a disk with a surface roughness in the range 100 to 150μin (Ra value) was obtained. The surface roughness of the disk was measured with a Mitutoyo SJ 210 roughness measuring tester which is shown in Figure C10.

*Figure C7***:** Surface of the disk after polishing with file

Polishing of Steel Disk with Surface Grinder

After polishing the disk with the files, a surface grinder shown in Figure C8 is used to get a smoother surface. A magnetic chuck in the surface grinder machine holds the work piece or the disk on it, while a silicon dioxide grinding wheel rotates at 100 rpm on contact with the disk. The feed rate was adjusted by hand. After polishing the disk with the surface grinder, a surface roughness in a range 40 to 60 μin (Ra value) was obtained.

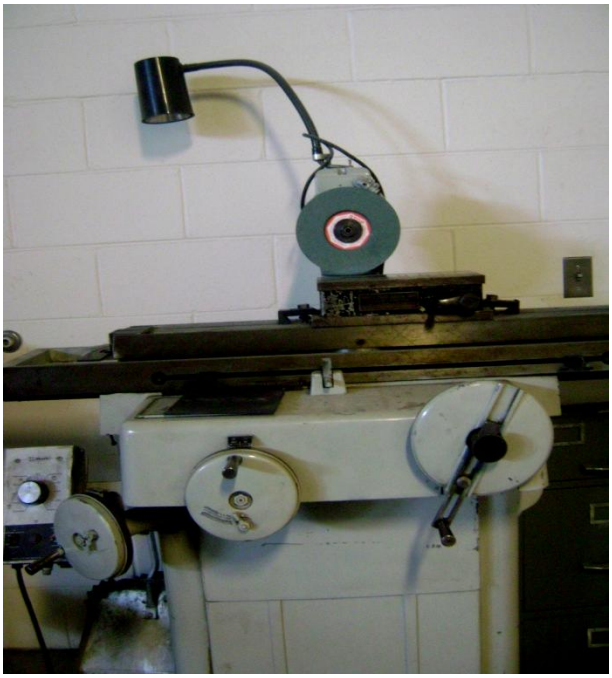

Figure C8: Surface grinder used for surface finish.

Polishing of Disk with Grit Paper

After polishing the disk with the surface grinder, a 240, 320, 400 and finally 600 grit sand paper sequences was used. This process yields a mirror like polished surface as presented in Figure C9. Finally, the disk surfaces are tested to have a roughness in the range of 1 to 10 μin (Ra value).

Figure C9: Final polished surface

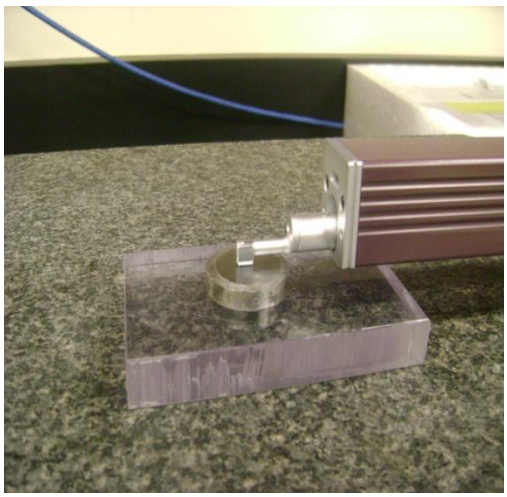

(a) Stylus movement along the surface (b) Display of Ra value of the surface

Figure C10: Surface roughness test with Mitutoyo SJ 210.